AD-A174 080 FRAM IV AMBIENT NOISE: (100 HZ-500 HZ) DATA ANALYSIS (U) SCIENCE APPLICATIONS INTERNATIONAL CORP MCLEAN VA R E KEENAN ET AL. NOV 85 SAIC-85/1901 N00014-84-C-0180 1/2

UNCLASSIFIED F/G 20/1 NL

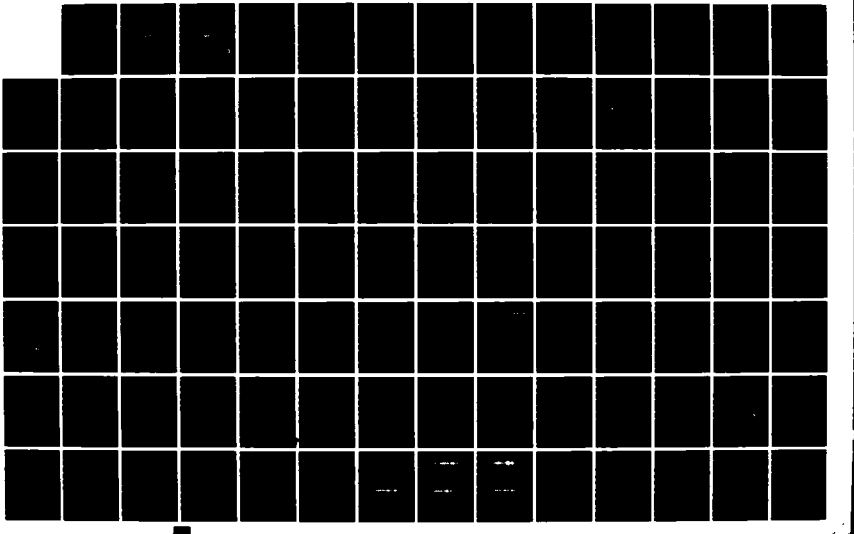

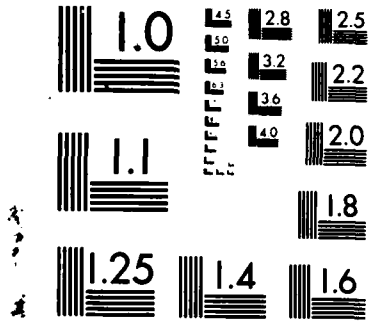

FRAM IV AMBIENT NOISE:
(100 Hz - 500 Hz) DATA ANALYSIS

SAIC-85/1901

SAIC™
Science Applications International Corporation

FRAM IV AMBIENT NOISE:
(100 Hz - 500 Hz) DATA ANALYSIS

SAIC-85/1901

Science Applications International Corporation

Post Office Box 1303, 1710 Goodridge Drive, McLean, Virginia 22102, (703) 821-4300

FRAM IV AMBIENT NOISE:
(100 Hz - 500 Hz) DATA ANALYSIS

SAIC-85/1901

Final Report for Task 27.3

November 1985

Prepared
by

Ruth Eta Keenan
Laurie A. Gainey
Navy Systems Division
Woods Hole, MA 02543

Prepared
for

NORDA/AEAS Program
NSTL Station, MS 39529

Contract No. N00014-84-C-0180

SCIENCE APPLICATIONS INTERNATIONAL CORPORATION

1710 Goodridge Drive
P.O. Box 1303
McLean, VA 22102
(703) 821-4300

SAIC
Science Applications International Corporation

Unclassified

SECURITY CLASSIFICATION OF THIS PAGE (When Data Entered)

REPORT DOCUMENTATION PAGE		READ INSTRUCTIONS BEFORE COMPLETING FORM
1. REPORT NUMBER SAIC-85/1901	2. GOVT ACCESSION NO. ADA174080	3. RECIPIENT'S CATALOG NUMBER
4. TITLE (and Subtitle) FRAM IV Ambient Noise: (100 Hz - 500 Hz) Data Analysis		5. TYPE OF REPORT & PERIOD COVERED Final Report 6. PERFORMING ORG. REPORT NUMBER SAIC-85/1901
7. AUTHOR(s) Ruth Eta Keenan Laurie A. Gainey		8. CONTRACT OR GRANT NUMBER(s) N00014-84-C-0180
9. PERFORMING ORGANIZATION NAME AND ADDRESS Science Applications International Corp. 1710 Goodridge Drive McLean, VA 22102		10. PROGRAM ELEMENT, PROJECT, TASK AREA & WORK UNIT NUMBERS Task 27.3
11. CONTROLLING OFFICE NAME AND ADDRESS Naval Ocean Research and Development Activity NSTL Station, MS 39529		12. REPORT DATE November 1985 13. NUMBER OF PAGES
14. MONITORING AGENCY NAME & ADDRESS(If different from Controlling Office) Office of Naval Research Dept of the Navy 800 N. Quincy Street Arlington, VA 22217		15. SECURITY CLASS. (of this report) Unclassified 15a. DECLASSIFICATION/ DOWNGRADING SCHEDULE

16. DISTRIBUTION STATEMENT (of this Report)

Unlimited

17. DISTRIBUTION STATEMENT (of the abstract entered in Block 20, if different from Report)

Unlimited

18. SUPPLEMENTARY NOTES

19. KEY WORDS (Continue on reverse side if necessary and identify by block number)

FRAM IV	spectra
mid-frequency	ice
ambient noise	thermal
Arctic	hydrophone

20. ABSTRACT (Continue on reverse side if necessary and identify by block number)

Ambient noise from horizontal and vertical hydrophones collected during FRAM IV is examined in the 100-Hz to 500-Hz frequency region. Potential ambient noise generating mechanisms are reviewed. Characteristic signatures of distinguishable noise events heard during FRAM IV are cataloged. The ambient noise spectral levels at 100 Hz, 200 Hz and 300 Hz are compared with the air temperature fluctuations over the 14-day period of the FRAM IV exercise.

DD FORM 1 JAN 73 1473 EDITION OF 1 NOV 65 IS OBSOLETE
S/N 0102-LF-014-6601

Unclassified

SECURITY CLASSIFICATION OF THIS PAGE (When Data Entered)

TABLE OF CONTENTS

LIST OF FIGURES

LIST OF FIGURES (Continued)

LIST OF FIGURES (Continued)

LIST OF FIGURES (Continued)

LIST OF FIGURES (Continued)

LIST OF TABLES

ACKNOWLEDGMENTS

This has been a lively and interesting project and could not have been accomplished without the help of many people. It has been a pleasure working with the individuals mentioned below.

This work has been a joint effort with the MIT Arctic Ambient Noise group. I have had many enlightening discussions with Dr. Ira Dyer, Ms. Chi-Fang Chen and Mr. Peter Stein about the nature of thermal ice noise and how best to find it in our data.

On several occasions I supplemented our data with additional data located at the Naval Underwater Systems Center (NUSC) in New London and would like to thank Dr. Fred DiNapoli, Mr. Mike Fecher and Mr. Bob Dullea for their help.

Most of the data was analyzed at Woods Hole Oceanographic Institution (WHOI) using the instrumentation of the MIT/WHOI Arctic group. Mr. Keith von der Heydt and Mr. Dave Goldstein helped initiate me to the proper use of this equipment. I would especially like to thank Keith for taking the time to help unravel some of the 'mysteries' of the data reduction.

This work has been sponsored by the NORDA AEAS Arctic program. The advice and support of Mr. G.A. Gotthardt and Mr. B.N. Wheatley are especially appreciated.

Section 1
INTRODUCTION

The FRAM IV exercise recorded ambient noise in a 0-2500 Hz bandwidth on analog tape in the spring of 1982. This report documents the SAIC contribution to the joint MIT-SAIC study of the mid-frequency (100 Hz to 1000 Hz) ambient noise recorded on these analog tapes. Section 2 discusses the mechanisms generating mid-frequency ambient noise in the Arctic. Section 3 describes the experimental configuration and Section 4 the data reduction methods. The characteristic signatures of various sounds heard on the data tapes are characterized in Section 5. Section 6 discusses the ambient noise spectra. Spectral levels are correlated with environmental parameters. Section 7 summarizes the conclusions of this study.

Mellen (1984) previously surveyed the ambient noise on these analog tapes to determine the range of ambient noise levels. He examined the hydrophone at a 30-meter depth for the entire exercise and his summary of the 20-Hz and 100-Hz levels for the entire period is included in Section 6.

Section 2
THERMAL STRESS MECHANISMS

Ice is subject to thermal, Coriolis, wind and current forces which produce stress in the ice. Noise is generated by the 'catastrophic' relief of the ice stress, such as ridge-building and ice-cracking.

Ice stress levels, hence the ambient noise levels, are seasonal. In the summer months ambient noise is at a minimum because the ice stress is at a minimum; the ice is more plastic allowing it to yield rather than fracture and, additionally, polynas (open pools of water) allow the ice floes to move freely with the current and wind forces, minimizing stress within the ice floe. In the fall and winter, the growth of new ice constrains ice motion, increasing the stress, increasing the noise level accordingly.

Buck (1982) has shown (Figure 2.1) that the ambient noise is at a minimum in the summer and increases throughout the fall and winter for the mean, 5th and 95th percentile noise levels. The 5th percentile indicates that level of noise which is greater than the ambient noise level 5 percent of the time, and the 95th percentile indicates that level of noise which is greater than the ambient noise level 95 percent of the time.

Dyer (1983) characterized the ambient noise pressure spectra to be composed of three competing spectral components (Figure 2.2). From about 1 to 100 Hz there is a broad spectrum peaked between 10-20 Hz. Shepard (Shepard 1979, Chen 1982) observed that the spectral peak at 10-20 Hz has an ω^2 shape below the peak and an ω^{-2} above the peak. A second broadly peaked spectrum, which is not always present,

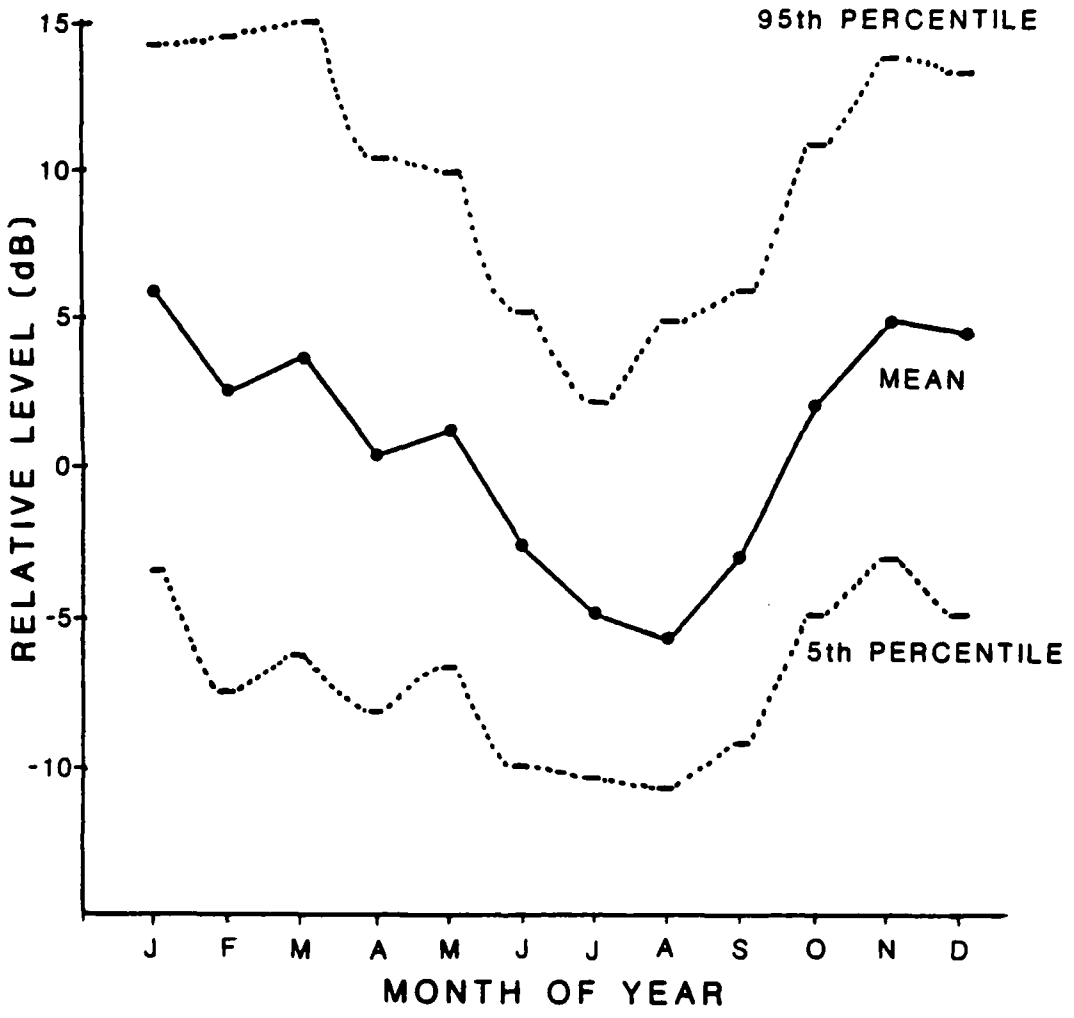

Figure 2.1. Seasonal Dependence of Arctic Ambient Noise (Buck, 1982)

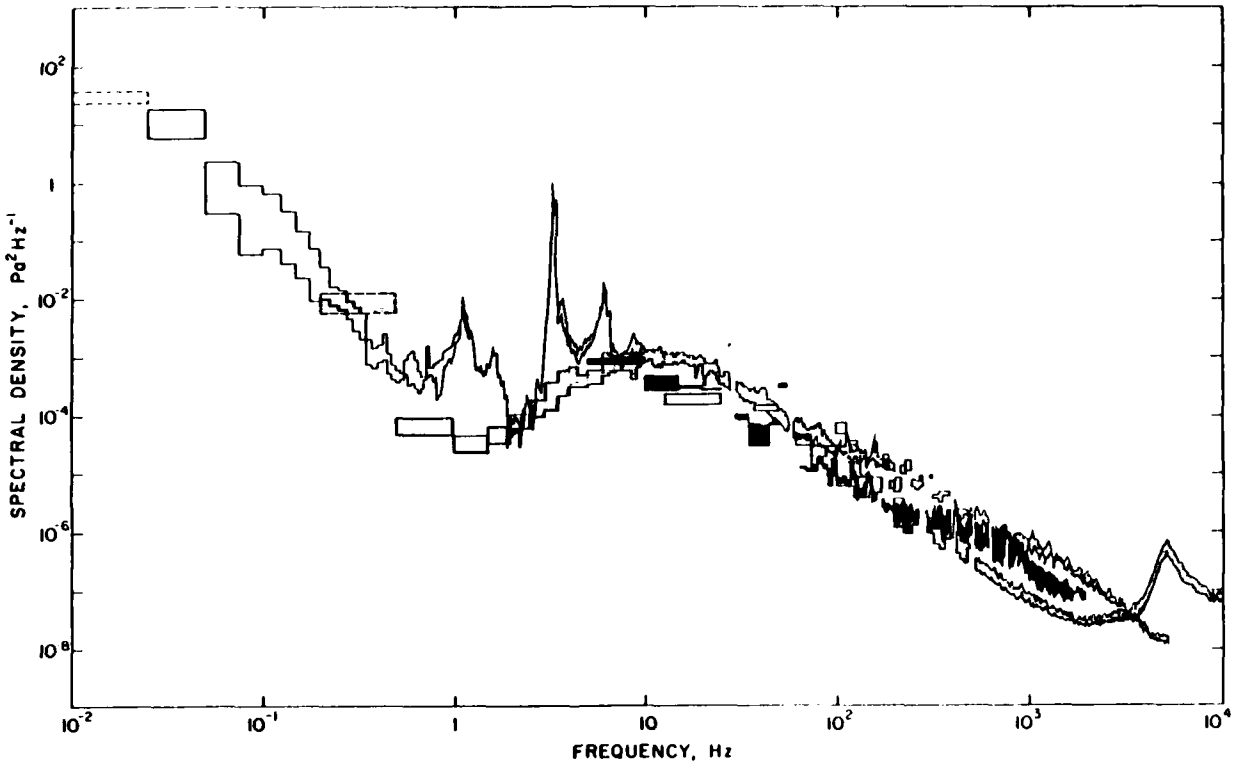

Figure 2.2. Composite Arctic Ambient Noise Spectra (Dyer, 1983)

extends from 150 to 5000 Hz. This feature has been associated with atmospheric cooling. The third component, which is not always present, has a spectral peak about 5000 Hz. This peak has been associated with wind carrying loose snow and ice particles which generate noise on impact with the ice surface.

Data taken by Milne (1967) in the Canadian Archipelago graphically demonstrates that when the air temperature cools the surface of the ice cools and contracts, resulting in surface cracks that generate sound. Milne observed a diurnal variation of ambient noise in the shallow water of the Canadian Archipelago that clearly correlated with the daily temperature variations. His results for spectral levels in the 150-300 Hz band are illustrated in Figure 2.3. This frequency band showed the highest correlation with the temperature variations which oscillated approximately 10°C every day.

Pressure spectra (Milne, 1967) measured in octave bands are shown in Figure 2.4. Spectrum A, labeled residual impulsive noise, was recorded during a long (several days) warming trend. Spectrum B is for a period where the temperature was rising but there were some drops in temperature producing negative gradients. Spectra C, D and E represent cooling periods. This thermal noise shown in Figure 2.4 is peaking in the mid-frequency (100 Hz to 1000 Hz) region, which corresponds to the second broadly peaked spectra noted by Dyer and illustrated in Figure 2.2.

The intensity of the ice-cracking noise has been observed to be a function not so much of the absolute temperature but of the temperature gradient, and a negative temperature gradient (cooling) is more likely to produce ice

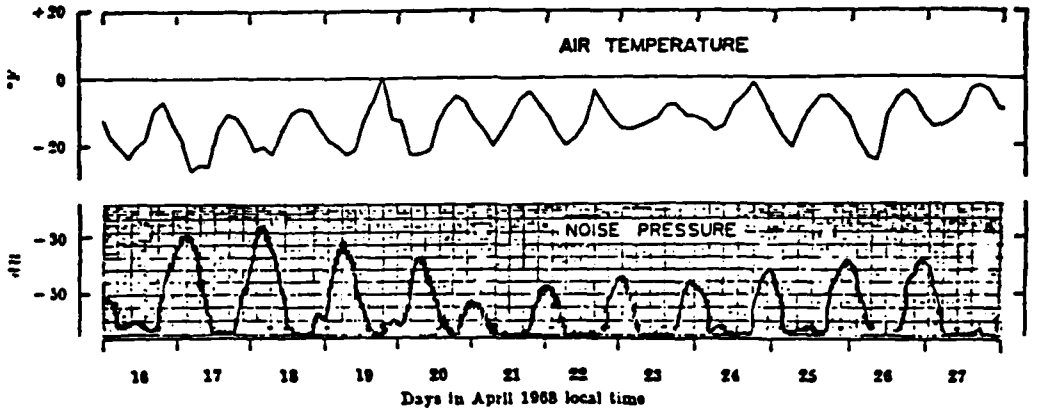

Figure 2.3. Pressure vs Temperature Correlation (Milne, 1969)

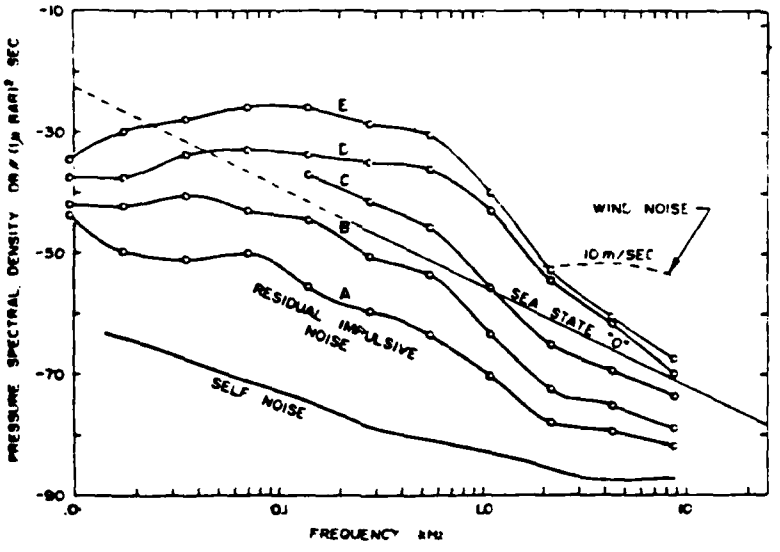

Figure 2.4. Thermal Ambient Noise Spectra (Milne, 1967)

noise than a positive temperature gradient. This is supported by Figure 2.4 as the temperature was dropping faster for Spectrum E than for Spectrum C.

Thermal stress is greatest at the ice surface. This is because ice is a poor conductor of heat so the thermal gradient between the air temperature at the surface and the deep ice temperature must be accommodated near the top layer of the ice. Milne and Ganton (1965) made visual observations of individual cracks on the surface of frozen leads that indicated the crack planes were vertically oriented and that the cracks appeared to penetrate to a depth of a few inches.

Figure 2.5 illustrates the pressure pulses recorded by Milne (1967) from ice-cracking events. Milne proposed a simple environmental model (the geometry is illustrated in Figure 2.6) to relate noise sources to the observed noise statistics. An omnidirectional hydrophone is located at depth h (Figure 2.6) in a half space bounded by the ice surface. Annular areas of width ΔR at horizontal ranges R are assumed to contain independent noise sources with an average emission rate of ε impulses per unit area per second. The radiation pattern $\cos^m\theta$ is assigned to each source, where theta is the incident angle and m defines the directivity. The ice-cracking pulses illustrated in Figure 2.5 were assumed to have a damped sinusoidal waveform

$$u(t) = \exp \frac{-t}{\tau_o} \sin \omega_o t \qquad t > 0$$

τ_o = time constant of the pulse envelope
ω_o = frequency within the envelope

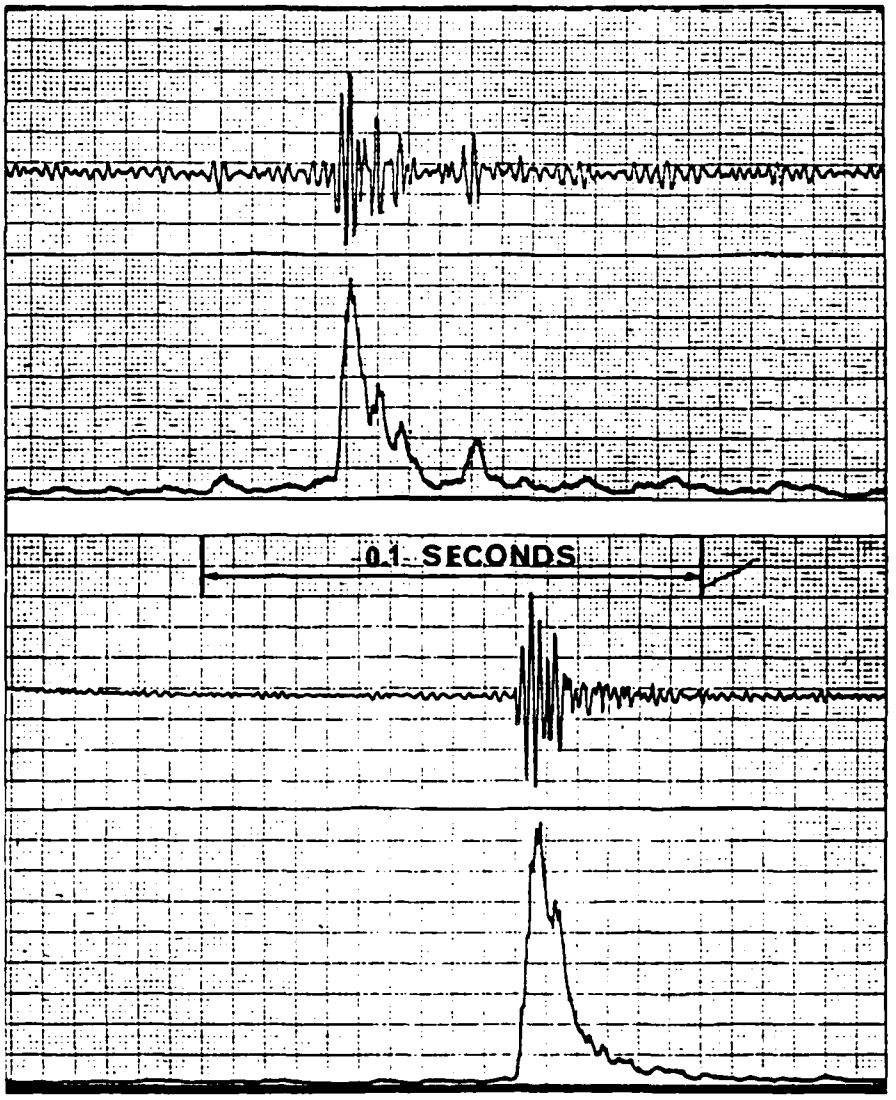

Figure 2.5. Pressure Pulses from Ice-Cracking Events (Milne, 1969)

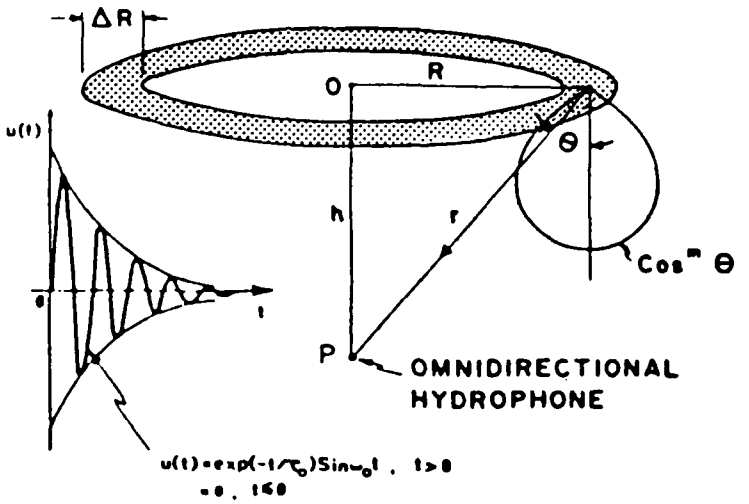

Figure 2.6. Milne Environmental Model (1969)

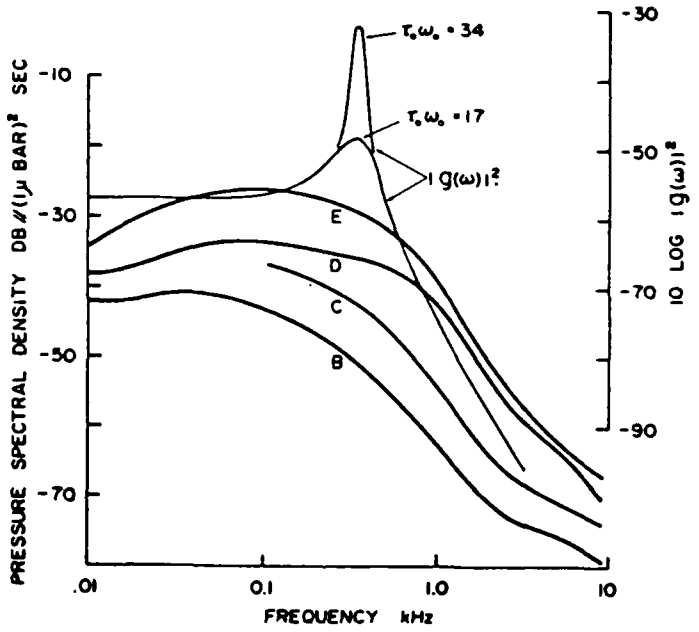

Figure 2.7. Milne Ice-Cracking Spectra (1969)

The spectral density predicted by this model will be

$$\phi(\omega) = 1/2\ \varepsilon^{m-1}\ \sigma_o^2 |g(\omega)|^2$$

$g(\omega)$ = the Fourier transform of the pulse wave

σ_o^2 = the mean square pressure amplitude of the pulse

Milne compared (illustrated in Figure 2.7) the observed ice-cracking spectra with computed spectra. His model shows spectra that are more peaked than observed. By including impulsive noises of different frequencies the predicted spectra could be broadened.

An individual crack relieves the stress over a limited surface. Three types of cracking modes for an elastic media are illustrated in Figure 2.8. Mode I cracking, due to the tensile forces of the surface of the ice trying to contract, is similar to the cracking associated with a muddy riverbed drying up. This motion would create an impulsive popping type of noise. Mode II cracking, a differential up/down sliding of the ice surface, could be caused by a bending moment. Mode III cracking, a parallel shearing of the crack surface, would require differential forces in the ice itself. Cracking of Types II and III would create a rubbing kind of noise.

An increase in the stress will reduce the area relieved by an individual crack requiring more cracks per unit area to relieve the overall stress. Thus as stress increases, the number of cracks per unit area increase raising the ambient noise levels. Milne (1967) observed the thermal noise to be Poisson distributed, which would be consistent with this type of mechanism.

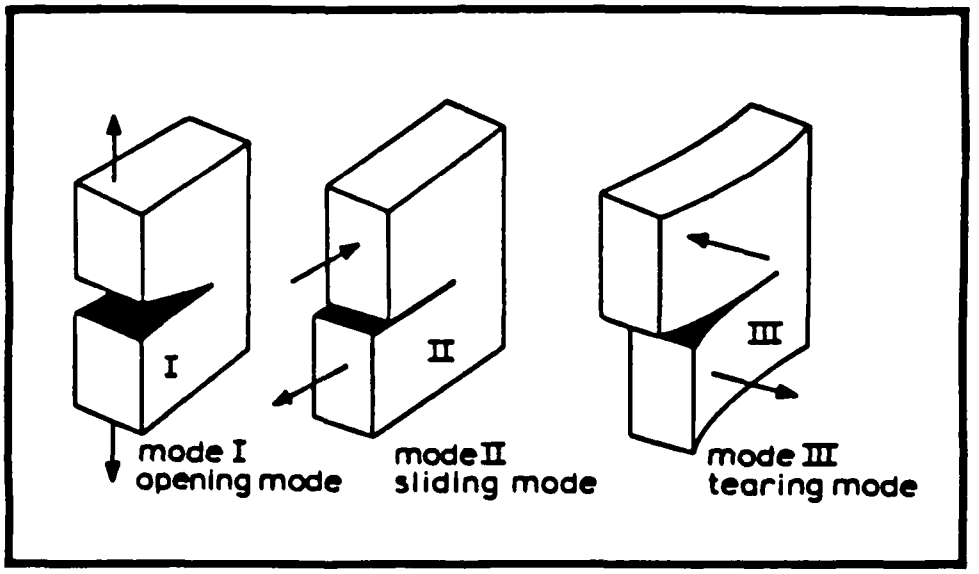

Figure 2.8. Ice Cracking Modes (Broek, 1982)

This report leaves the reader with this general description of the thermal noise mechanism. A detailed theoretical thermal noise model is being developed by Ms. Chi-Fang Chen (MIT) in partial fulfillment of the Ph.D. requirements at MIT.

Section 3
DATA

The multi-institutional FRAM exercises were organized in the spring of 1980 through 1984 to collect oceanographic and acoustic data in the Arctic Ocean. This study uses data from the FRAM IV exercise collected on the MIT/WHOI horizontal array and the NRL vertical array.

3.1 MIT/WHOI Horizontal Array

The MIT/WHOI horizontal array consisted of 29 hydrophones and 4 geophones. The hydrophones were placed at 91 meters below the ice surface, and the geophones were frozen into the ice surface. The hydrophone elements had a ±5V response (linear response ±4V). The hydrophone response was flat between 100 and 1000 Hz as indicated in the USRD calibration in Table 3.1 and the sensitivity was 158.6 dB re 1μPa per volt on the three hydrophones tested.

The exponential configuration of the elements was selected to optimize beamforming below 80 Hz. The array had an East-West aperture of 1280 meters and a North-South aperture of 1300 meters. The location of the hydrophone and geophone elements, with respect to hydrophone 1, apex phone, is listed in Table 3.2 and illustrated in Figure 3.1. Three hydrophones that were not part of the beamforming portion of the array were tapped by the NUSC analog system. These hydrophones were denoted hairy, strapped, and 90-lb, and were used to study strum. The 90-lb hydrophone was weighted by a 90-lb weight at the bottom; the hairy hydrophone had a faired surface on the cable and the strapped hydrophone had the suspension system used in the other hydrophones removed.

Table 3.1 USRD Calibration

HYDROPHONE (H) GEOPHONE (G)	RANGE (M)	BEARING (DEG)	DEPTH (M)
H1	0	0	91
H2	23	0	91
H3	42	0	91
H4	82	0	91
H5	161	0	91
H6	321	0	91
H7	642	0	91
H8	19	180	91
H9	40	180	91
H10	80	180	91
H11	160	180	91
H12	321	180	91
H13	438	180	91
H14	20	90	91
H15	41	90	91
H16	80	90	91
H17	160	90	91
H18	322	90	91
H19	20	270	91
H20	80	270	91
H21	160	270	91
H22	324	270	91
H23	647	270	91
H24	971	270	91
H29	638	90	91
H30	872	0	91
G1	0	0	0
G2	160	0	0
G3	160	270	0
G4	226	315	0
HAIRY	50	225	91
STRAPPED	155	354	91
90 lb	136	6	91

Table 3.2 Location of Hydrophone and Geophone Elements

HYDROPHONE	DEPTH (M)
V1	960
V2	870
V3	782
V4	690
V5	630
V6	600
V7	570
V8	540
V9	510
V10	480
V11	450
V12	420
V13	390
V14	360
V15	350
V16	335
V17	330
V18	300
V19	270
V20	NOT WORKING
V21	210
V22	180
V23	150
V24	140
V25	125
V26	120
V27	90
V28	60
V29	30

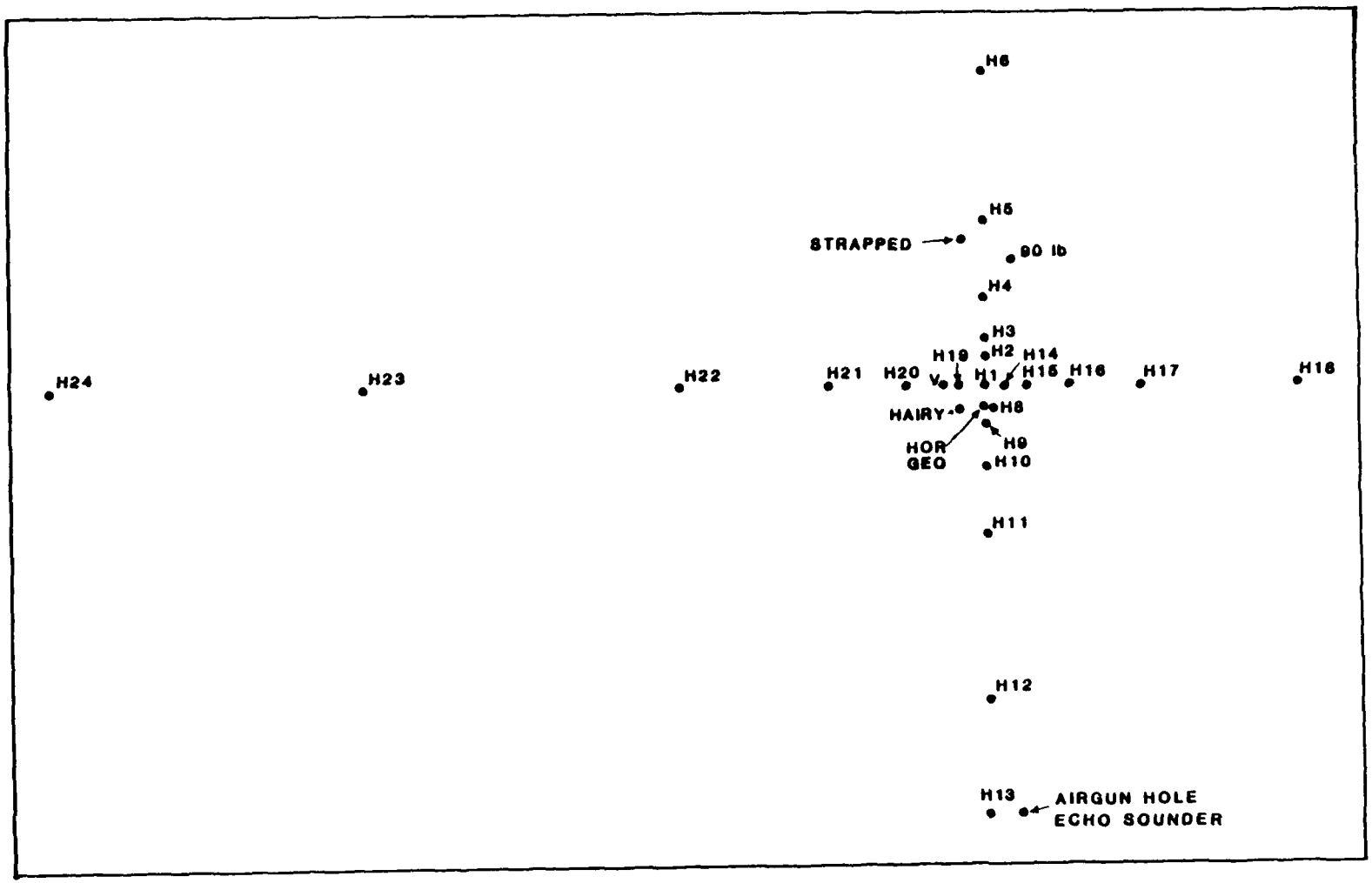

Figure 3.1. Schematic of Receiving Array

A digital 24-channel recorder with a 120 dB dynamic range was used for the horizontal array. Thus, at any one time only 24 of the 33 elements were being recorded. This system used an anti-aliasing filter (see Figure 3.2) that limited the high-frequency response to 80 Hz. This study had access to these digital tapes which were used to check the consistency of the analog data reduction.

3.2 NRL Vertical Array

The NRL vertical array consisted of 28 elements at depths ranging from 30 meters to 960 meters below the surface of the ice. The vertical array was located approximately 40 meters west of the horizontal apex hydrophone, as illustrated in Figure 3.1. The depths of the vertical elements are listed in Table 3.2.

Conversations with T.C. Yang and R. Dicus at the Naval Research Laboratory (NRL) confirmed that the frequency response of the hydrophones and system (preamp and postamp) electronics was flat. The variable gain amplifier (see Figure 3.2) had a cutoff frequency (6 dB/octave rolloff) that was dependent upon the gain setting, the higher the gain the lower the cutoff.

The NRL analog system had a 28-channel capability and was used to collect data from the vertical array. Before recording on the NRL tapes a 400-Hz low pass filter was inserted. This study did not have access to these tapes.

3.3 NUSC Recordings

The Naval Underwater Systems Center (NUSC) made analog recordings from hydrophones/geophones selected from

FRAM IV DATA ACQUISITION

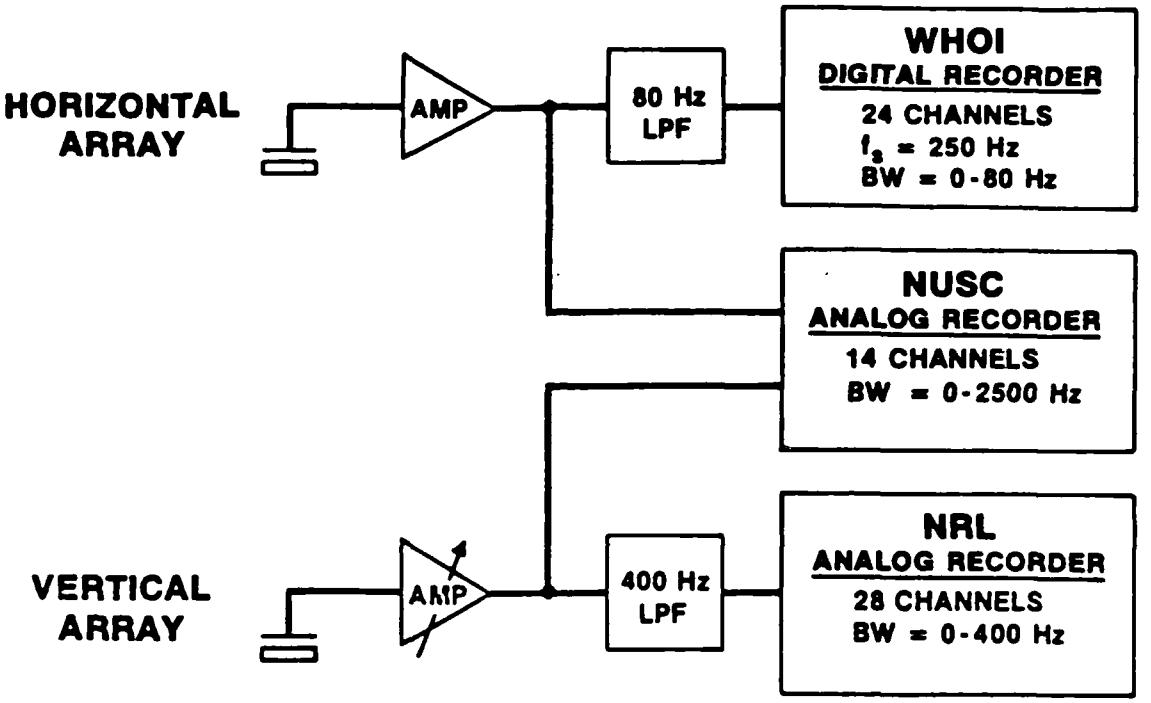

Figure 3.2. Data Acquisition Summary

both the horizontal and vertical array. The NUSC analog Honeywell recorder had a 14-channel, 75-dB dynamic range capability. Data from twelve elements selected from the horizontal and vertical arrays, was recorded on the first twelve channels. The remaining two channels on the NUSC recorder were used for time code and tape synchronization channels. The Honeywell recorder was played at Wide Band I, 3-3/4 IPS which limited the bandwidth to 2500 Hz.

The configuration of the FM recorder was changed frequently during the exercise. Appendix A lists the FM recorder configuration for the analog data available at WHOI beginning on Day 15.

Several of these analog tapes had two channels digitized by NUSC at a 5952.38-Hz sampling rate using a 2400-Hz anti-aliasing filter. Some of these digital tapes were analyzed with a VAX floating-point array processor but none of this work is included in this report.

Section 4
DATA PROCESSING

The data processing setup used for this study at WHOI consisted of playing the NUSC analog tapes on an EMI recorder through a Spectral Dynamics SD345 FFT Analyzer. A Kronhite filter, 24-dB/octave rolloff, was occasionally used to help analyze the data.

A VAX Floating Point Array Processor was used to process the high-frequency NUSC digital tapes.

Some of the low-frequency WHOI/MIT digital tapes were processed on the MIT/WHOI HP acquisition system to verify analog data.

Other analog tapes from FRAM IV were played at NUSC/NLL, who provided us with some spectral levels to extend the pressure time series.

4.1 Calibration Tone

Due to variations in system electronics between tape recorders, a baseline voltage must be established. A 500-Hz, 1V-RMS calibration tone was recorded on each channel at the end of FRAM IV. These calibration tones were played through our data processing system to check the fidelity of our reproduction.

Figure 4.1a shows the power spectra of the 500-Hz calibration tone with the wideband-I option ON. It was evident from listening to the pure tone and from Figure 4.1a that the calibration tone is faithfully reproduced in this

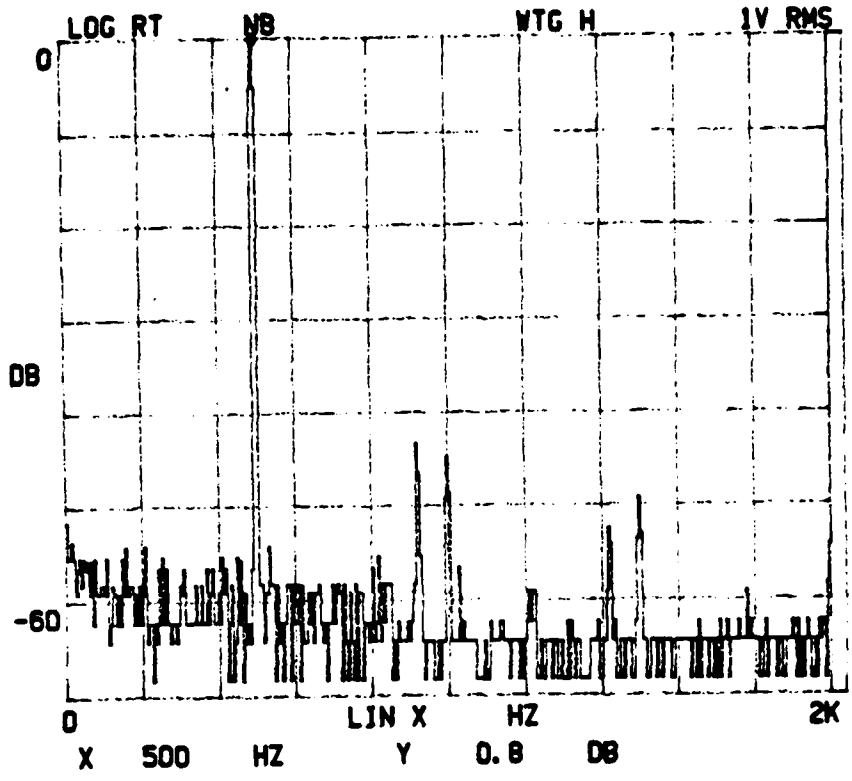

Figure 4.1a

Calibration Tone,
Wide Band.

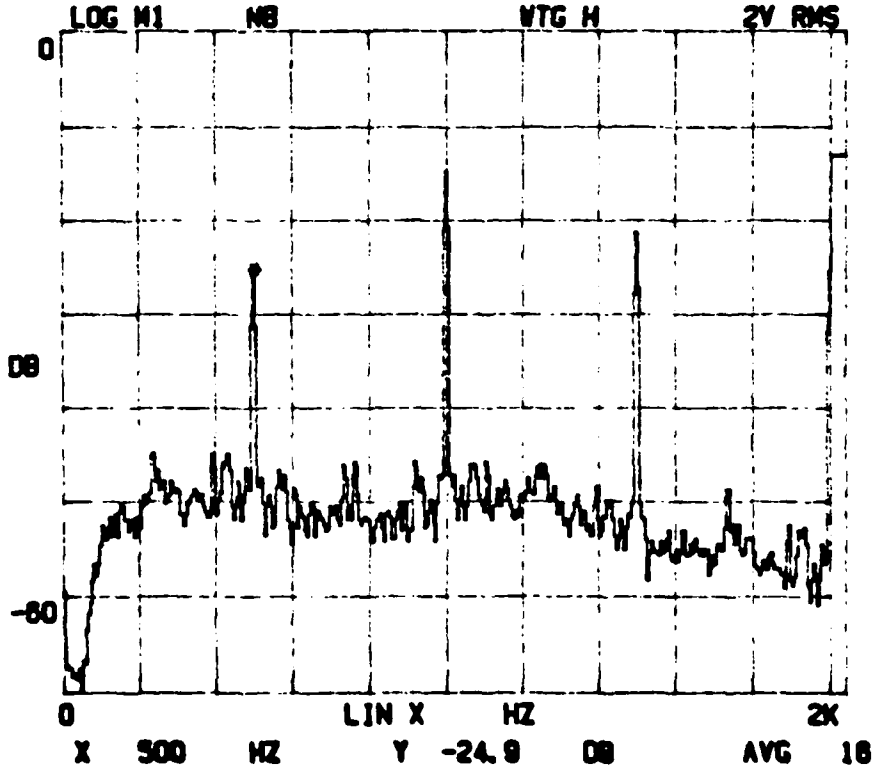

Figure 4.1b

Calibration Tone,
Without Wide Band.

mode (the dynamic range of the spectrum analyzer is 65 dB). The cursor has been placed in the 500-Hz frequency bin and reads at a +0.8-dB level with respect to the 1V-RMS reference voltage. Table 4.1 lists the 500-Hz level measured on each channel of the EMI recorder.

Table 4.1 EMI Recorder

FM CHANNEL	500-Hz LEVEL
1	+.8
2	+.8
3	+.8
4	+.8
5	+.8
6	+.7
7	+.8
8	+.8
9	+.7
10	+.8
11	+.8
12	+.7

Figure 4.1b reproduces Figure 4.1a without the wideband I option. It was obvious from listening to the tape and from Figure 4.1b that the 500-Hz tone is obscured in the noise. All the remaining analysis used the wideband option to faithfully reproduce the data.

4.2 Spectrum Analyzer

The SD345 Spectrascope was used at WHOI and provides figures for the plots in the report unless noted otherwise. The SD345 is a microprocessor-based, 1024-point FFT analyzer. Sixteen frequency ranges can be selected in a 1,2,5 sequence from 1 Hz to 100 kHz full scale. The sampling rate is 2.56 times the full scale frequency range selected. Thus a full scale of 5 kHz represents 1024 samples at a

12.8-kHz rate for a total time series of 0.08 seconds. A full scale of 100 Hz represents a 4.0-second time series. The SD345 offers 400 lines of resolution, hence the 5-kHz full scale frequency range would have a 12.5-Hz resolution and the 100-Hz full scale frequency range would have a .25-Hz resolution.

The time series displays 512 points, every other point sampled. A 5-kHz full scale setting represents 80 ms sampled every .156 ms in the time display.

The SD345 has a transient arm feature which was used to capture events discussed in Section 5. The transient arm can be selected to trigger on positive or negative voltages exceeding a predetermined threshold. The display shows 10% of the time series preceding the event. Again the time series only displays every other point sampled to generate the spectra.

The pressure spectra can be displayed in the power spectra density format or the Fourier transform format. The PSD format (Figure 4.2) is displayed in engineering units (EU) squared per Hz. The bandwidth and Hanning window corrections (-10 log [1.5 * BW]) are automatically applied to the output. To convert to dB re 1V the equivalence between volts and engineering units must be programmed into the SD345. In this case 1mV was set equal to 1 engineering unit. The 500-Hz tone has a level -7.88 dB re $1V^2$. The Fourier transform format (see Figure 4.1a) displays the spectra in dB relative to the reference voltage in the top right hand corner of the display. No corrections are made for the bandwidth or Hanning window. The 500-Hz level is .8 dB and if we correct for the bandwidth and Hanning window, -10 log(1.5*5) we get a level of -7.88 dB re 1V. Since this display is

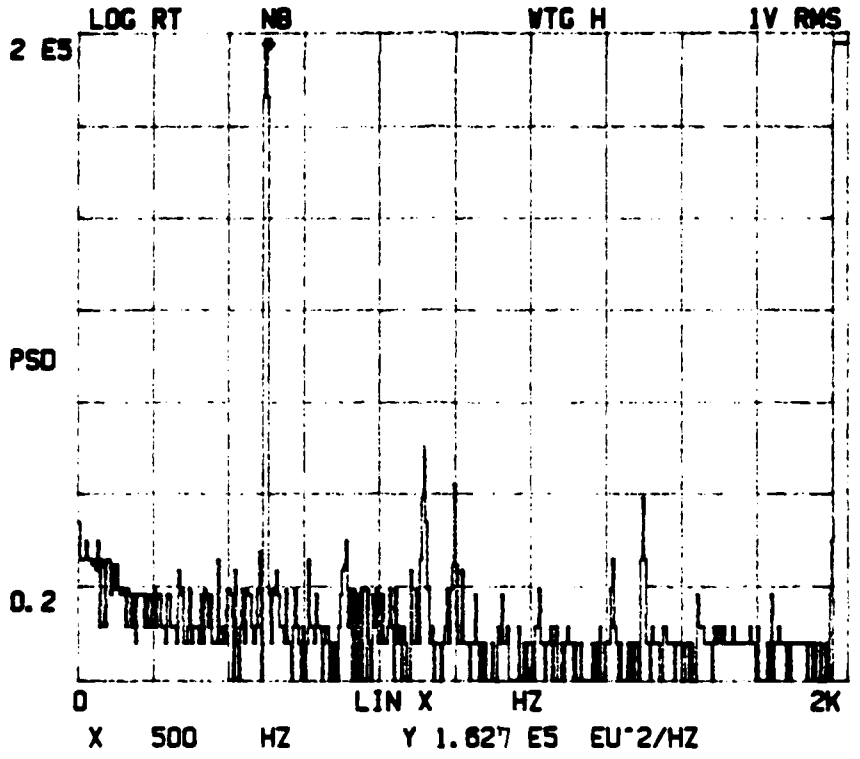

Figure 4.2. Calibration Tone, PSD Format

relative to the reference voltage and the SD345 has a 65-dB dynamic range some care is required to avoid the noise floor in these displays. Since such an error would be immediately obvious and as this display offers a dB scale we have opted to use it for the presentation of spectra in this report. Equation (4.1) is used to convert the output of this display to absolute pressure level (dB re 1μPa re 1Hz).

$$DBA = DBL - VLT - HYD - BW - TG - CAL - HAN \quad (4.1)$$

where:

DBA = absolute dB
DBL = dB level from SD345 plot
VLT = 20 log(1V RMS/reference voltage)
HYD = hydrophone sensitivity
= -159 dB re 1μPa re 1V
BW = 10 log(bandwidth)
TG = TAPE GAIN
= 24 dB for horizontal phones
= 38 dB for vertical phones
CAL = correction for calibration tone
HAN = Hanning window correction
= 10 log(1.5)

To verify that Equation (4.1) is correct we compare the spectral levels from the MIT/WHOI digital tapes with a spectra from the analog tape. Figure 4.3 represents a 516-second average spectral plot for hydrophone 24 starting at Day 15 at 01:15:00. The levels depicted in this plot represent absolute levels referenced to 1μPa and 1 Hz. Figure 4.4 is the compatible spectra using the SD345. The same time average and hydrophone were selected. As Figure 4.3 does not contain any special windowing, Figure 4.4 was created using

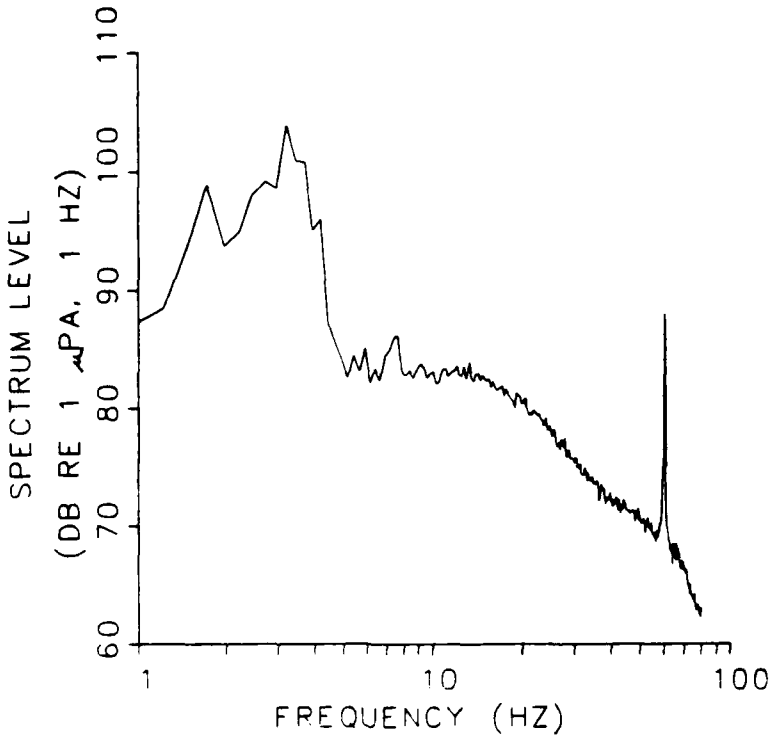

Figure 4.3. 100-Hz Spectra Using MIT/WHOI Digital Data

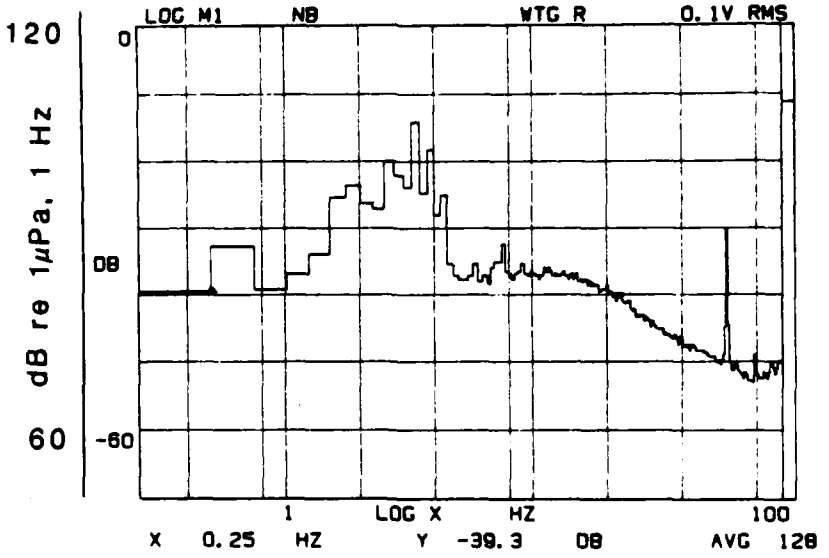

Figure 4.4. 100-Hz Spectra Using NUSC Analog Data

the rectangular window. The 20-Hz level in Figure 4.3 is 81 dB re 1μPa re 1 Hz and in Figure 4.4 it is -40 dB. Using Equation 4.1 where

DBL = -40
VLT = 20
HYD = -159
BW = -6
TG = 24
CAL = .8
DBA = -39.5 + 120.2

The absolute level in Figure 4.4 would also be 81 dB. At 40 Hz the level in Figure 4.3 is about 73 dB re 1μPa re 1 Hz and in Figure 4.4 it is approximately -47 dB or 73 dB re 1μPa re 1 Hz.

4.3 Stability of Average Spectra

Figures 4.5a through 4.5j illustrate the spectra of increasing the number of averages from 1 to 256, by a factor of 2. To plot pressure level versus time we wanted to trade off between stable spectra levels (long term samples) and spectra representative of ambient noise events uncontaminated by camp activity (short term samples). Comparing the plots in Figure 4.5 illustrates that the spectra become fairly stable at N = 16 and very stable at N = 128. It is easy to read off mean levels from the 128-average spectra and there is no difference in the spectral levels of increased averages.

4.4 Interchannel Consistency

The consistency of spectral levels is examined between channels on the analog tape. For this comparison the

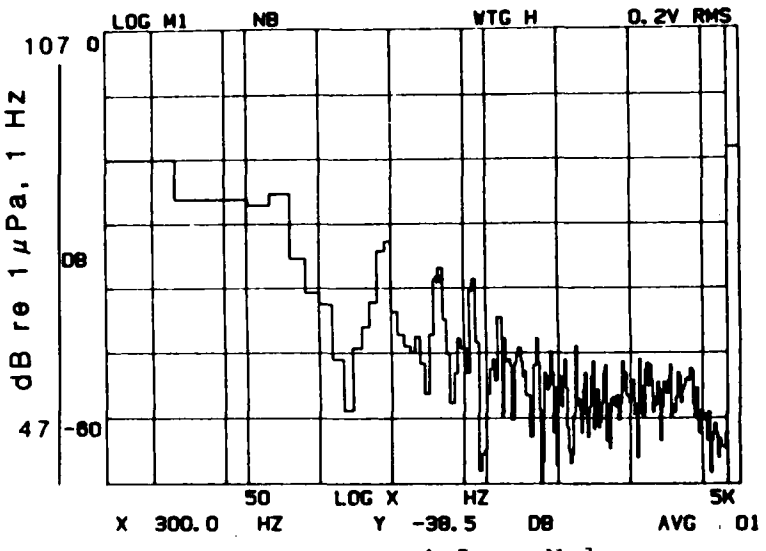

Figure 4.5a. N=1

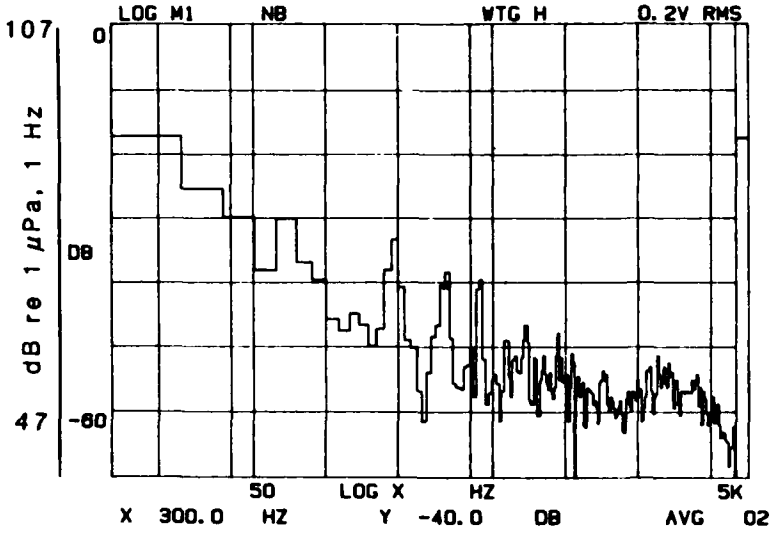

Figure 4.5b. N=2

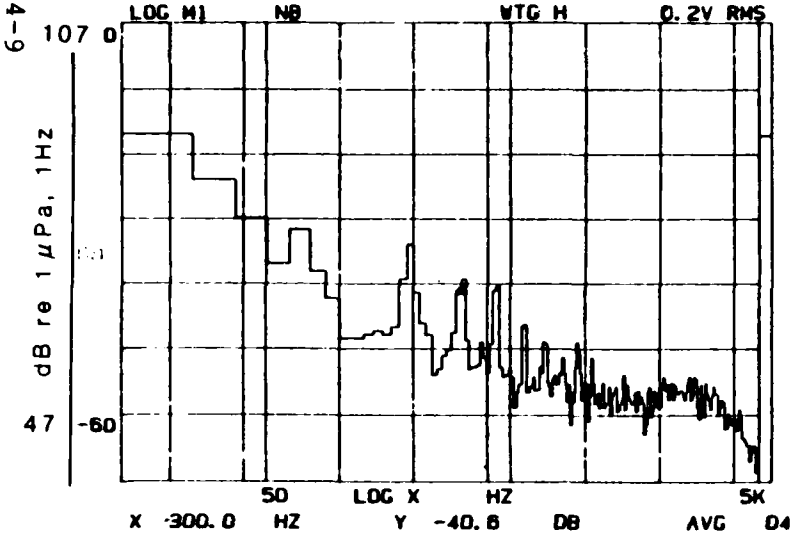

Figure 4.5c. N=4

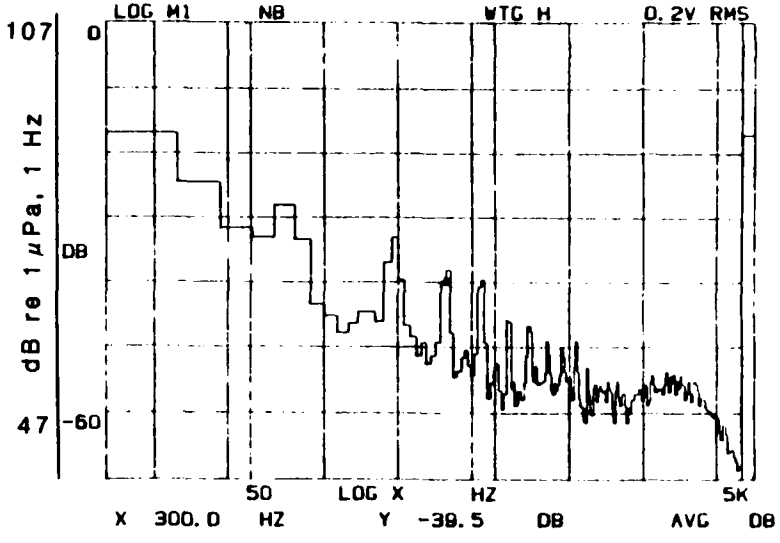

Figure 4.5d. N=8

Figures 4.5a-j. Average 5K Spectra for Various Time Averages of a Quiet Period on Day 15 at 03:37:00, FM Channel 1, Kronhite: 0-20K Hz.

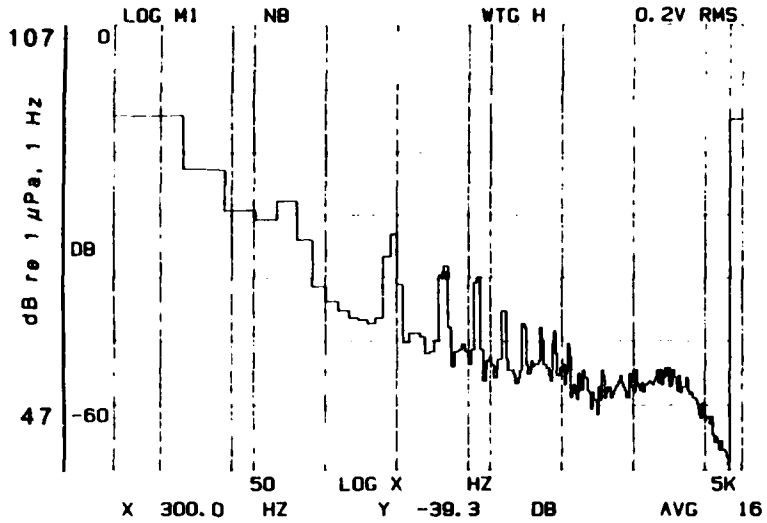

Figure 4.5e. N=16

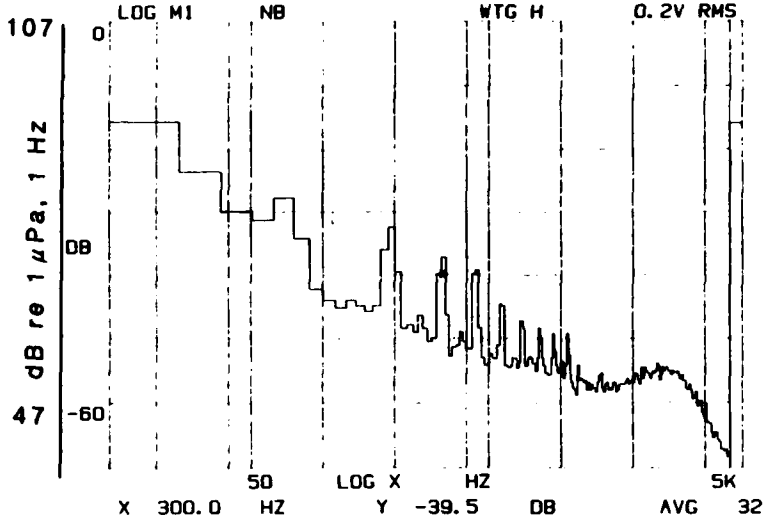

Figure 4.5f. N=32

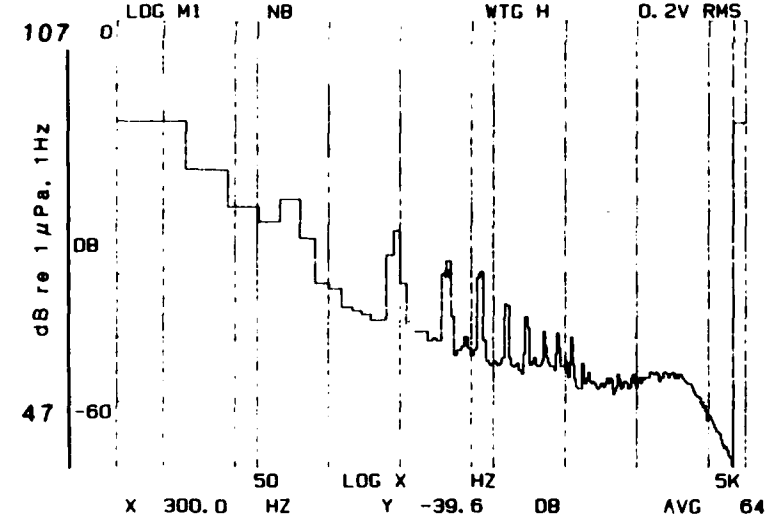

Figure 4.5g. N=64

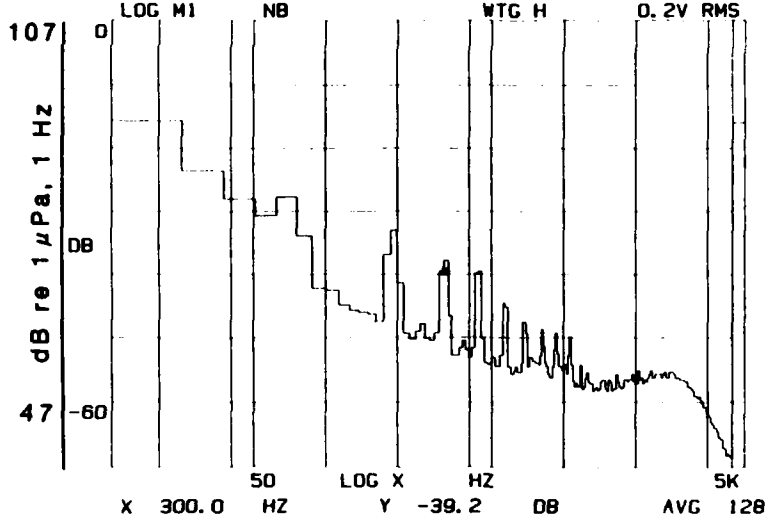

Figure 4.5h. N=128

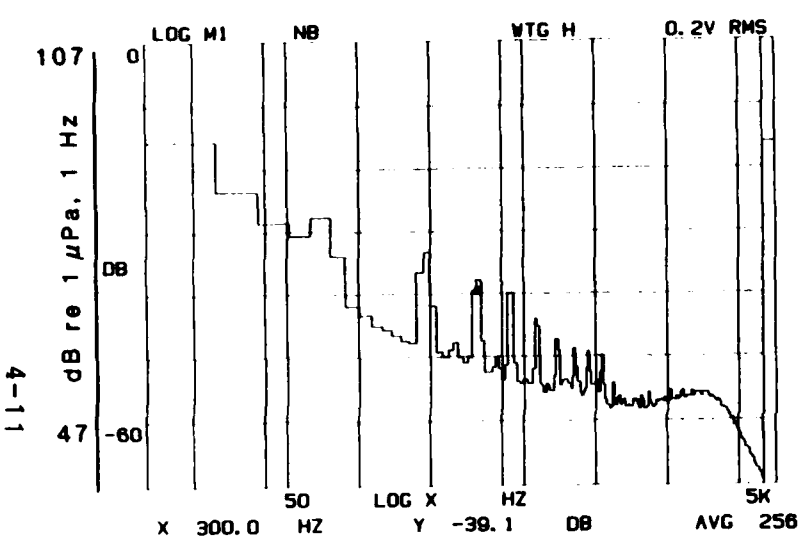

Figure 4.5i. N=256

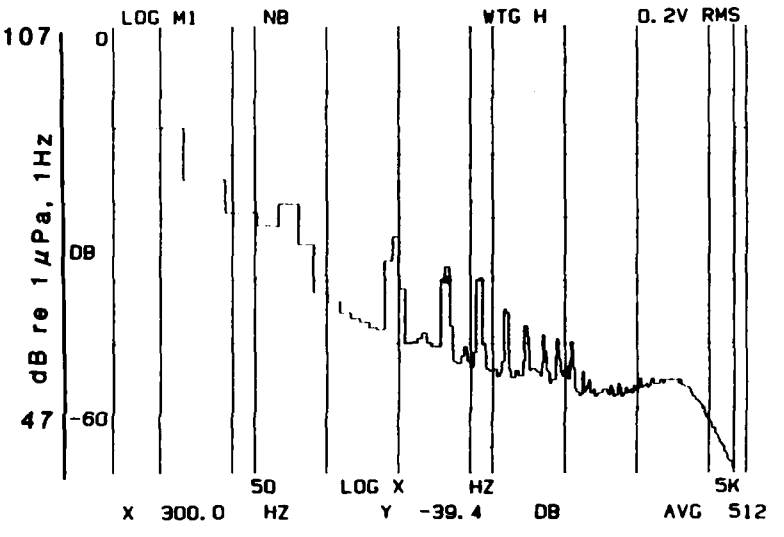

Figure 4.5j. N=512

5-kHz scale was selected on the spectral dynamics to show all the data available on the tape. A 128-average spectral output (at the 5-kHz setting this represents a 10.24-second average) from all the analog channels are compared in Figure 4.6 at 18:17:00 on Day 15. This was a quiet period on all the hydrophones and no notations appear in the logbook. All the horizontal phones (FM channels 1,3,5,7,9) and the geophones (FM channels 11,12) are in agreement with each other as are all the vertical phones (FM channels 2, 4, 6, 8, 10); however, the spectra of the vertical and horizontal phones disagree.

After accounting for the 14-dB difference in gain settings between horizontal and vertical phones, the spectral levels between horizontal and vertical phones agree up to 700 Hz; the vertical phones continue to roll off and the horizontal phones show constant, then increasing levels. As both horizontal and vertical hydrophones have flat frequency responses in this range the difference between vertical and horizontal is unaccountable at this time. Therefore this study will not use data above 500 Hz.

4.5 Generator Lines

It has been suggested that generator harmonics (lines at multiples of 60 Hz) invalidate the horizontal phone data. In Figure 4.7a the spectra of FM channel 3 (the horizontal strapped hydrophone) shows a 2.5-Hz resolution. If this figure is compared with a spectra generated on another spectrum analyzer with a 1.5-Hz resolution, it will be evident that the generator lines are very narrow band and one can read the spectral levels between the lines. Figure 4.7b shows FM Ch 3 and FM Ch 4 from 100 to 900 Hz. Notice that FM Ch 4, which is the 90 m vertical hydrophone, also shows

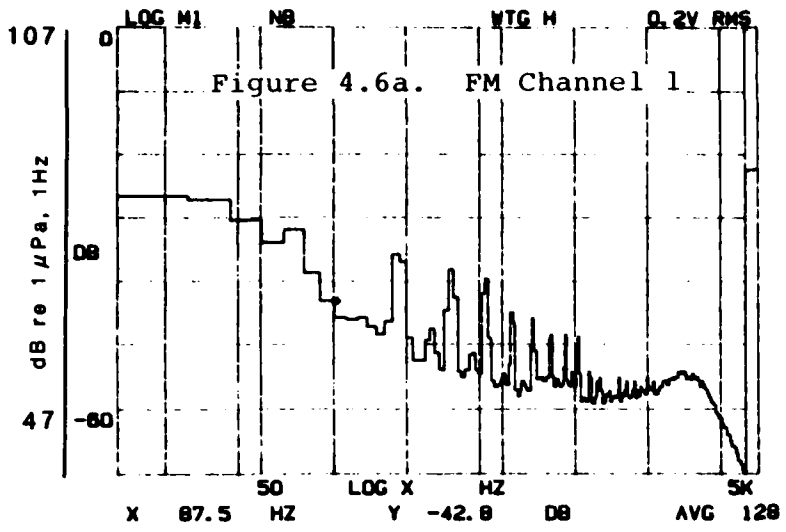

Figure 4.6a. FM Channel 1

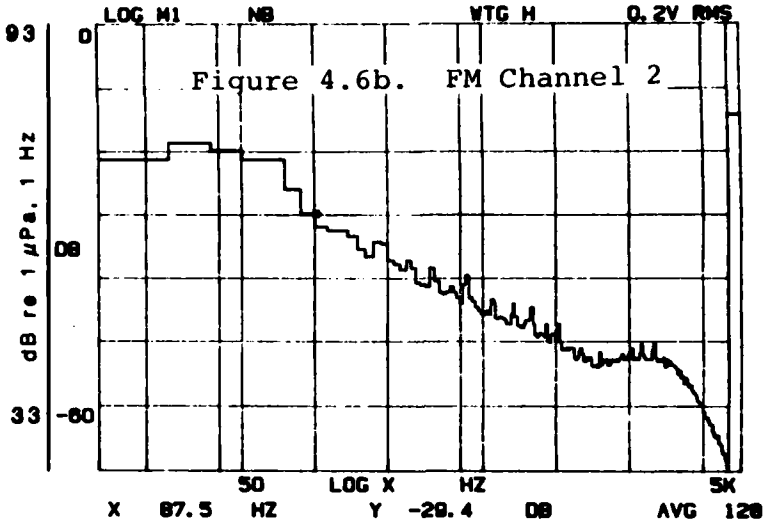

Figure 4.6b. FM Channel 2

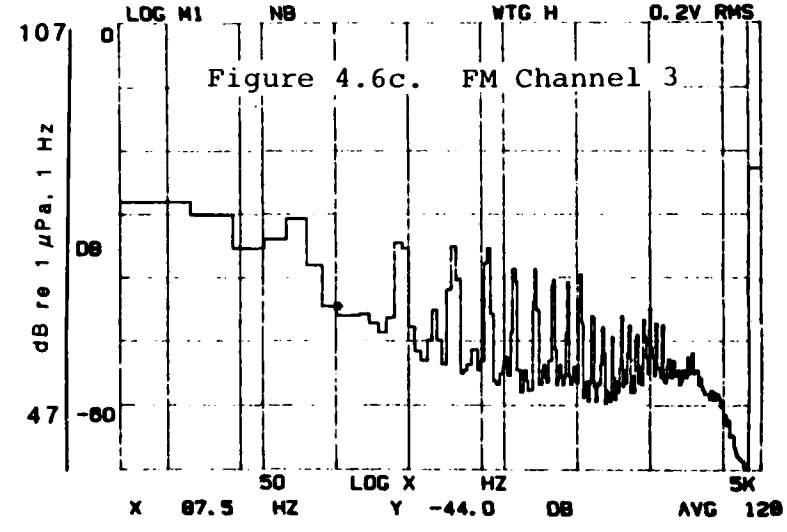

Figure 4.6c. FM Channel 3

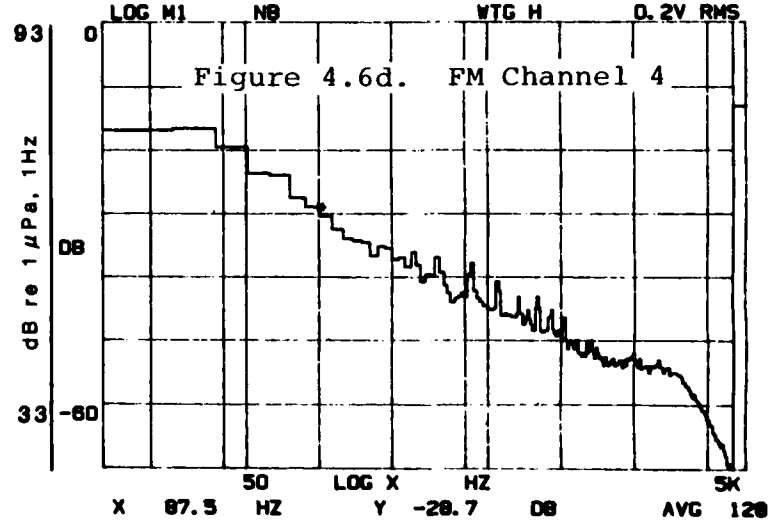

Figure 4.6d. FM Channel 4

Figure 4.6a-1 Average 5K Spectra (N=128) of a Quiet Period on Day 15 at 18:17:00 for Various Channels, Kronhite: 0-20K Hz.

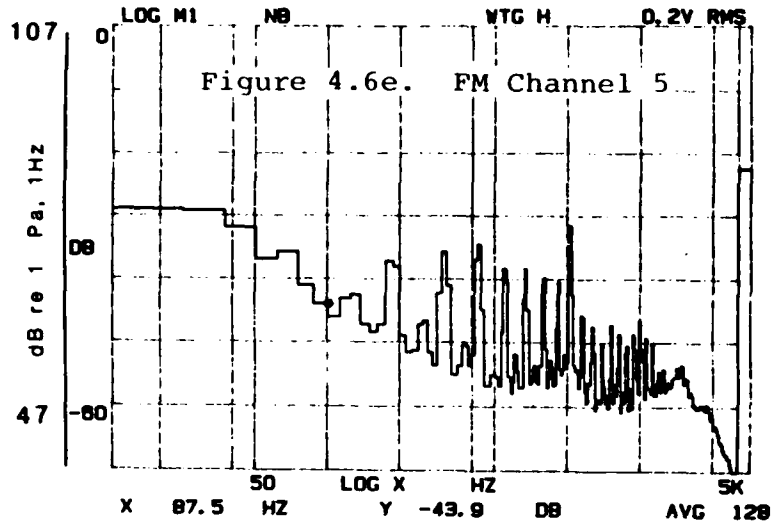

Figure 4.6e. FM Channel 5

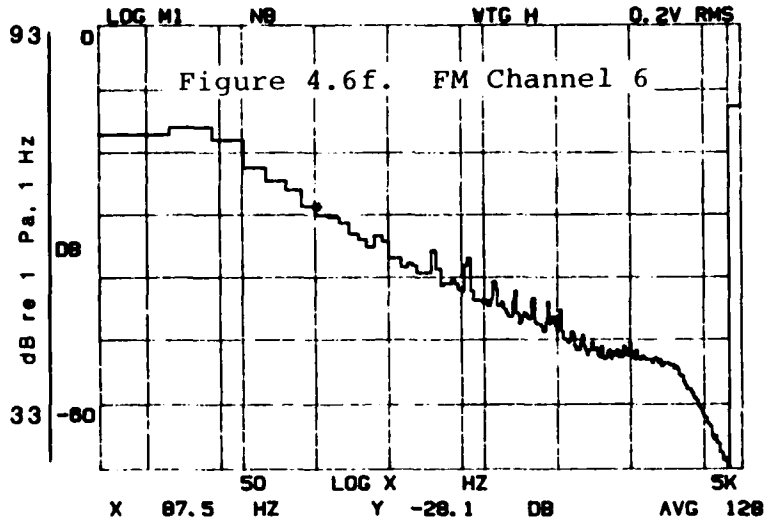

Figure 4.6f. FM Channel 6

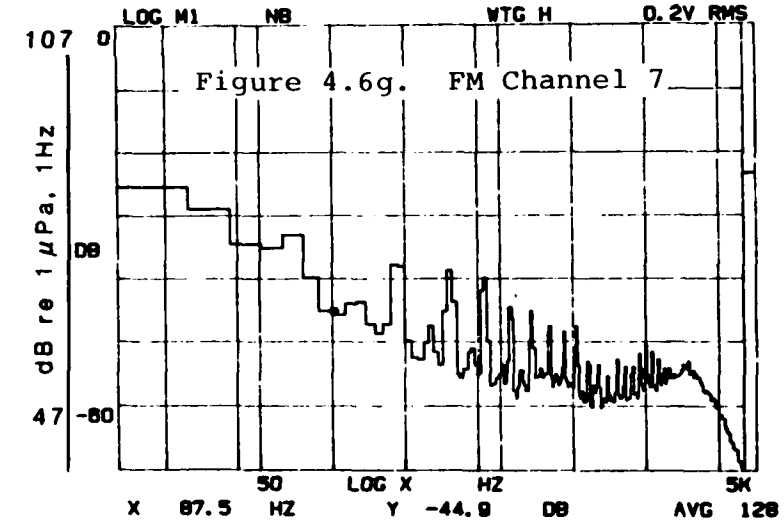

Figure 4.6g. FM Channel 7

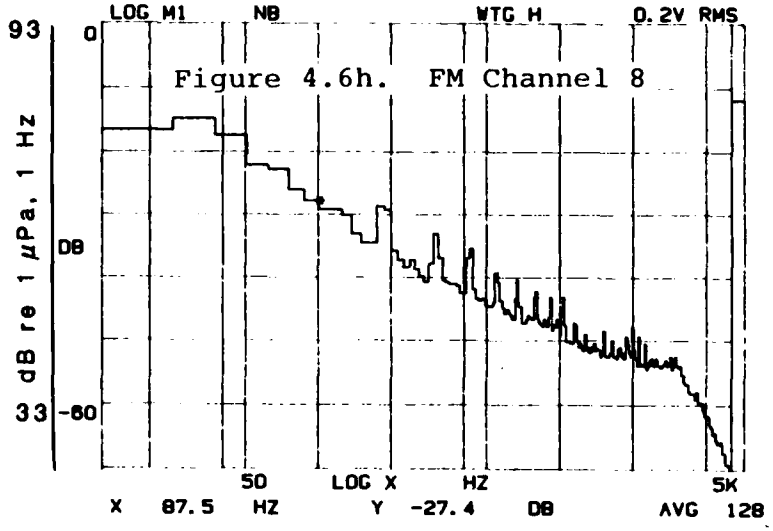

Figure 4.6h. FM Channel 8

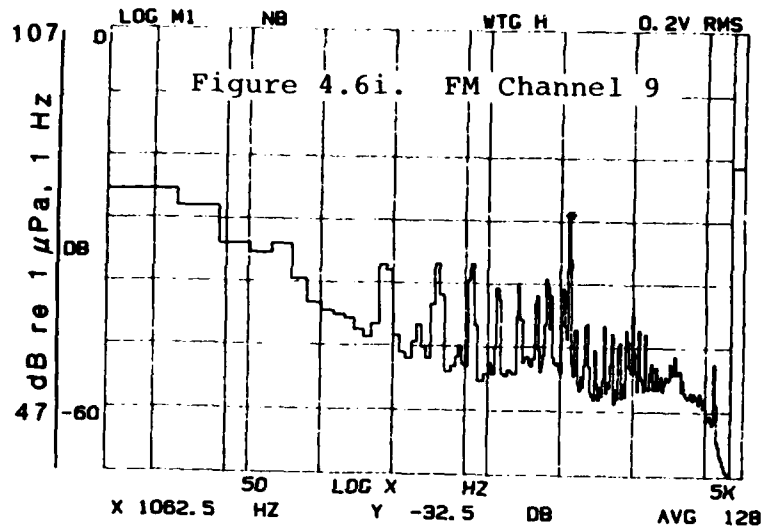

Figure 4.6i. FM Channel 9

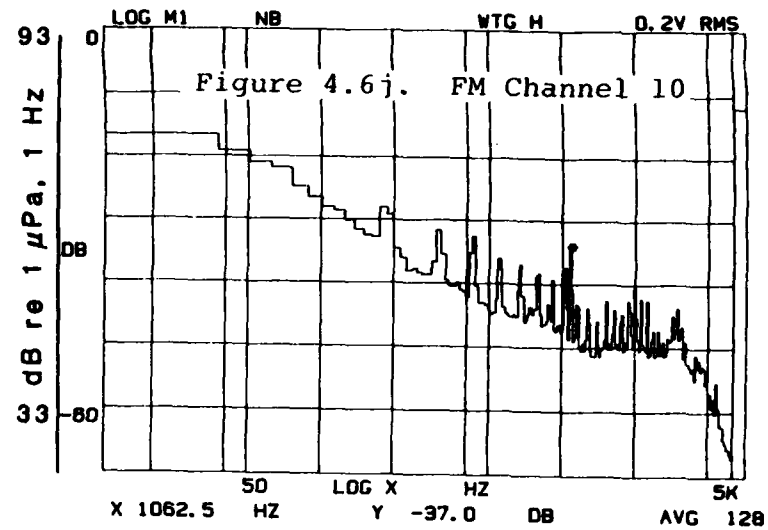

Figure 4.6j. FM Channel 10

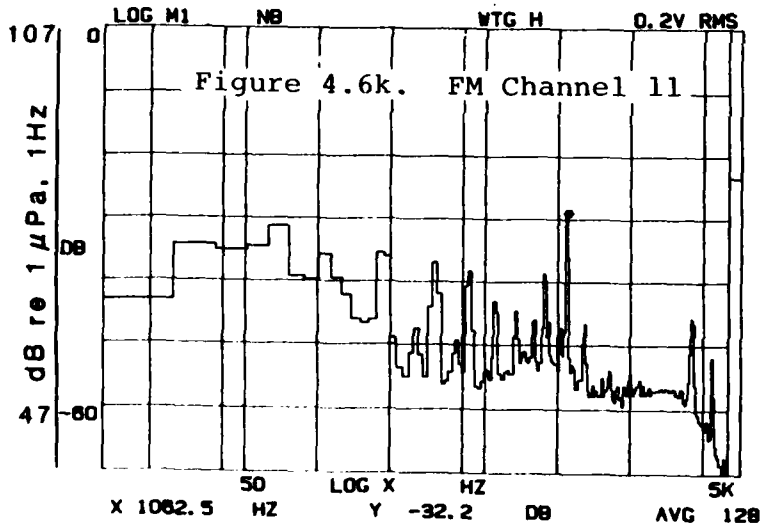

Figure 4.6k. FM Channel 11

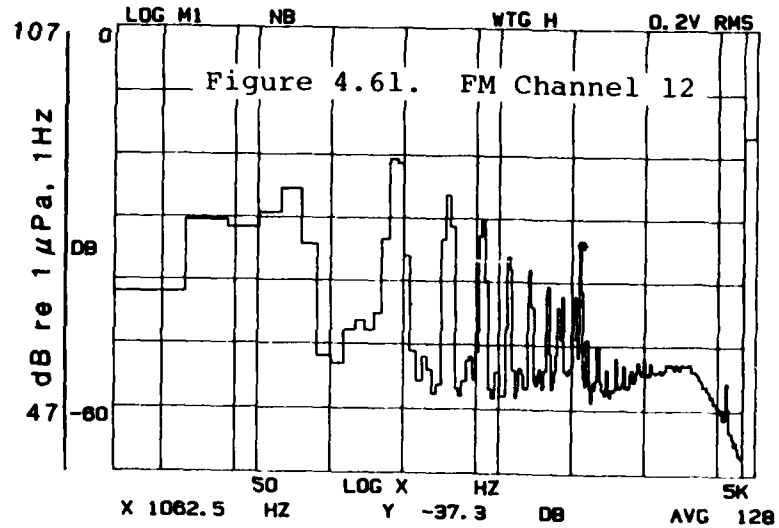

Figure 4.6l. FM Channel 12

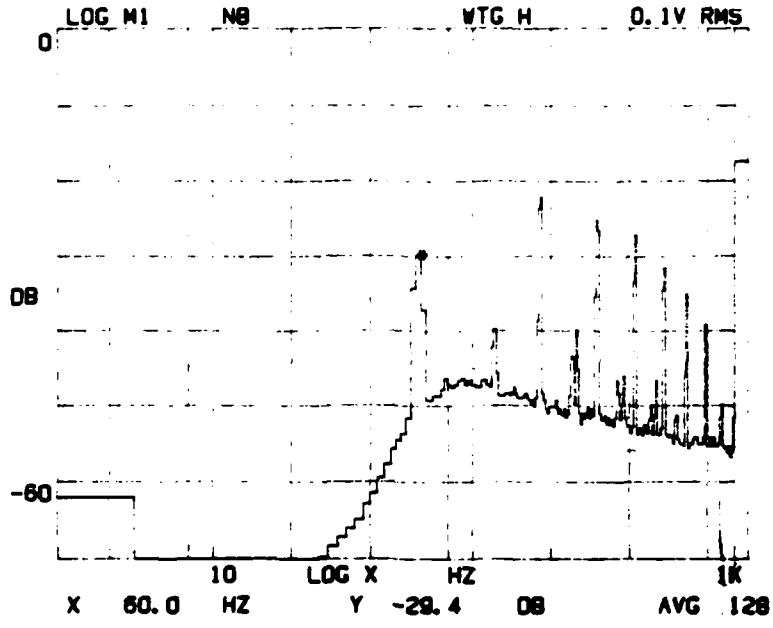

Figure 4.7a. Average 1K Spectra (N=128) of a Quiet Period on Day 16 at 00:24:50, FM Channel 3, 2.5 Hz Resolution, Kronhite: 80 Hz - 20 kHz

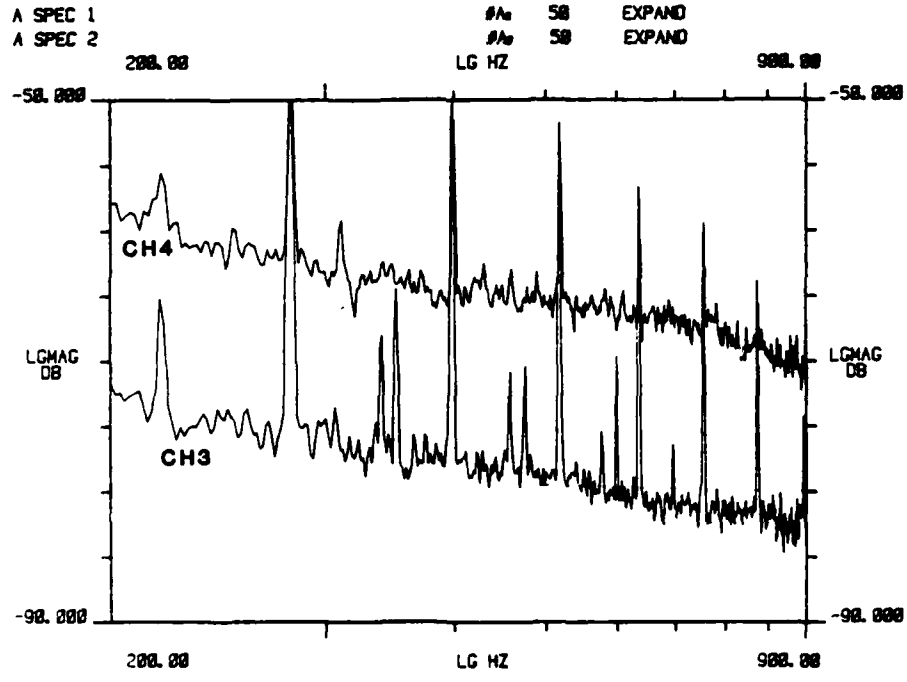

Figure 4.7b. Average 100-900 Hz Spectra of a Quiet Period on Day 16 at 00:24:50, FM Channel 3 and FM Channel 4, 1.5 Hz Resolution

generator lines although they are not as energetic. The 100-Hz level from Figure 4.7a is about 62 dB re 1μPa. To correct the spectral levels shown on Figure 4.7b one need only add the hydrophone sensitivity and tape gain (135 dB for the horizontal phone and 121 dB for the vertical phone). The 100-Hz level for the horizontal and vertical phone in Figure 4.7b is 63 dB re 1μPa.

4.6 Strum

In Mellen's survey of this data he rejected the horizontal hydrophone data to avoid the problems of cable flutter (strum) because strum "creates a problem with the limited dynamic range of the analog recorder." The vertical array being weighted by the length of the array will suffer less from strum than the horizontal phones. While this may be a potential hazard with the horizontal hydrophone data it is not a frequent problem nor an undetectable problem. In most cases the strum is within the dynamic range of the recorder and is only an inconvenience that can be easily filtered out. The unfiltered time series for horizontal hydrophones 1 and 24 (Figures 4.8a and 4.8c) are compared with the 30-m vertical hydrophone (Figure 4.8b) at 04:03:00 on Day 15. The vertical phone suffers no noticeable strum; on hydrophone 1 there is a .5V peak-to-peak variation induced by the strum and on hydrophone 24 a 1V peak-to-peak variation. All the hydrophones are within the 3V peak-to-peak voltage that will be linearly recorded. We searched the data tapes to find a case where the strum exceeded the dynamic range and found FM channel 5, Figure 4.8d, on Day 20 at 20:25. The time series shows nonlinear response and the loud periodic clanging noise which was obviously artificial was not observed on any other channel. The 9-Hz level is 147 dB re 1μPa and the 100-Hz level, influenced by clipped data is

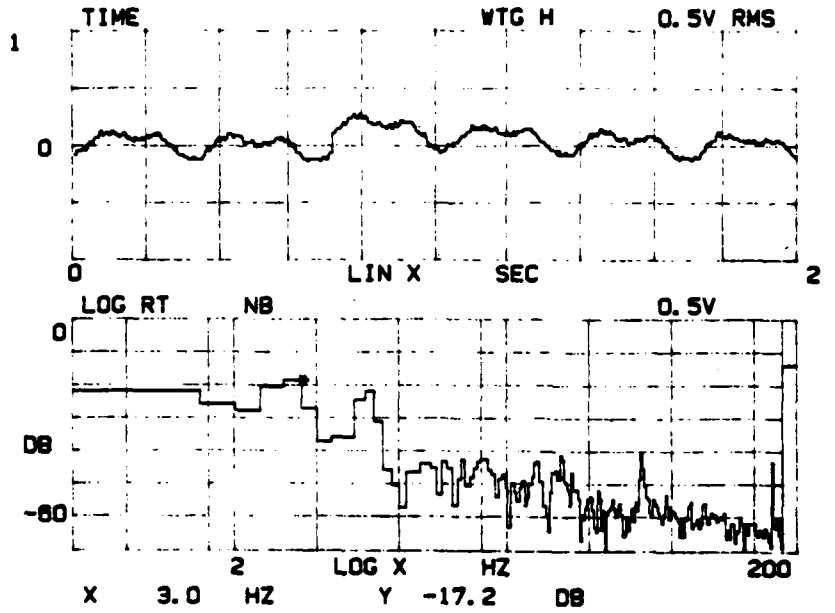

Figure 4.8a. Strum Time Series of 2 Seconds on Day 15 at 04:03:00, FM Channel 1, No Filter

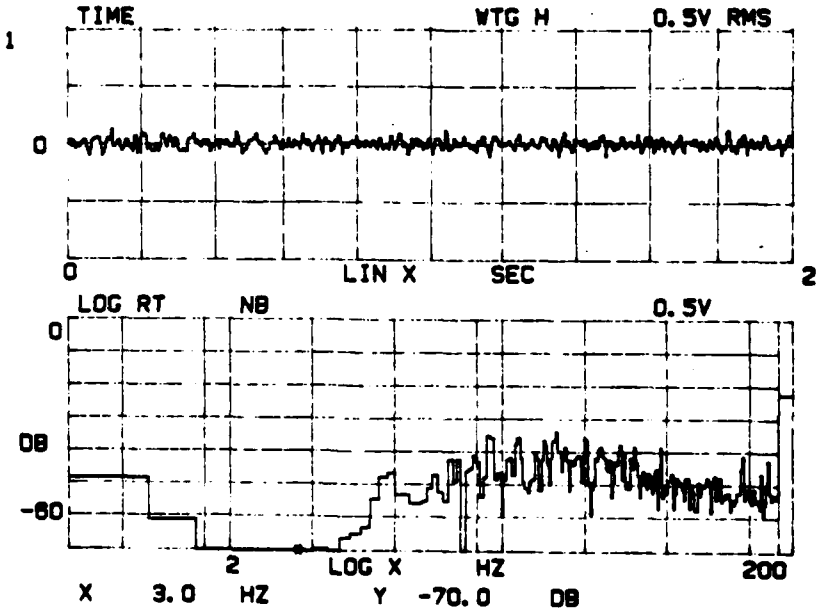

Figure 4.8b. Strum Time Series of 2 Seconds on Day 15 at 04:03:00, FM Channel 2, No Filter

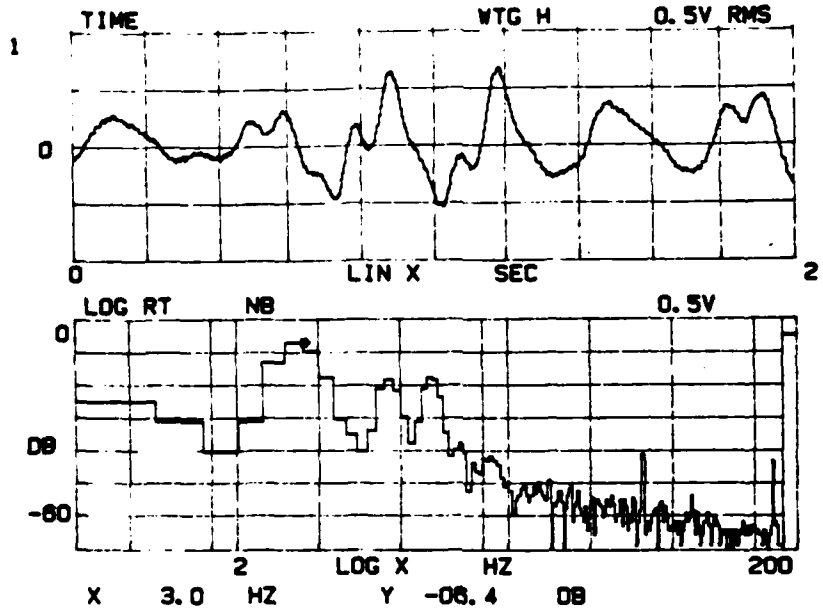

Figure 4.8c. Strum Time Series of 2 Seconds on Day 15 at 04:03:00, FM Channel 9, No Filter

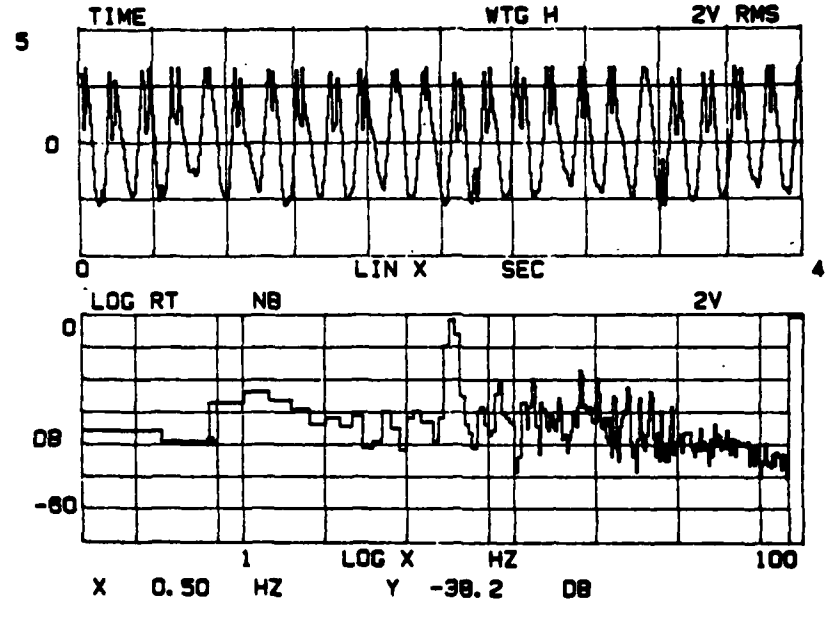

Figure 4.8d. Strum Time Series of 4 Seconds on Day 16 at 2025, FM Channel 5, No Filter

100 dB re 1 μPa. Thus excessive strum can be detected and avoided. The more "normal" strum illustrated in Figure 4.8a does not contaminate the higher frequencies but it can mask the time series signature of the noise events, thus a Kronhite filter was included to attenuate the strum signature.

Section 5
CHARACTERISTIC SIGNATURES

This section categorizes the types of noises heard on the analog tapes. We distinguish between ambient noise and manmade noise. We first describe the known manmade noises and then discuss the ice noises.

5.1 Airgun Noise

In this exercise an airgun was located at a range of 430 meters and bearing of 175 degrees from the apex phone, as illustrated in Figure 3.1. It operated every twenty minutes on the hour throughout much of the experiment, but was sometimes down for repairs and sometimes operated more often.

The airgun noise is a very distinctive, loud sound that dies much like the rumble of thunder. It can be heard on all channels.

Figure 5.1a shows a 20-second time series of the airgun on FM channel 1 (hydrophone 1). The initial burst is followed by bottom-interacting paths about 5 seconds later. The entire event lasts approximately 8 seconds. Figure 5.1b (a 1-KHz full scale average of 64 spectra, approximately 26 seconds, during the airgun signature) shows the peak frequency of the airgun to be 20 Hz.

5.2 Shot Noise

There were two types of shot experiments, refraction and reverberation. Refraction shots were set at various distances from the camp to measure the arrival structure of

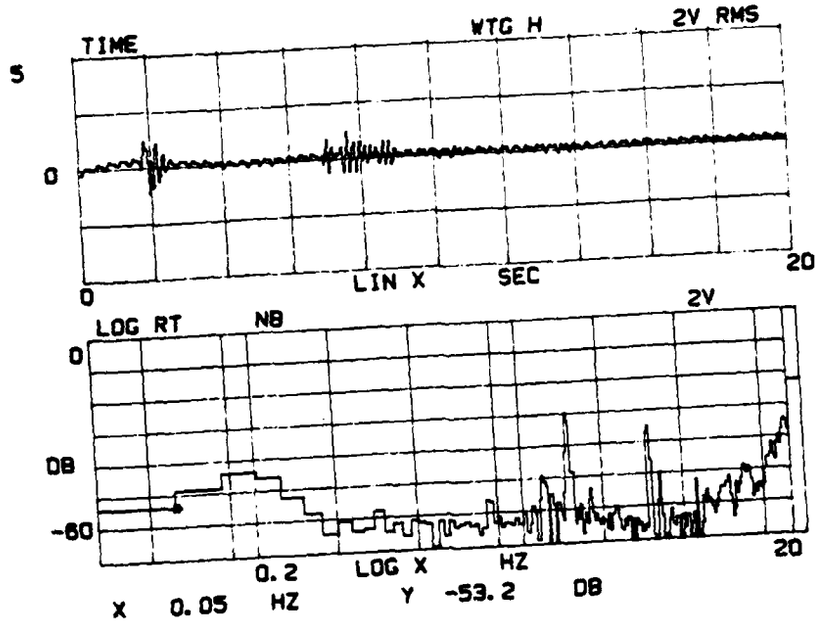

Figure 5.1a. Sample of a 20-sec Airgun Event on Day 15 at 04:00:00, FM Channel 1, No Filter

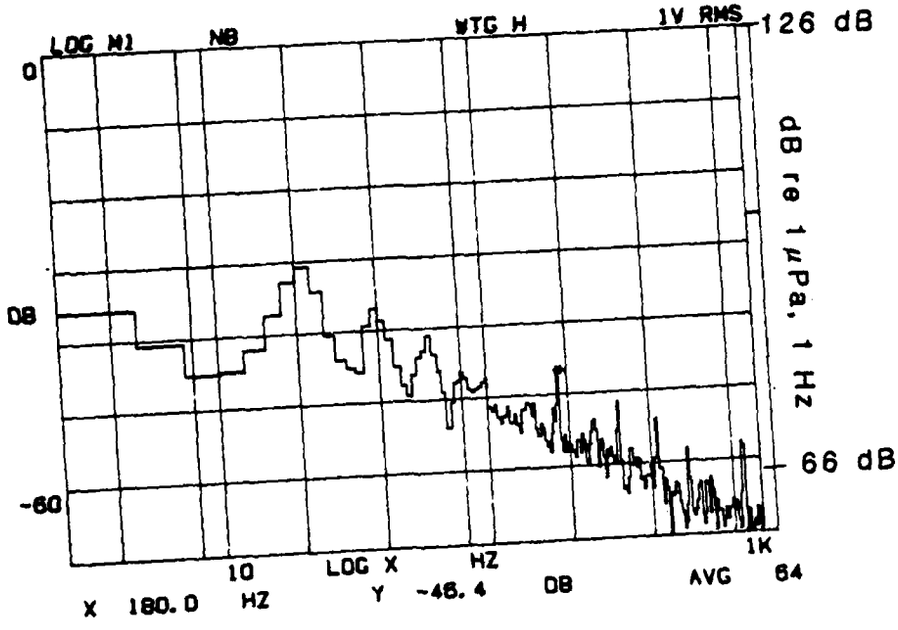

Figure 5.1b. Average 1K Spectra (N=64) of an Airgun Event on Day 15 at 00:20:05, FM Channel 1, Kronhite: 0-20K Hz

energy propagating through the sea floor. Reverberation shots were set near camp to study the basin reverberation characteristics. The shot noises lasted longer than the airgun and overloaded all of the hydrophones.

A 55-lb shot set on Day 15, 20 km from the camp, is illustrated on FM channel 1 (hydrophone 5) at 17:59:58 in Figure 5.2a in an 80-msec time series. This entire event, which lasted 60 seconds, is illustrated in Figure 5.2b. (The change in level in the time series between Figures 5.2a and 5.2b is due to the anti-aliasing filter in the SD345. The 80-second sample corresponds to a 5-Hz spectra so all frequencies above 5 Hz are filtered out, effectively reducing the voltage.)

A 880-lb reverberation shot set on Day 16 at 00:00:07, 5 km from the camp, is illustrated on FM channel 3 (strapped hydrophone) at 00:02:14; this event lasted 3 to 5 minutes.

5.3 3.5-kHz Projector

A 3.5-kHz projector (echo sounder) was placed in a hole near the airgun (see Figure 3.1). Although 3.5 kHz is beyond the 2500-Hz bandwidth of the recording system the echo sounder was loud enough to be recorded by the tape. The echo sounder makes a clicking noise every 2 seconds and can be heard on all the hydrophones.

The signature varied somewhat but a typical time series is illustrated in Figure 5.3a for 20 ms and 5.3b for 4 ms to expand the pulse. Figure 5.3c shows a typical spectra contaminated by the echo sounder on a 5k-scale. The 3500-Hz peak is clearly evident in the spectra and effects the nearby frequency bins.

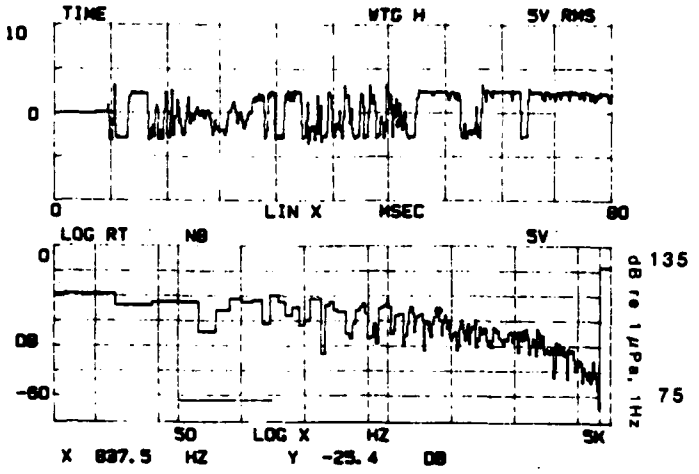

Figure 5.2a

Sample (80 msec) of a 55# Shot at 20 km on Day 15 at 17:59:58, FM Channel 1, No Filter

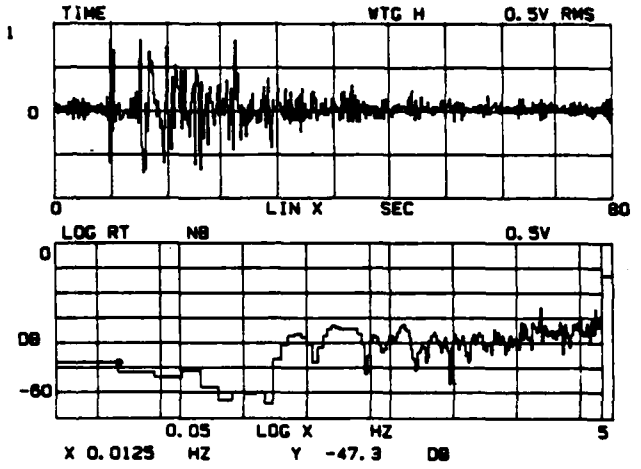

Figure 5.2b

Sample (80 sec) of a 55# Shot at 20 km on Day 15 at 17:59:58, FM Channel 1, No Filter

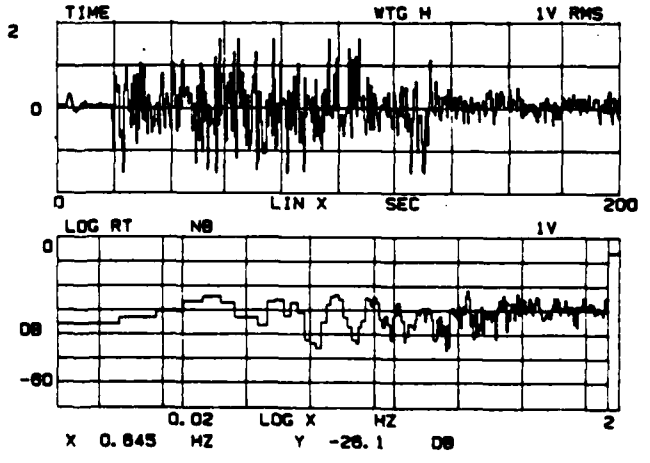

Figure 5.2c

Sample (200 sec) of a 880# Shot at 5 km on Day 16 at 00:02:14, FM Channel 3, No Filter

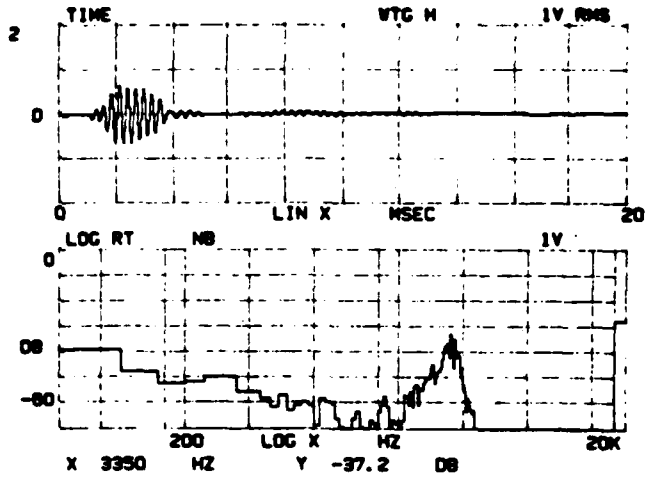

Figure 5.3a

Sample (20 msec) of 3.5K Projector on Day 15 at 17:16:01, FM Channel 1, No Filter

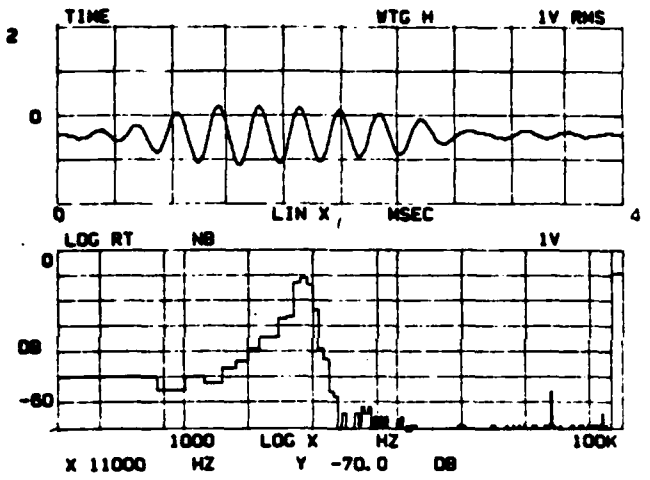

Figure 5.3b

Sample (4 msec) of 3.5K Projector on Day 15 at 17:16:01, FM Channel 1, No Filter

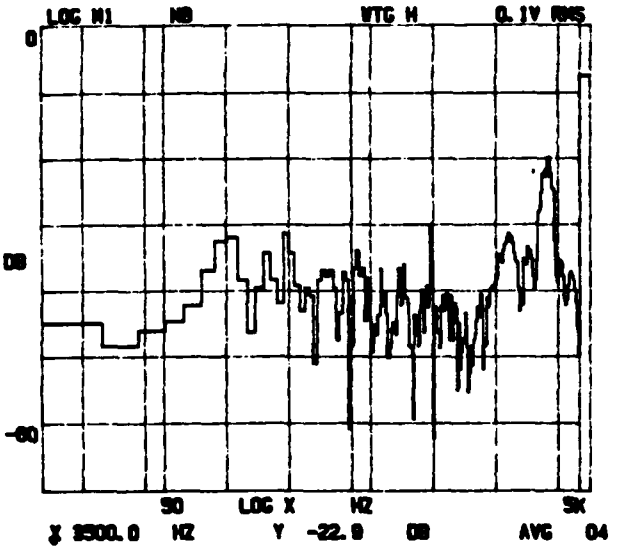

Figure 5.3c

Average 5K Spectra (N=04) of a 3.5K Projector on Day 17 at 07:45:00, FM Channel 1, No Filter

Figure 5.3d through 5.3n illustrate the echo sounder signature of the same pulse on all the hydrophones on Day 16 at 03:25:23. The echo sounder was placed near hydrophone 13 (see Figure 3.1). All the FM channels, except Ch 9 were near the middle of the camp. The signal is distorted by background noise on FM Ch 5 and FM Ch 9. The vertical phones all show anomalous behavior which has been attributed to overloading the recording system. Notice the maximum horizontal voltage is 1V peak-to-peak whereas the vertical displays 5V peak to peak. The low frequency tail, as a feature on the vertical phones, has been attributed to the recovery time of the electronics. It is possible that the increased gain on the vertical system caused the recorder to overload on these channels.

5.4 Helicopter Noise

At times the log indicates a helicopter in the vicinity of the camp. The noises heard on the hydrophones sound like a helicopter on land. The helicopter noise is due to the low pressure vortices shed by the blades. These vortices generate noise when the helix formed by the blade vortices impacts on the ground.

The spectra shown in Figure 5.4 is an unfiltered 5K 64-average (5.12-second average) of helicopter noise. The peak frequency is about 200 Hz and rolls off 40 dB/decade above 200 Hz.

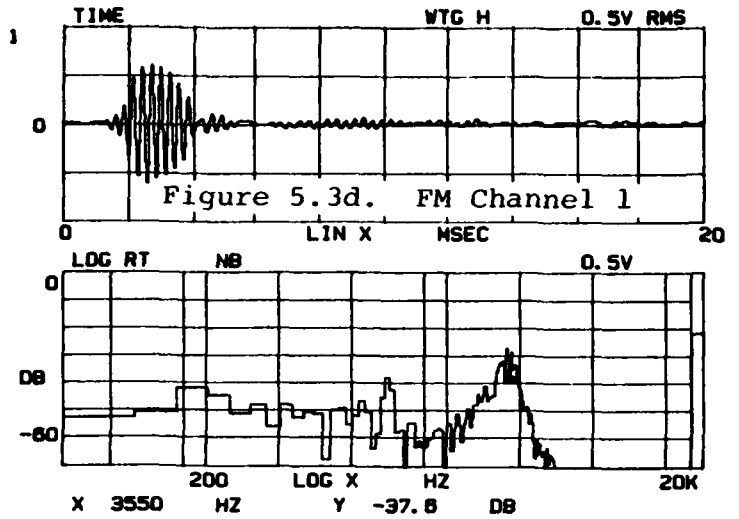

Figure 5.3d. FM Channel 1

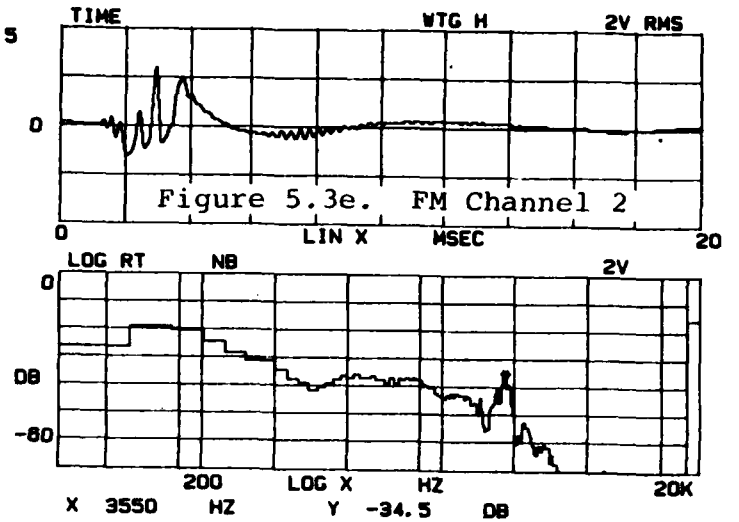

Figure 5.3e. FM Channel 2

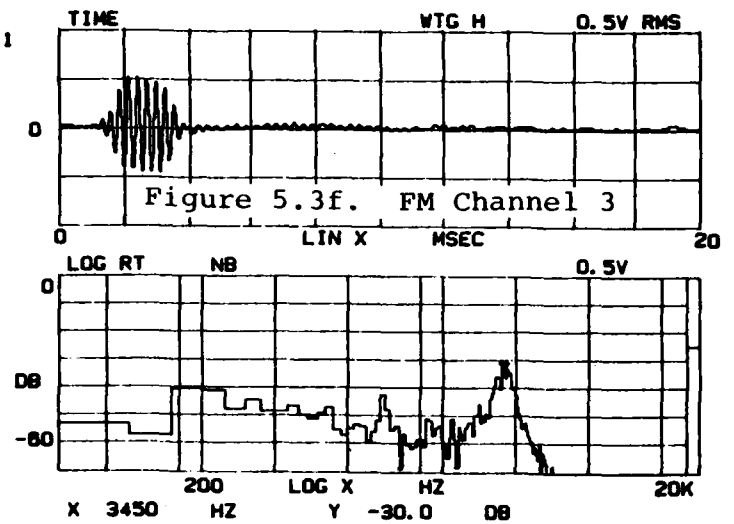

Figure 5.3f. FM Channel 3

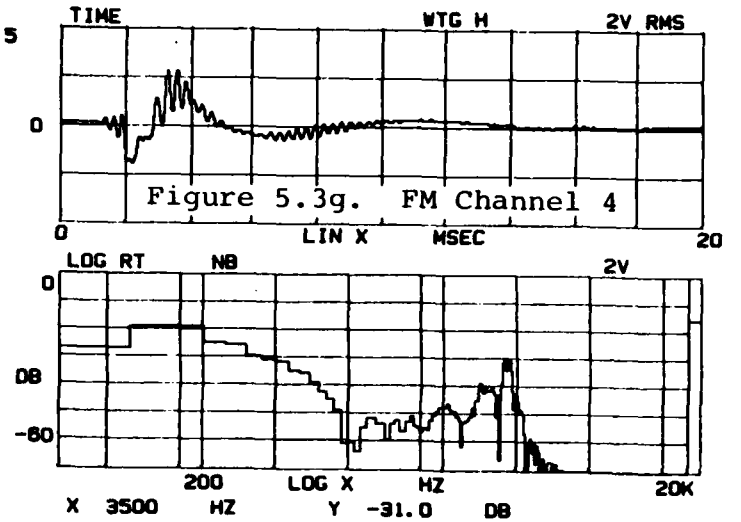

Figure 5.3g. FM Channel 4

Figure 5.3d-n. Sample (20 msec) of 3.5K Projector on Day 16 at 03:25:23 for Various FM Channels, Kronhite: 100-20K Hz

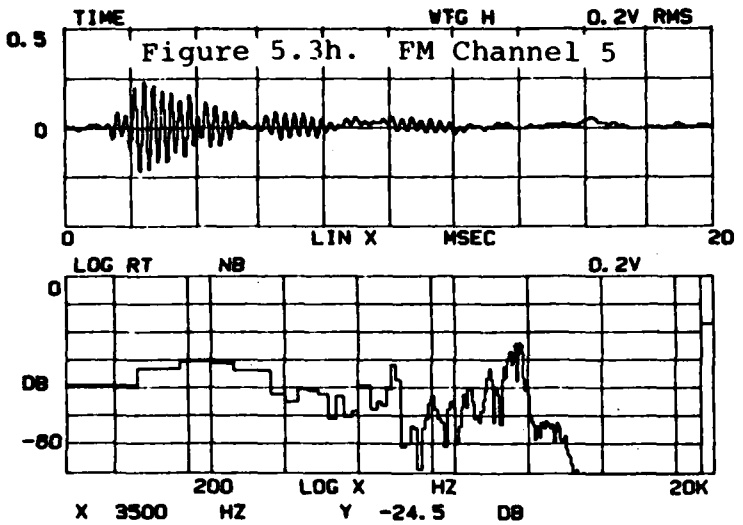

Figure 5.3h. FM Channel 5

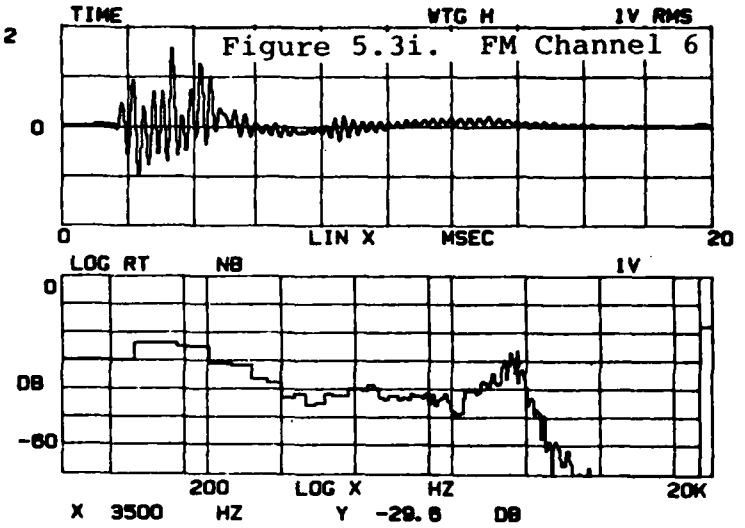

Figure 5.3i. FM Channel 6

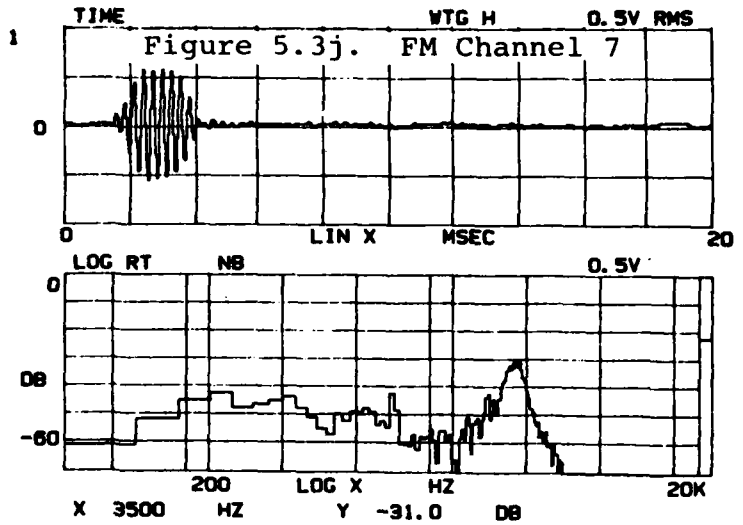

Figure 5.3j. FM Channel 7

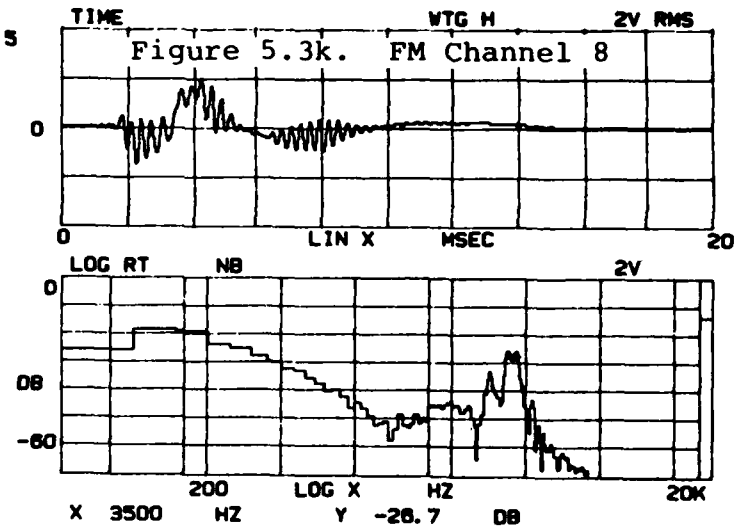

Figure 5.3k. FM Channel 8

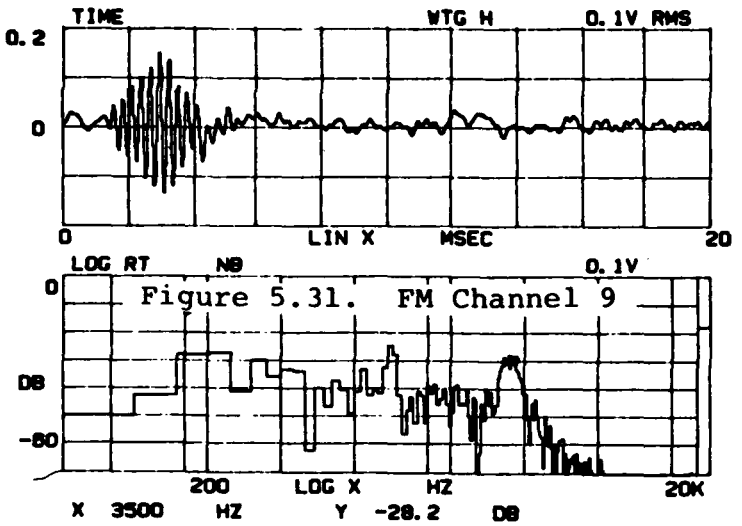

Figure 5.31. FM Channel 9

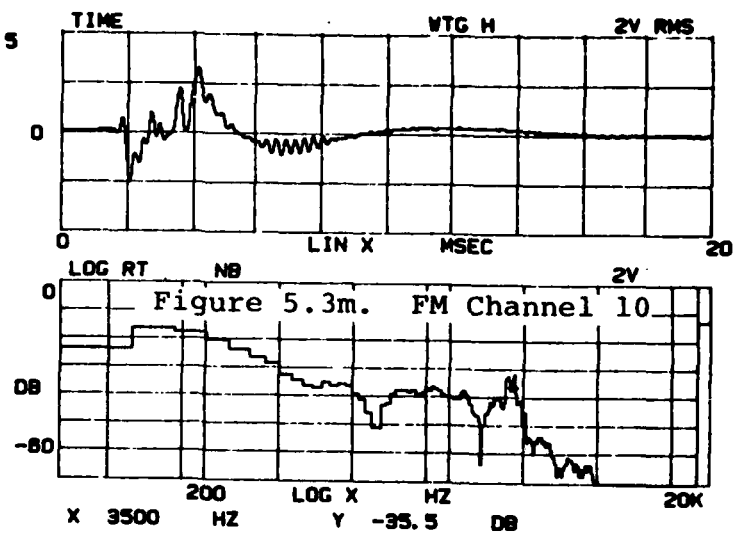

Figure 5.3m. FM Channel 10

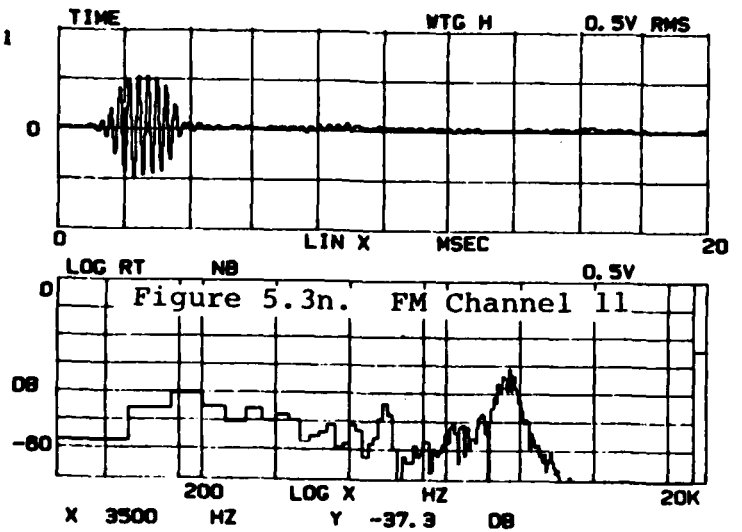

Figure 5.3n. FM Channel 11

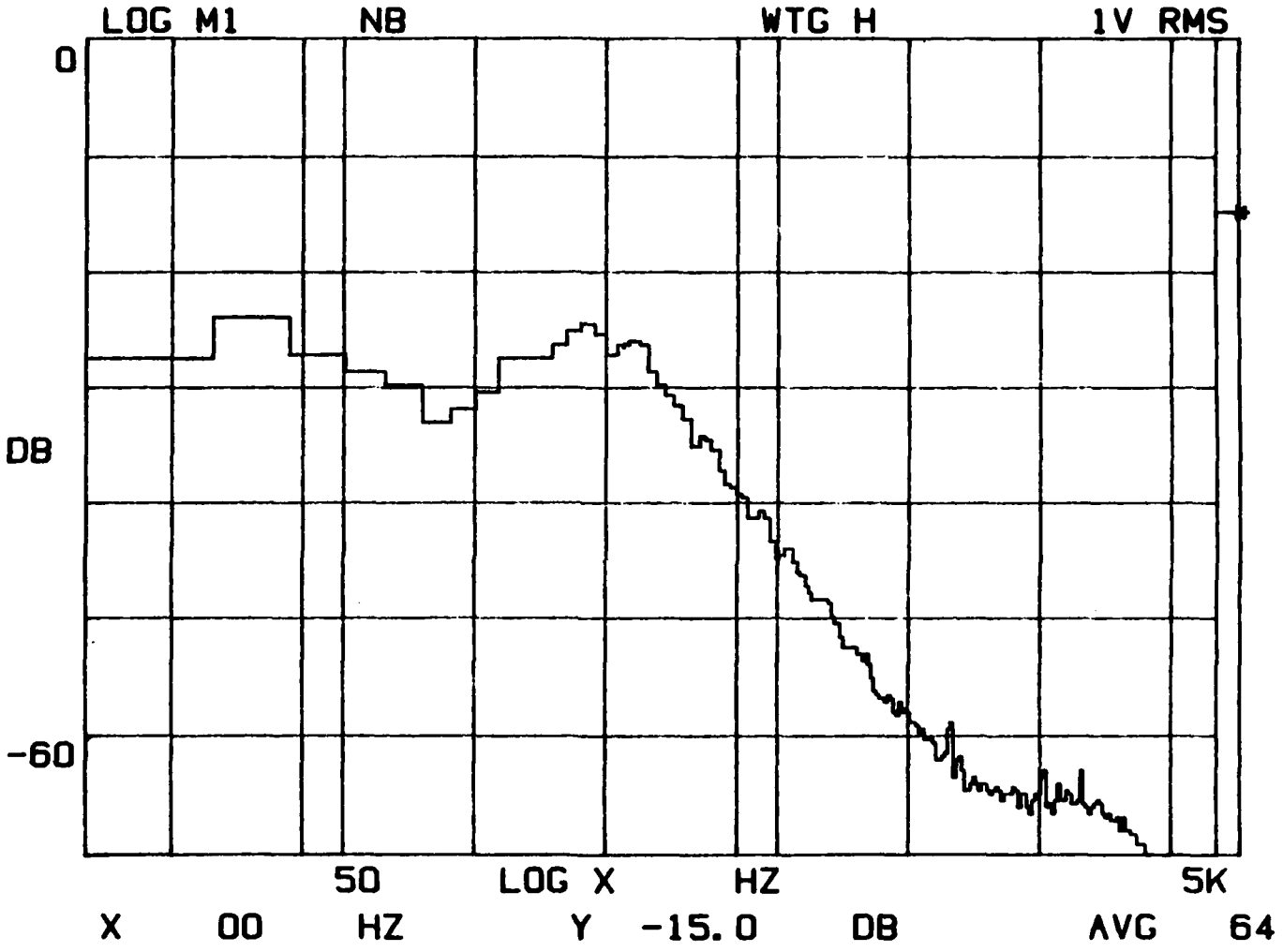

Figure 5.4. Average 5K Spectra (N=64) of Helicopter Noise on Day 15 at 13:26:58, FM Channel 2, No Filter

5.5 Snowmobile Noise

Snowmobile noise is distinguished by the motor hum and the scratching on the ice. Figure 5.5a illustrates a 4-second time series. Figure 5.5b shows a spectra before the snowmobile event and Figure 5.5c illustrates a spectra during the snowmobile event. All the frequencies greater than 50 Hz are affected and no clear peak frequency is obvious.

5.6 Walking Noise

Walking noises can be heard on the hydrophone as they would be heard on the ice. The crunching of snow and ice beneath each footstep make it easy to distinguish walking noises. These noises are very common on the hydrophones located closer to the center of camp activity, especially the vertical array. Fortunately, one can avoid the walking noise contamination by listening to other hydrophones.

Figure 5.6a shows a time series of a walking event. Notice that the events are about 280-msec apart indicating the walker is taking approximately 3 steps per second.

The next few figures demonstrate the changes in the spectra during the walking event. Figure 5.6b is a spectra before the walking begins. Figure 5.6c is a few seconds into the event, notice the increase in levels between 600 Hz and 3000 Hz. A few seconds later, Figure 5.6d, the frequencies between 300 Hz and 600 Hz are also affected.

Figures 5.6e through 5.6p illustrate a walking event as recorded by all the hydrophones and filtered below 80 Hz. These figures show a 400-ms time series that was held

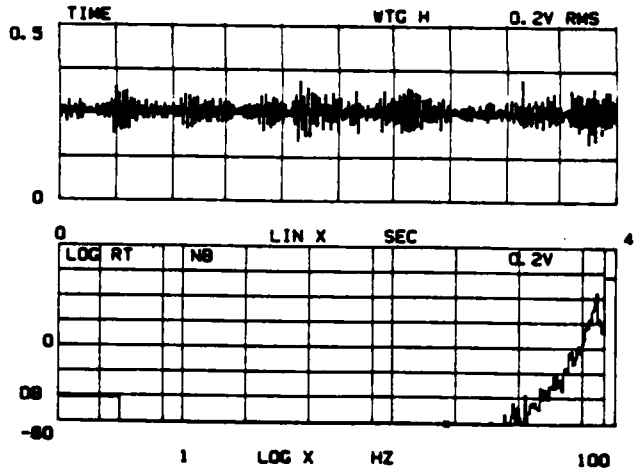

Figure 5.5a

Sample (4 sec) of Snowmobile Noise on Day 15 at 10:55:00, FM Channel 2, Kronhite: 100-20K Hz

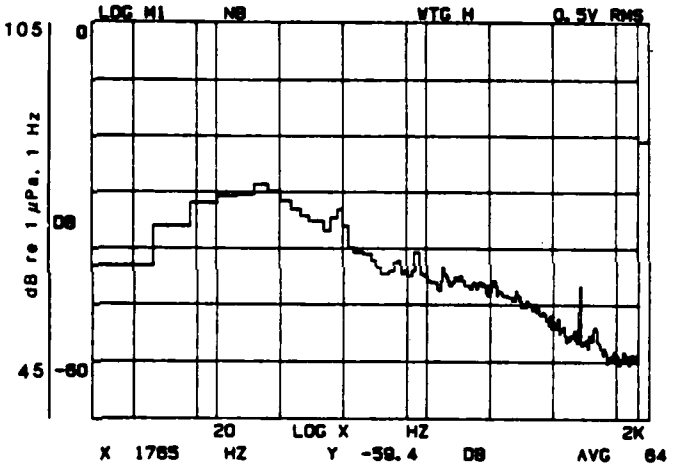

Figure 5.5b

Average 2K Spectra (N=64) Before Snowmobile Noise is Detected on Day 15 at 10:52:10, FM Channel 2, Kronhite: 0-20K Hz

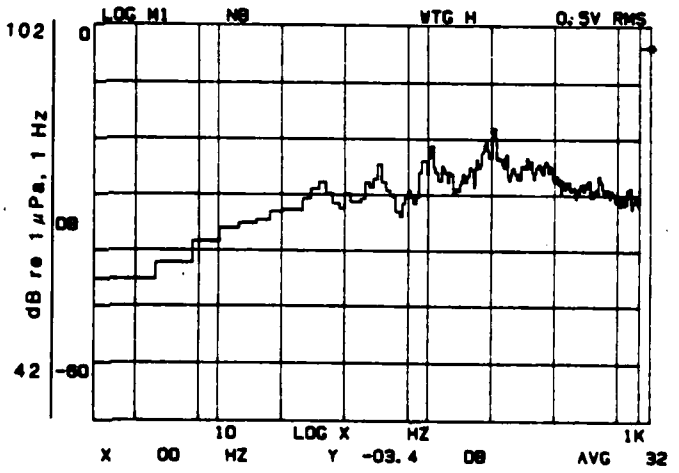

Figure 5.5c

Average 2K Spectra (N=64) During Snowmobile Noise on Day 15 at 10:55:10, FM Channel 2, Kronhite: 0-20K Hz

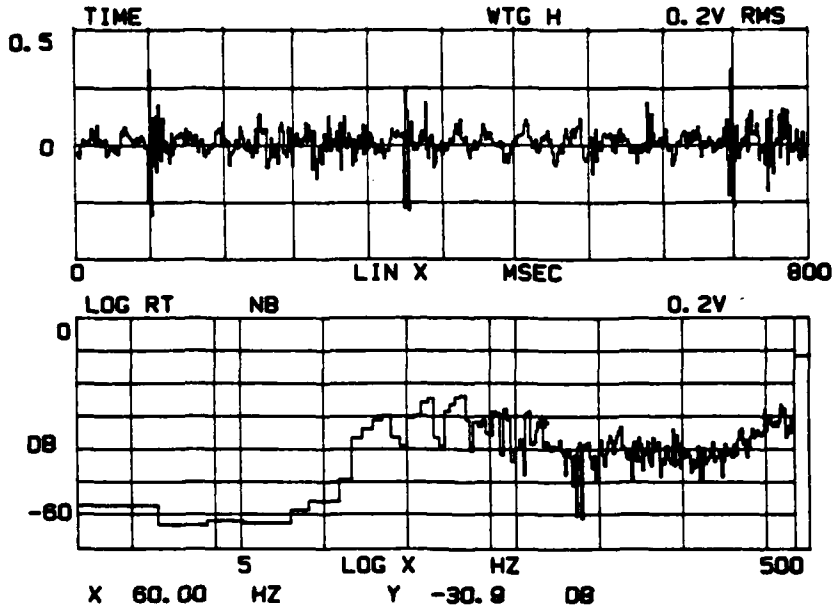

Figure 5.6a. Sample (800 msec) of a Walking Event on Day 15 at 04:57:10, FM Channel 2, Kronhite: 10-20K Hz

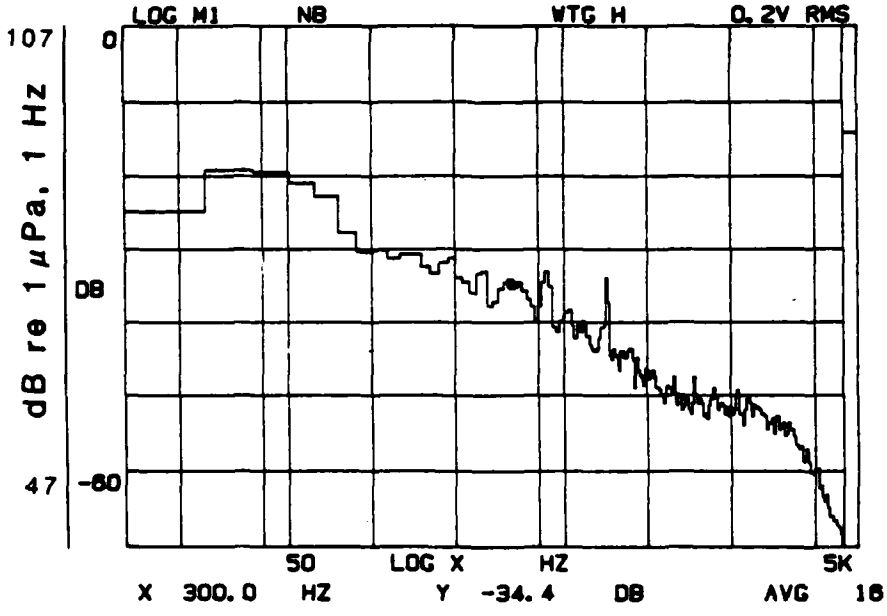

Figure 5.6b. Average 5K Spectra (N=16) Before Walking is Detected on Day 15 at 04:56:40, FM Channel 2, Kronhite: 10-20K Hz

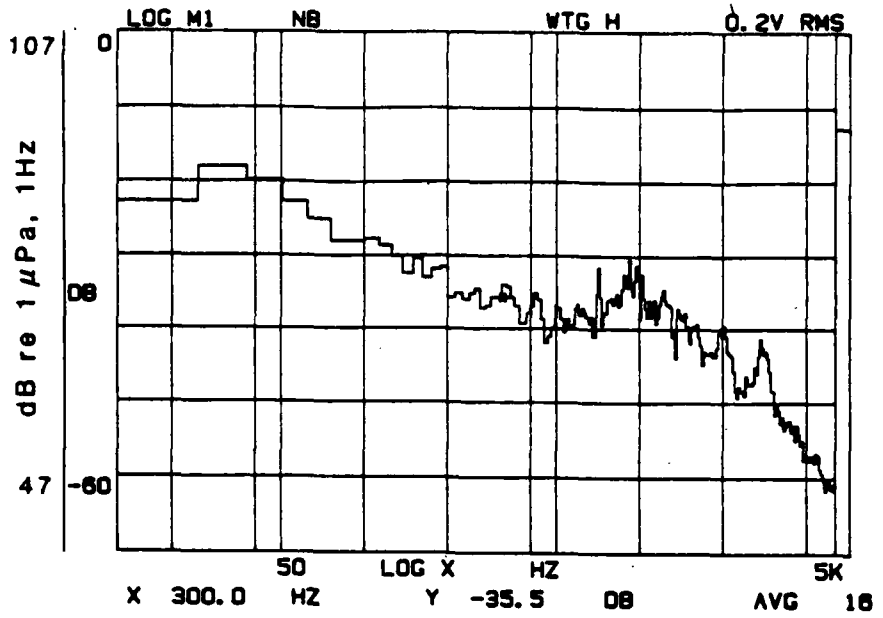

Figure 5.6c. Average 5K Spectra (N=16) of a Walking Event on Day 15 at 04:56:50, FM Channel 2, Kronhite: 10-20K

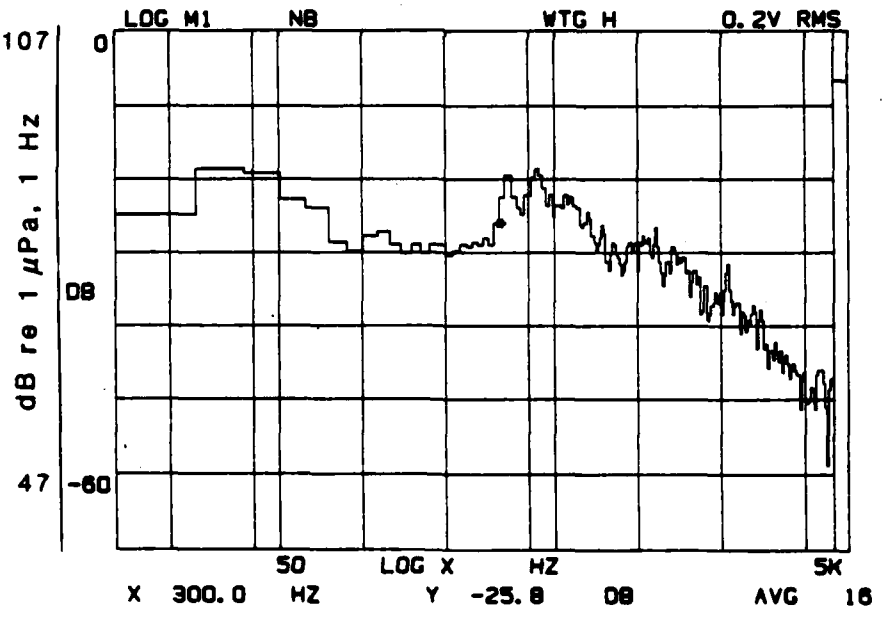

Figure 5.6d. Average 5K Spectra (N=16) of a Walking Event on Day 15 at 04:56:56, FM Channel 2, Kronhite: 10-20K

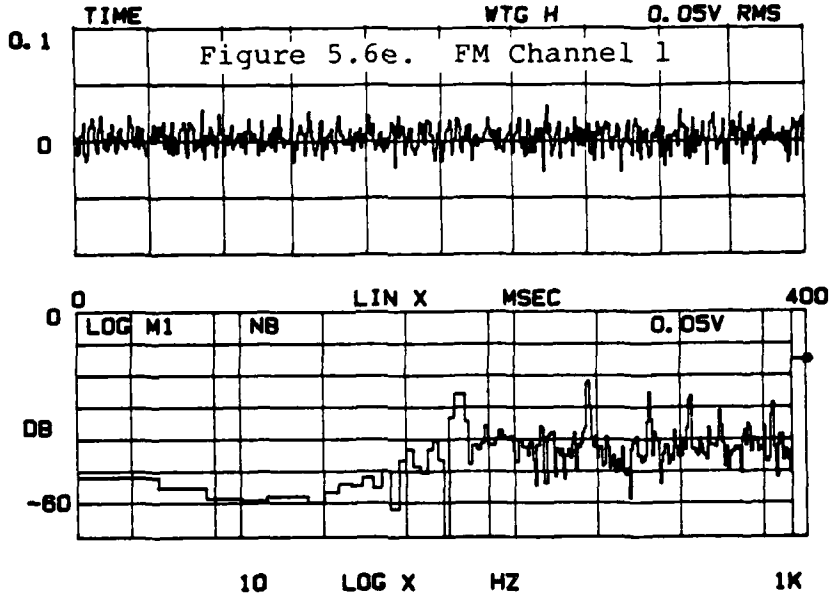

Figure 5.6e. FM Channel 1

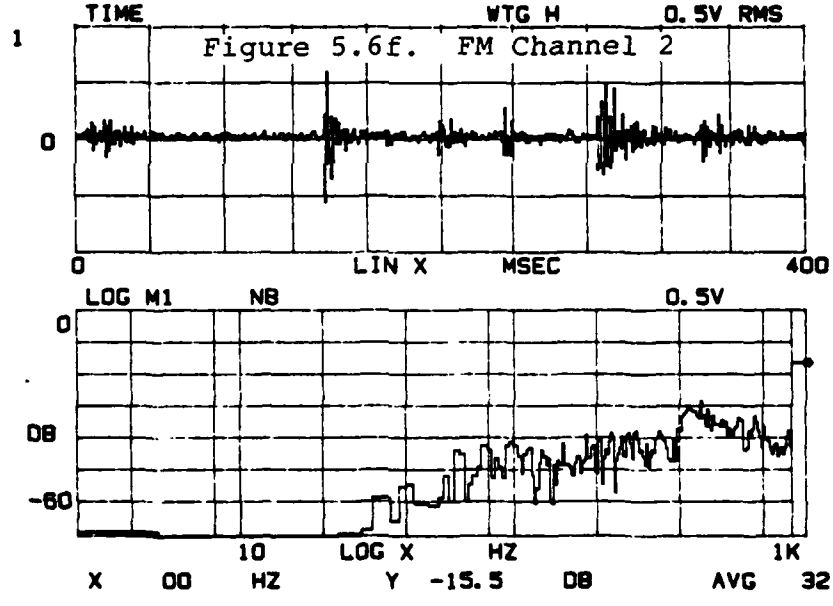

Figure 5.6f. FM Channel 2

Figures 5.6e-p. Sample (400 msec) for Various FM Channels when Walking Detected on Channel 2, on Day 15 at 04:56:57, Kronhite: 80-20K.

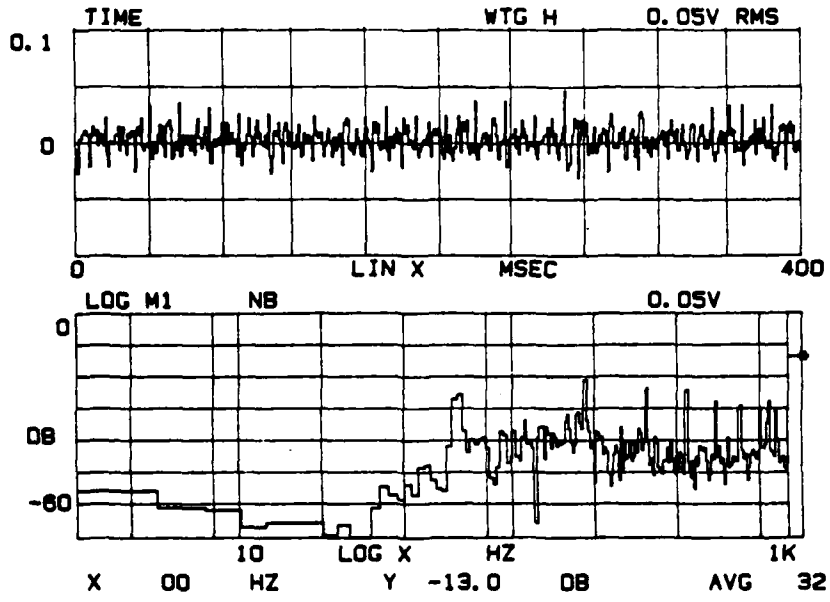

Figure 5.6g. FM Channel 3

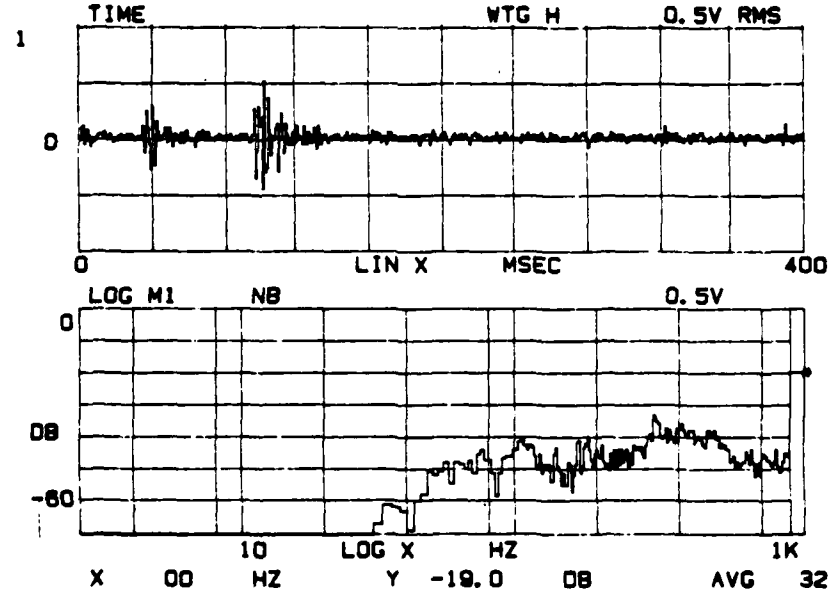

Figure 5.6h. FM Channel 4

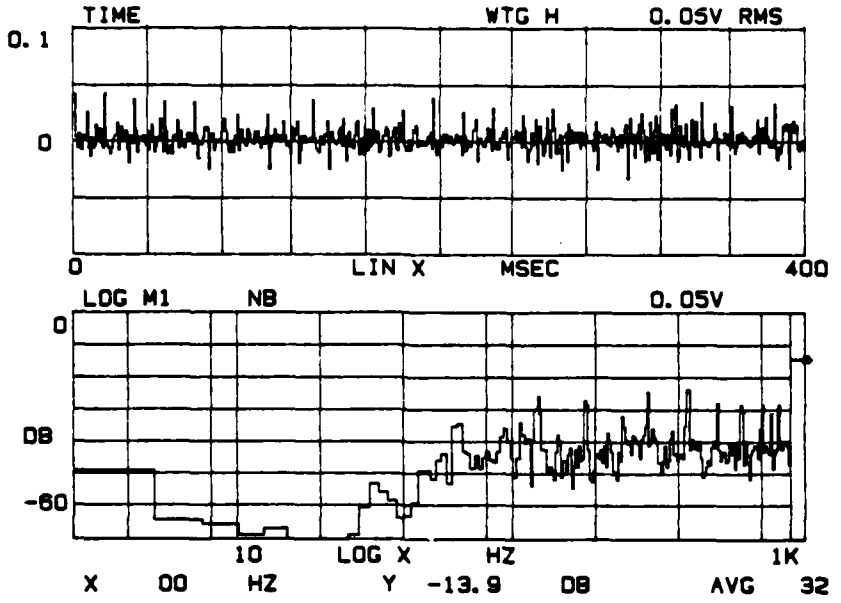

Figure 5.6i. FM Channel 5

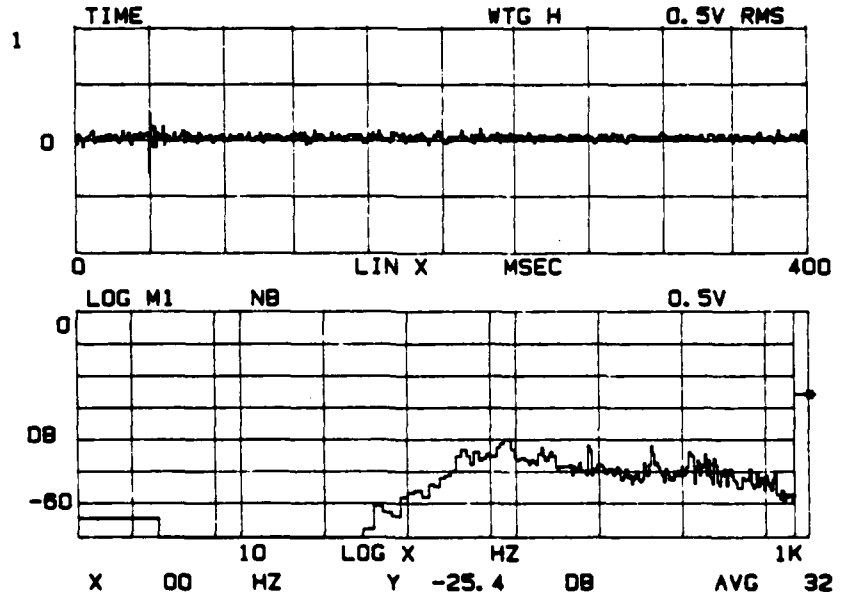

Figure 5.6j. FM Channel 6

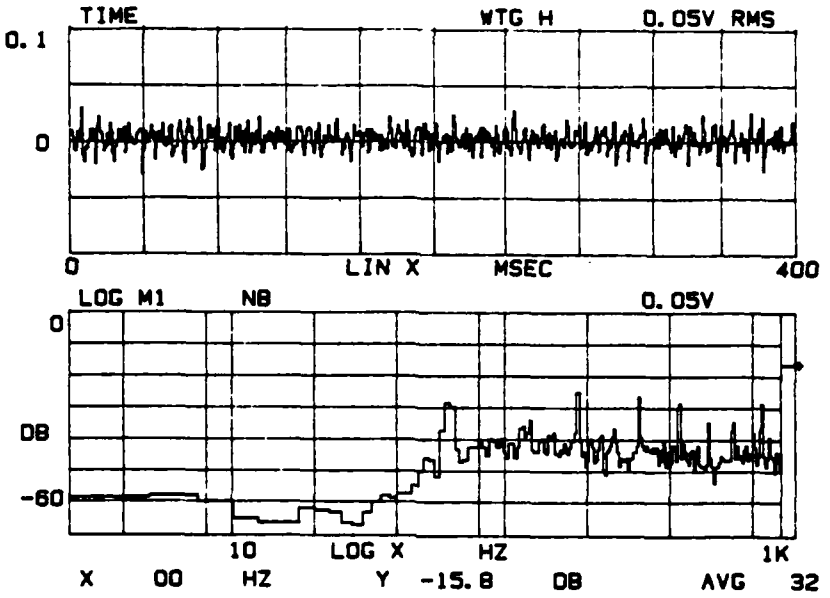

Figure 5.6k. FM Channel 7

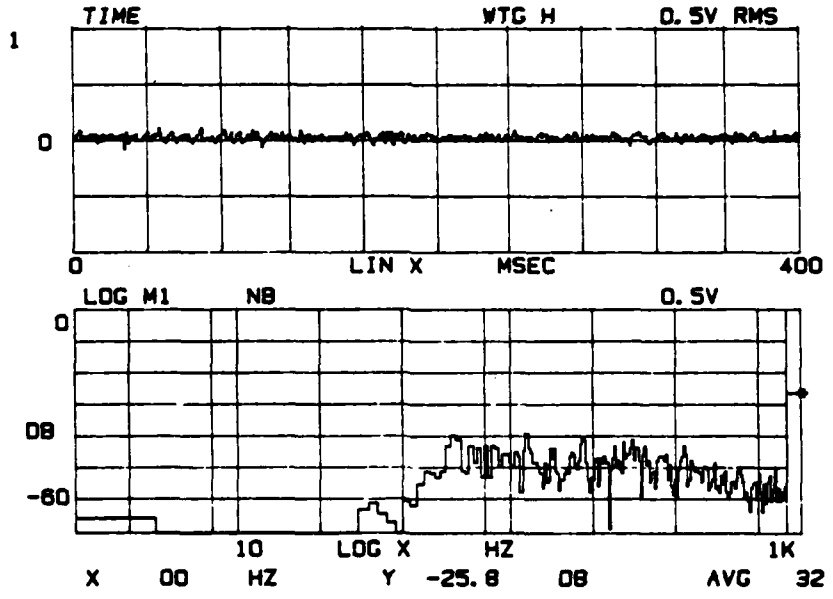

Figure 5.61. FM Channel 8

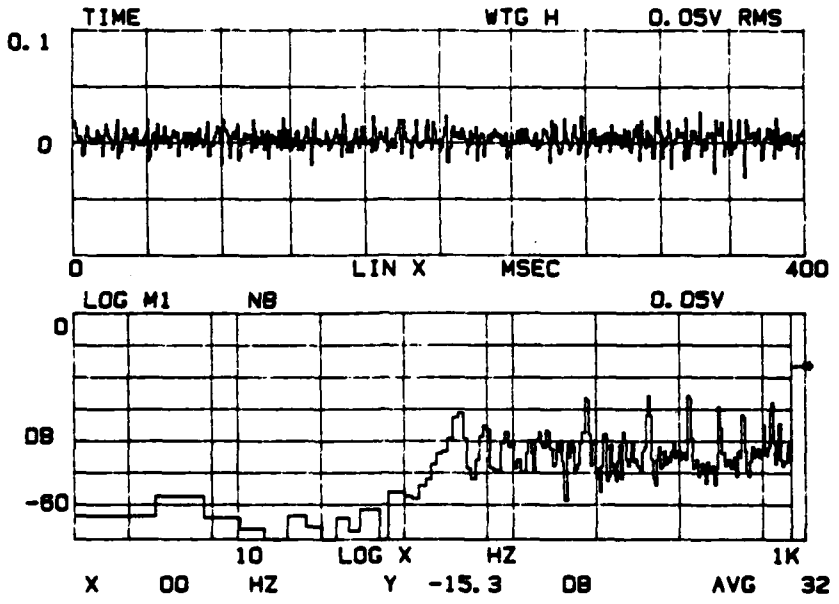

Figure 5.6m. FM Channel 9

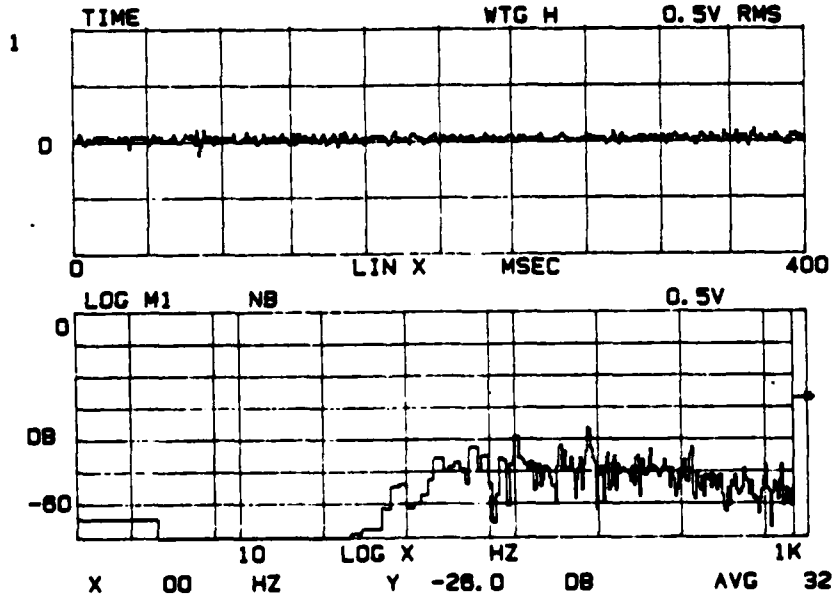

Figure 5.6n. FM Channel 10

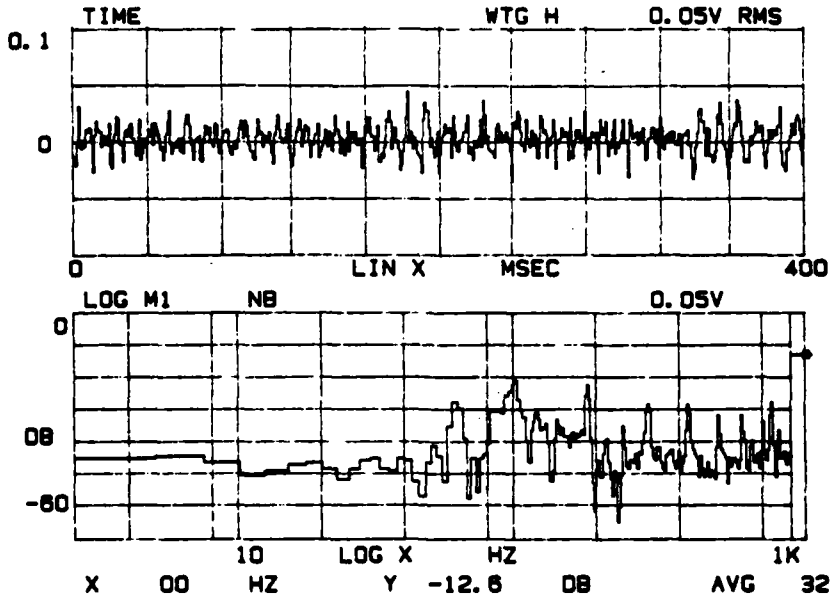

Figure 5.6o. FM Channel 11

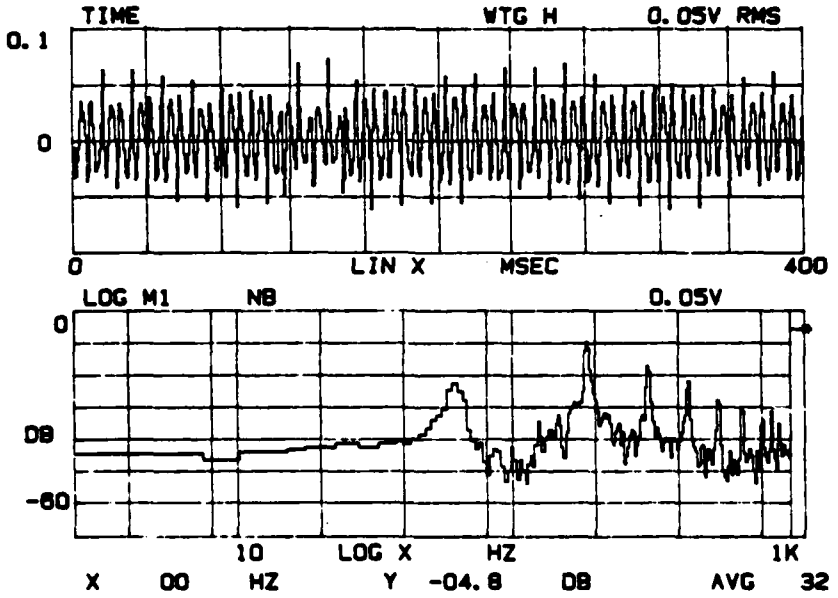

Figure 5.6p. FM Channel 12

at 04:56:57 on Day 15 and a 1-kHz spectra that began accumulating at 04:56:57 for 12.8 seconds, thus these spectra are not the instantaneous spectra used in previous figures. The event was found on FM channel 2, the 30m vertical phone, and sounded like someone walking towards the array. Part of the time series on this channel, Figure 5.6f, shows a 400-Hz level of -32 dB (78 dB re 1 μPa). The 400-Hz level on the 90m vertical phone, Figure 5.6h, is about 70 dB re 1 μPa. Spherical spreading from the 30m to 90m phone is approximately 9 dB which would account for this difference. The walking sound was more muffled on the 270m phone, Figure 5.6j, and didn't even become audible until 04:57:04. The 270m 400-Hz level was approximately 60 dB re 1 μPa. Spherical spreading from the 30 m to 270 m hydrophone is about 19 dB which would account for the difference between the 270m and 30m phones. The walking sound was barely heard on the 450m phone, Figure 5.6l and not at all on the 960m phone, Figure 5.6n. The only horizontal hydrophone on which the walking event could be heard was the apex phone, Figure 5.6e. The apex phone was closest (40m) to the vertical array. The walking event was very faint on the apex phone and could not be distinguished from the background noise until 04:57:04 through 04:57:10. The 400-Hz level on the apex phone is about 60 dB re 1 μPa.

5.7 Straf

Straf is a description of various noises heard on the ice. (The term straf was coined by Dyer and Stein from a reversal of the letters of the word, which they thought described the sound quite well). Thermal stress discussed in Section 2 is believed to be the underlying generating mechanism for straf. We expect straf to be due to the mode II ice cracking illustrated in Figure 2.8.

The duration of a straf event has been observed to vary from a few milliseconds to minutes. The peak frequency has been observed to vary from a 100 Hz to 500 Hz.

Straf was heard at various times on all the hydrophones and in most cases never on more than one hydrophone at the same time. In some instances straf was observed just prior to the airgun signature. On the vertical phones when we heard straf, we could also detect straf on the other vertical phones. The fact that straf is usually observed on only one hydrophone at a time is controversial. It might indicate straf is a very local event or that this is not real ambient noise. The continuation of this work will try to resolve this issue.

Figure 5.7a shows the time series of a quiet period on FM channel 1, the apex phone, right before a 20-msec straf event on this channel at 00:22:39 on Day 15, shown in Figure 5.7b. The straf event occurs abruptly in the middle of an otherwise quiet period. The peak frequency of the event is about 300 Hz as observed in the spectra in 5.7b. The peak-to-peak voltage before the event does not exceed .05V whereas it is almost .25V during the event. The 300-Hz level increases more than 15 dB. These spectra were filtered below 100 Hz. This event was not heard on any other channel.

Figure 5.7c illustrates a 200-ms straf event at 16:03 on Day 15 on the apex phone. It has a peak frequency in the 150-300 Hz region. The peak-to-peak level is 0.2V. This event was only heard on this channel.

Figure 5.7d shows the time series of a 500-ms straf event on the apex phone at 01:23:58 on Day 15. Notice the repetitive nature of this event which may be due to repeated

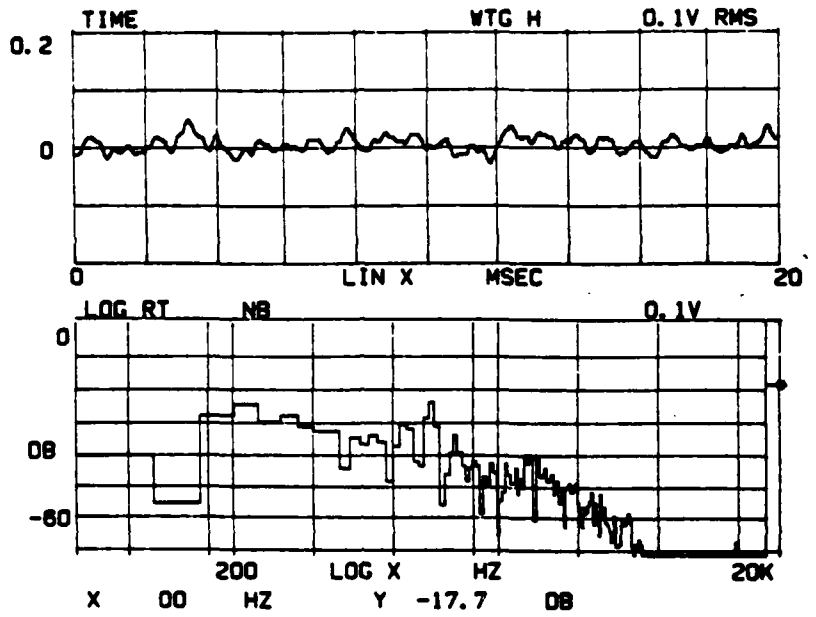

Figure 5.7a. Sample (20 msec) of Quiet Time Before Straf on Day 15 at 00:22:37, FM Channel 1, Kronhite: 100-20K Hz

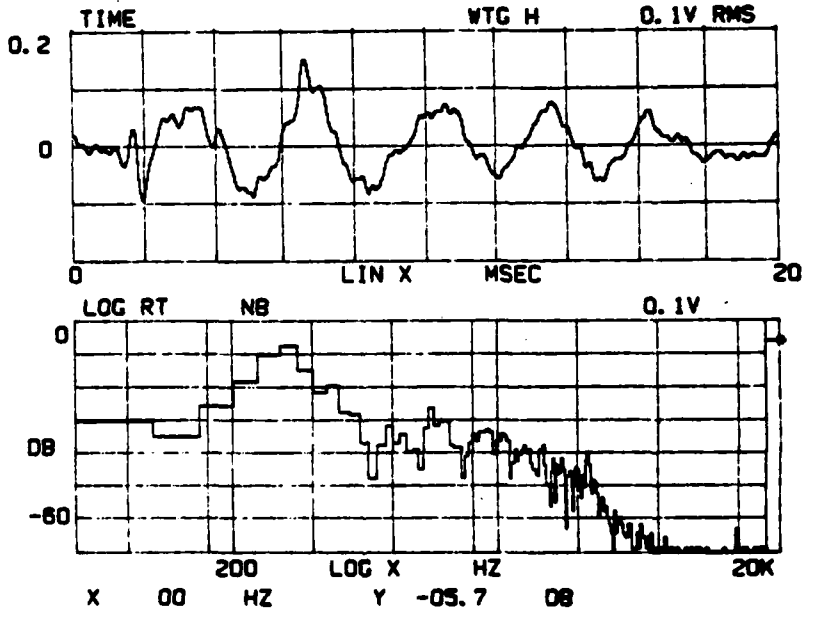

Figure 5.7b. Sample (20 msec) of Straf Event on Day 15 at 00:22:39, FM Channel 2, Kronhite: 100-20K Hz

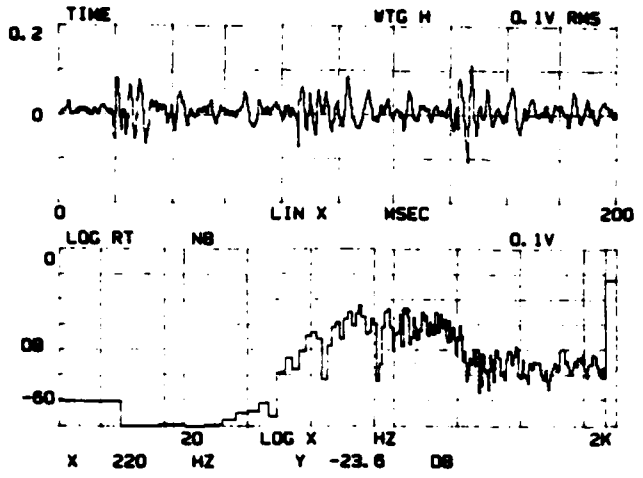

Figure 5.7c. 200-msec

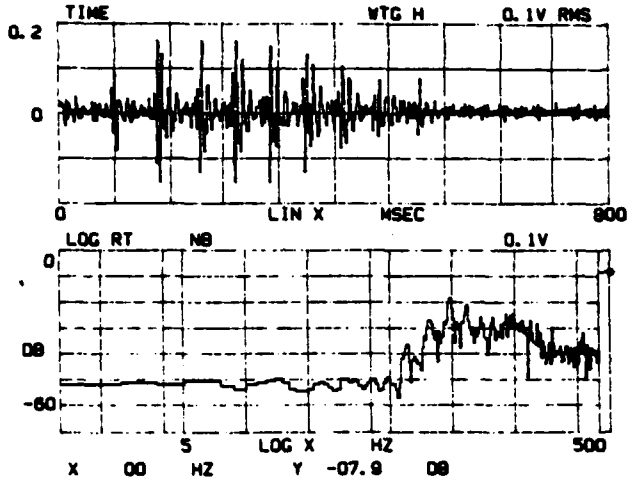

Figure 5.7d. 800-msec

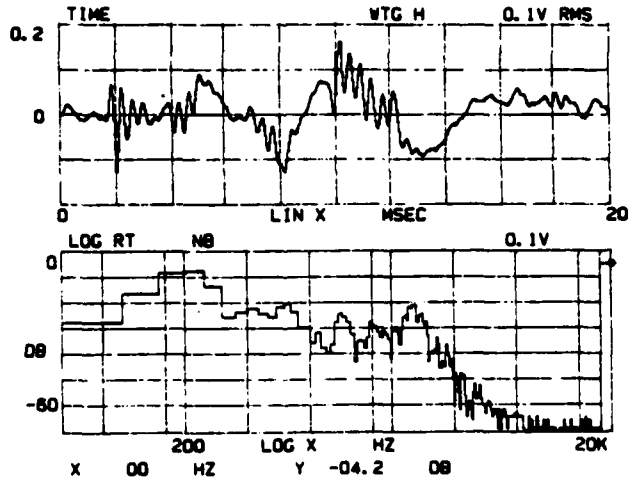

Figure 5.7e. 20-msec

Figures 5.7c-e. Time Samples of Varying Duration of Straf Event on Day 15 at 16:03:00, FM Channel 1, Kronhite: 100-20K Hz

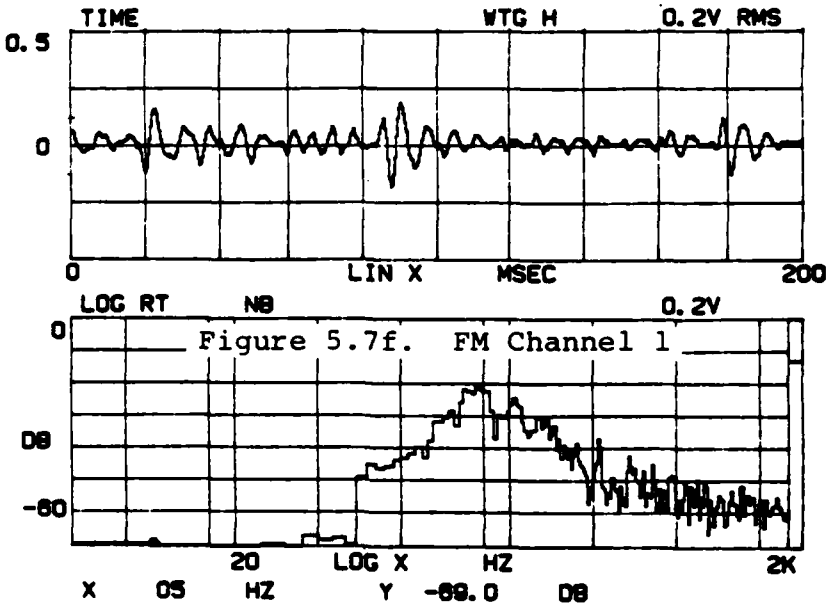

Figure 5.7f. FM Channel 1

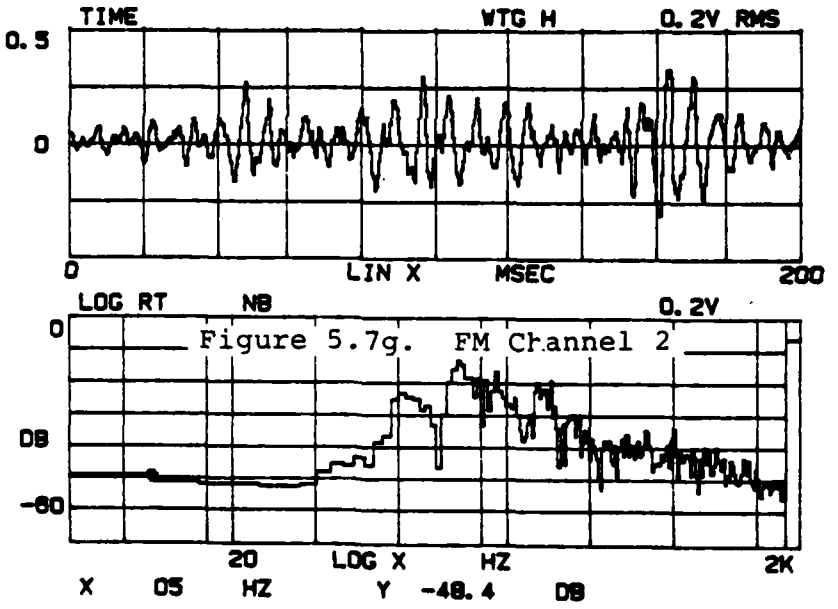

Figure 5.7g. FM Channel 2

Figures 5.7f-o. Sample (200 msec) of Straf Event on Day 16 at 00:18:42 for Various FM Channels, Kronhite: 100-20K

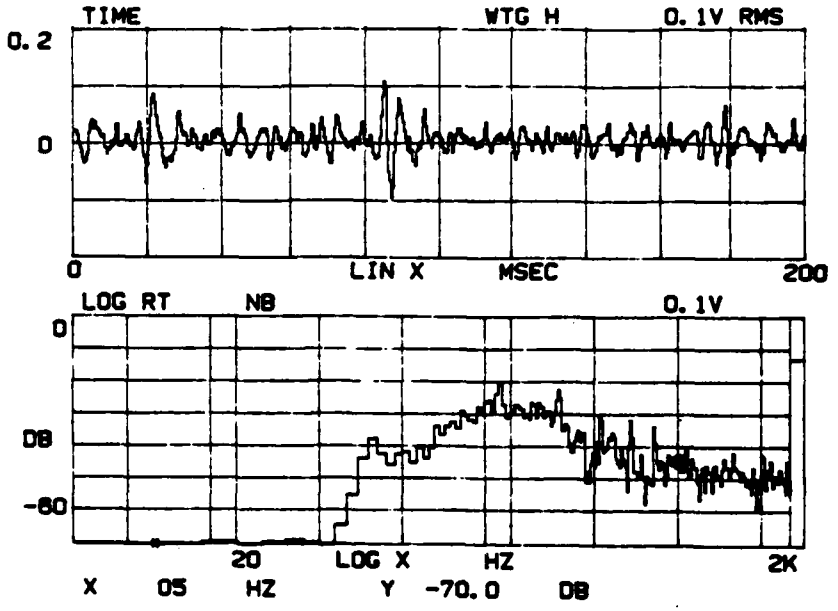

Figure 5.7h. FM Channel 3

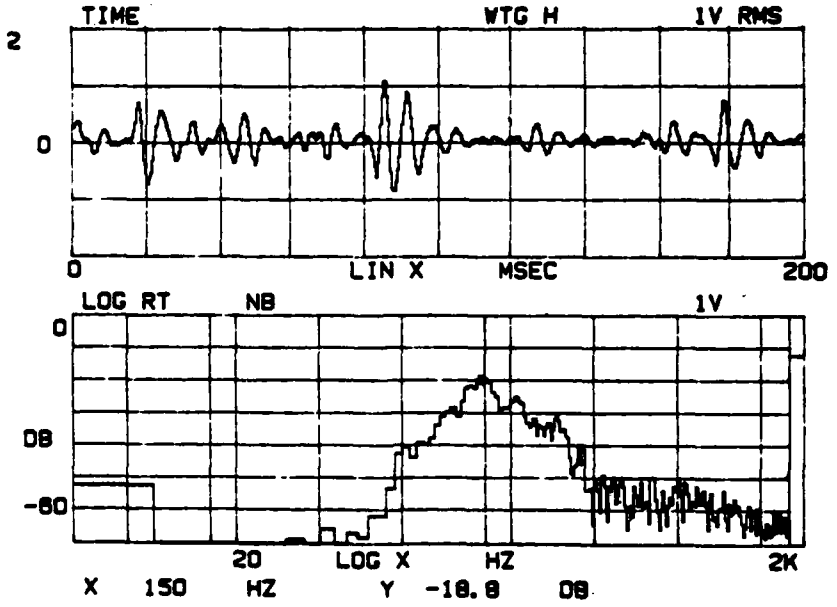

Figure 5.7i. FM Channel 4.

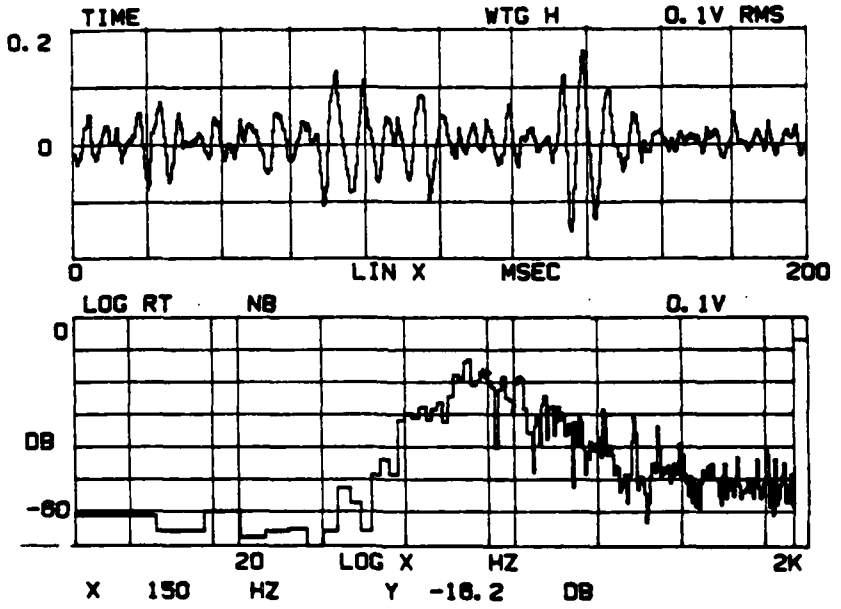

Figure 5.7j. FM Channel 5

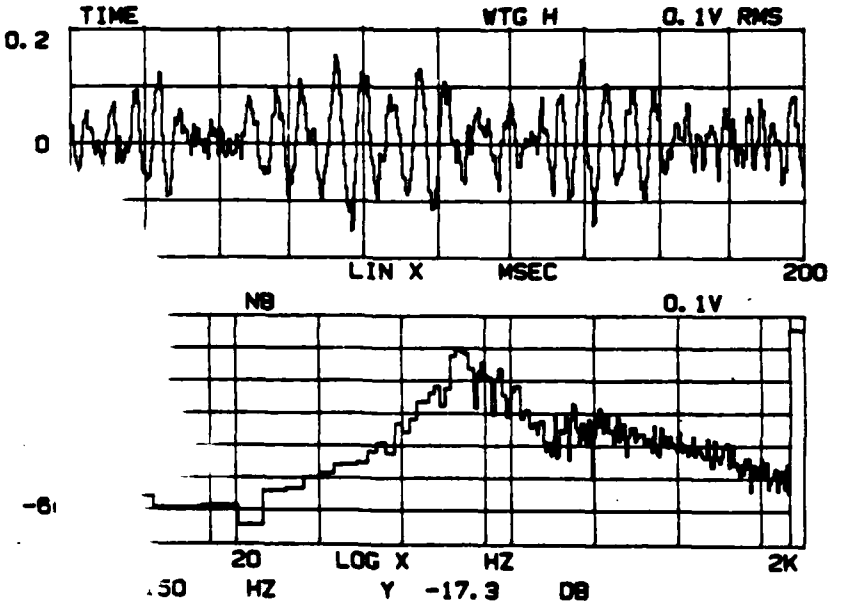

Figure 5.7k. FM Channel 6

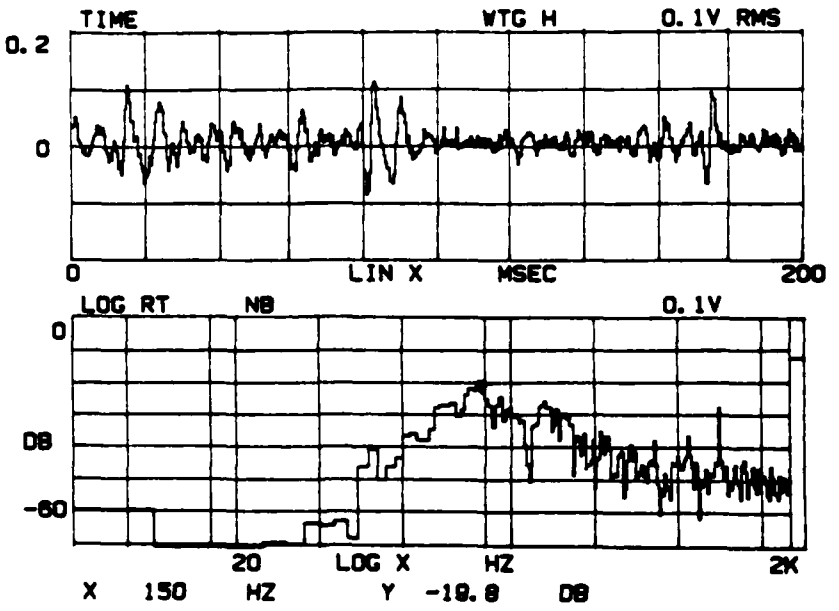

Figure 5.71. FM Channel 7

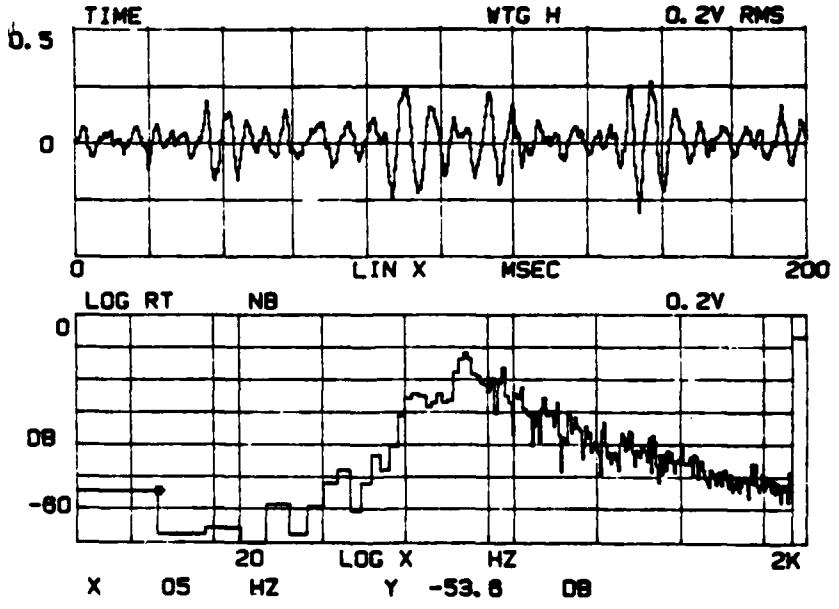

Figure 5.7m. FM Channel 8

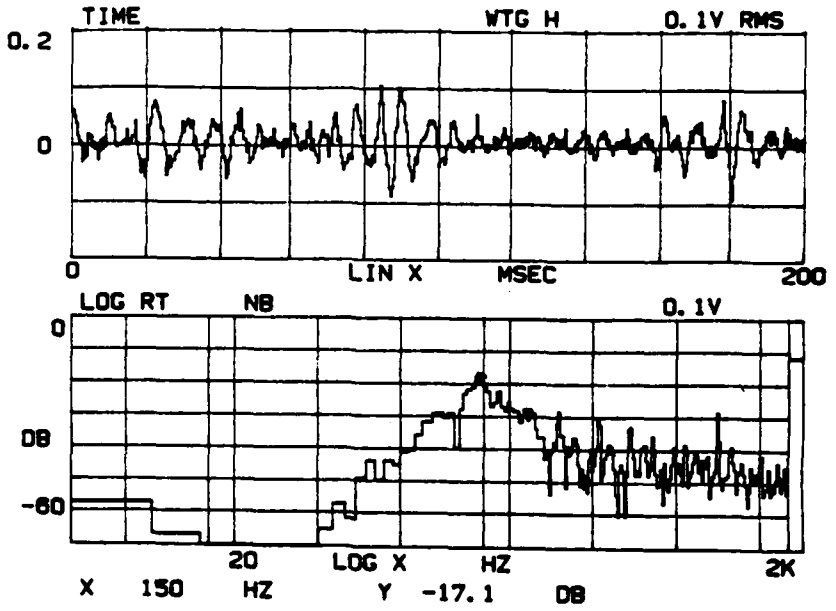

Figure 5.7n. FM Channel 9

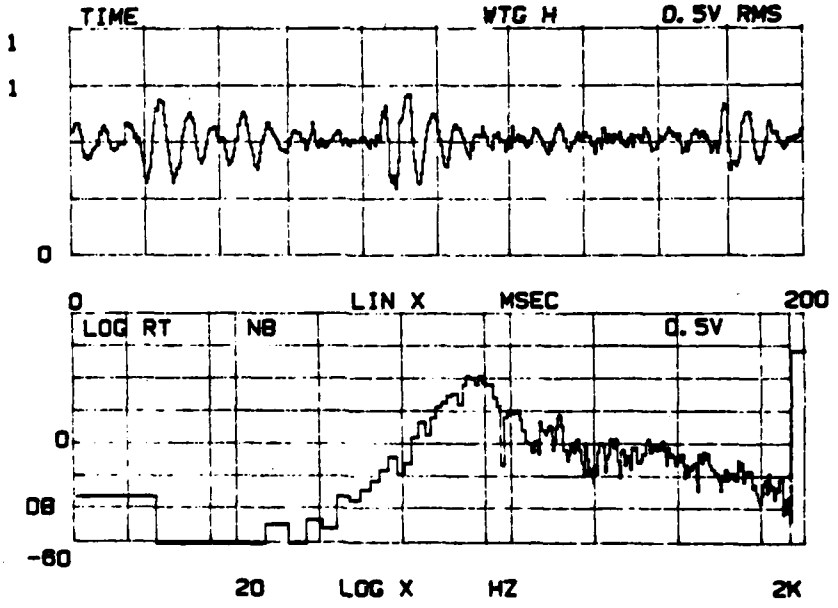

Figure 5.7o. FM Channel 10

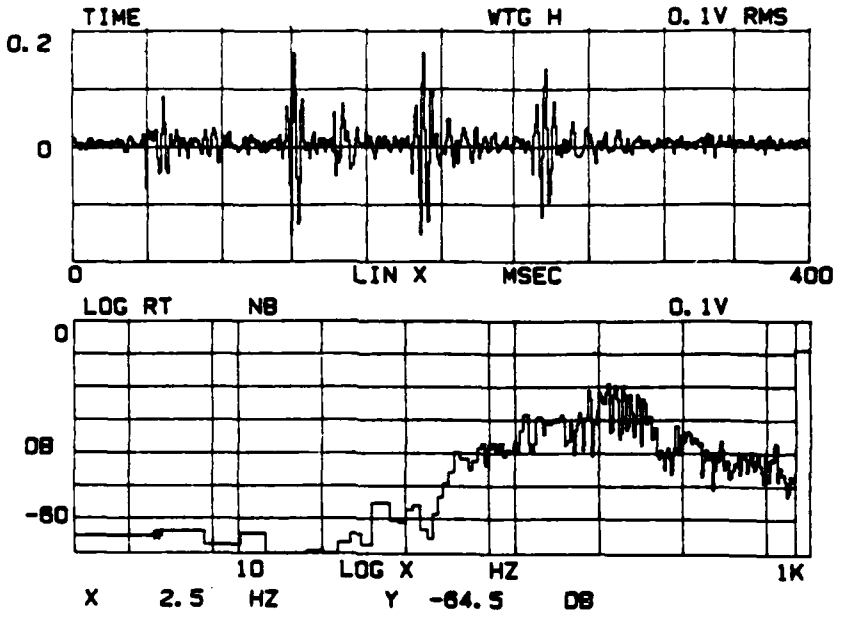

Figure 5.7p. Sample (400 msec) of Straf Event on Day 16 at 02:14:58, FM Channel 1, Kronhite: 80-20K Hz

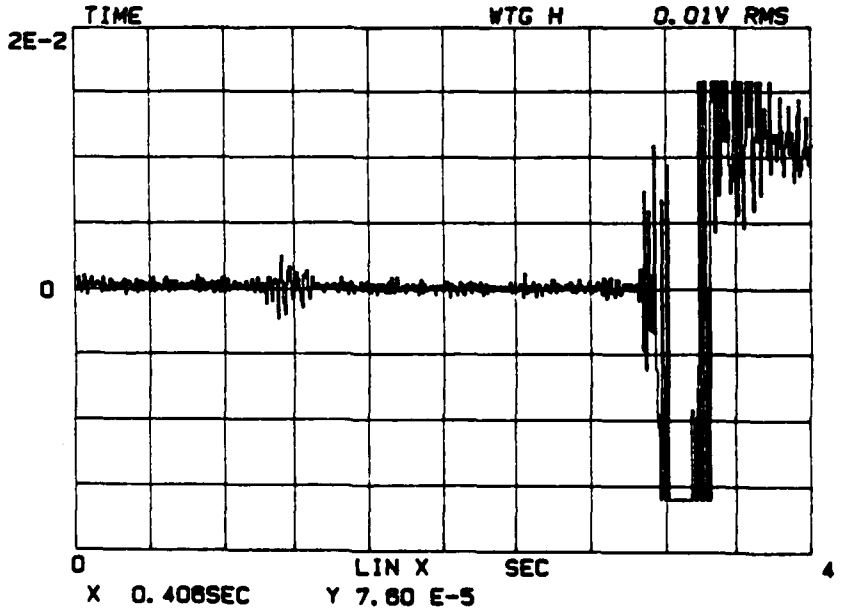

Figure 5.7q. Sample (400 sec) of Straf Before Airgun on Day 16 at 02:15:00, FM Channel 1, Kronhite: 150-20K

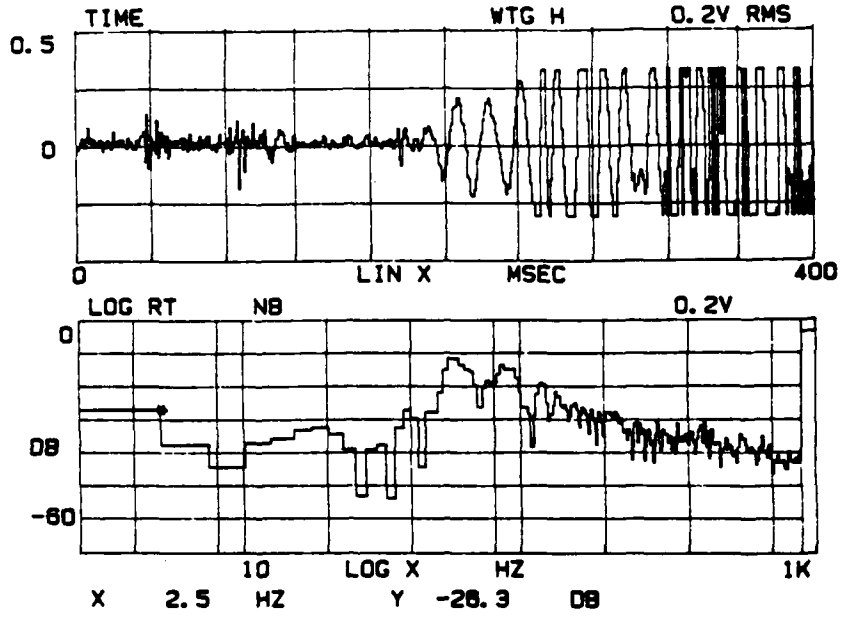

Figure 5.7r. Sample (400 msec) of Straf Before Airgun on Day 16 at 02:14:59, FM Channel 2

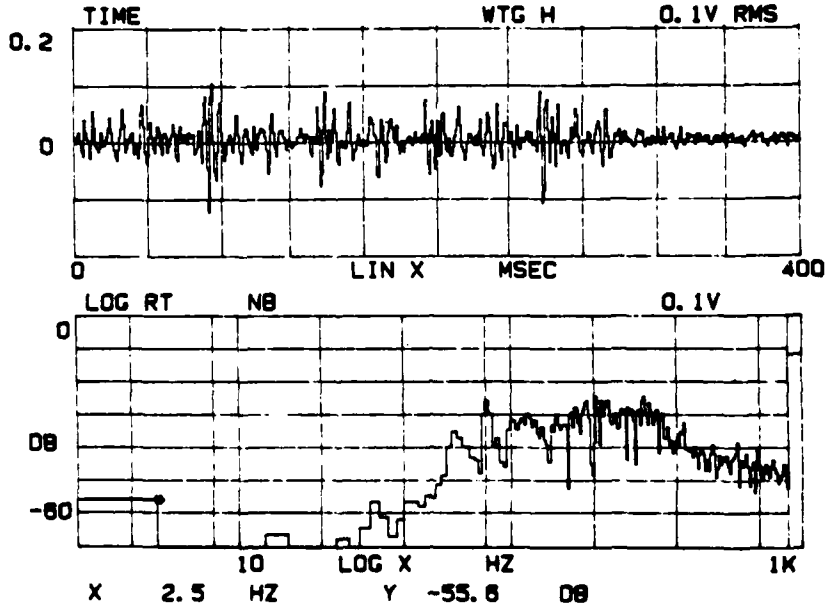

Figure 5.7s. Sample (400 msec) of Straf Before Airgun on Day 15 at 09:59:26, FM Channel 1, Kronhite: 80-20K Hz

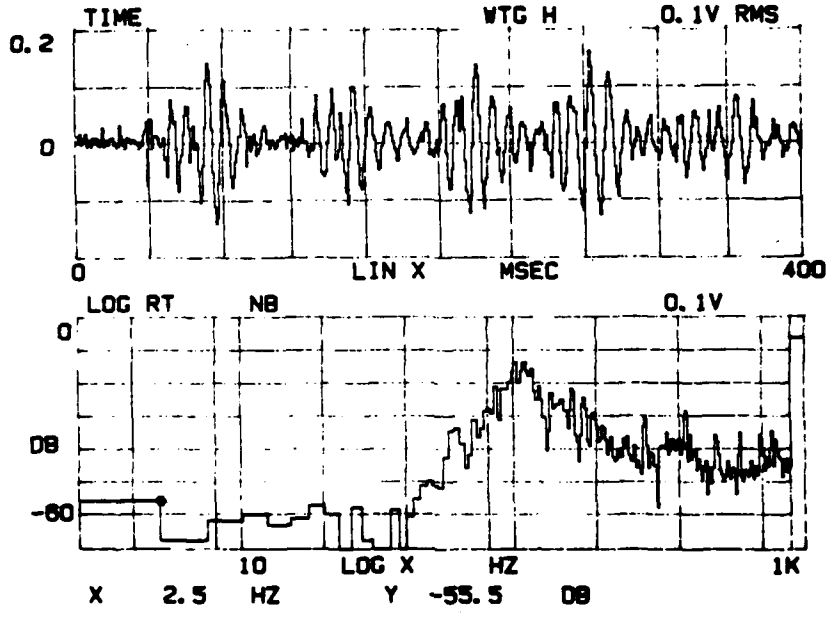

Figure 5.7t. Sample (400 msec) of Straf Before Airgun on Day 15 at 09:59:40, FM Channel 9, Kronhite: 80-20K Hz

rubbing, sticking then slipping. Figure 5.7e is a 20-msec time series of a portion of this event and illustrates the complex nature of this straf event. The peak-to-peak voltage is .25V and again this event was observed only on this channel.

Figures 5.7f through 5.7o illustrate a straf event detected on all channels. This was a 280-ms event at 00:18:42 on Day 16, however only 200-ms of the event is shown in these figures.

The peak frequency is about 150 Hz. Table 5.1 lists the absolute level at 150 Hz for each hydrophone. The peak-to-peak voltage on hydrophone 5 is almost .4V and close to 2V on the 90m vertical hydrophone (the 14-dB gain between vertical and horizontal would make that equivalent to .4V on a horizontal phone). This event is much louder than previous events observed on only one hydrophone. It seems unusual that the levels on the vertical array are so varied but further analysis requires we digitize and plot the time series of each hydrophone simultaneously to examine moveout.

Table 5.1 Absolute Level for Each Hydrophone at 150 Hz

H5	92
V30	81
Strapped	85
V90	93
Hairy	89
V270	80
90 lb	85
V450	81
H24	88
V960	86

It was observed while listening to the tapes that the straf was sometimes followed by the airgun noise. In Figure 5.7p straf, peaking around 300 Hz, was observed on the apex hydrophone. Two seconds later, Figure 5.7q, the airgun noise followed. In Figure 5.7r, on the 30m vertical hydrophone, straf preceeded the airgun noise by approximately 140ms. The airgun was approximately 430m from both hydrophones. The 140ms time difference is consistent with the time it takes a longitudinal wave traveling in the ice at 3000 m/sec to reach the hydrophone before the water wave (1500 m/s).

This suggests the longitudinal wave in the ice is sufficient to cause the same type of stress relief as thermal stress on the ice. No such explanation is plausible for the straf event on the apex hydrophone recorded 2 seconds prior to the airgun signature. This may have been an independent, coincidental event. This phenomenon will be examined further.

A straf event lasting 280ms, Figure 5.7s, was observed only on the apex phone at 09:59:26 on Day 15. It had a broad spectra peaked about 200 Hz. While listening to the other channels another straf event, Figure 5.7t, was detected on horizontal hydrophone 24 with a narrower peak about 100 Hz, at 09:59:40. Assuming the events are local, it shouldn't be unusual to find separate events occurring about the same time at different locations.

5.8 Pop

Every now and then a single pop can be heard on the tape. Again thermal stress relief is responsible for this noise, however in this case the mode I type of cracking,

illustrated in Figure 2.8, is the more likely generating mechanism.

Figures 5.8a through 5.8f show a pop that was heard on all of the vertical phones and one horizontal phone that was near the vertical array (Ch 1,2,4,6,8,10). Notice the polarity of the signal on channel 1 is reversed from the polarity of the signal on the vertical phones, this is because the horizontal hydrophones responded to a positive pressure with a negative pulse, opposite the vertical phones. This event has a peak frequency about 500 Hz. This event should be very useful in unraveling the propagation along the vertical array once the data is digitized and plotted simultaneously for all the hydrophones.

It is significant that near midnight a series of pops and straf events are observed. We expect this is due to the increased thermal stress, which is to be expected near midnight.

5.9 Seals

While analyzing the analog tapes we noticed a noise that sounded much like the wind howling on Day 15 at 09:53:56. Checking the other channels we observed that the noise was heard on FM channels 2,4,5,6,8,10 which are all the vertical hydrophones and the hairy hydrophone located closest to the vertical array. The signature of this noise shows some interesting characteristics. There was a distinct peak at 312.5 Hz on all channels (see Figure 5.9 series), and channel 6 exhibited the harmonics of the noise with a second peak at 625 Hz although this is not illustrated in the figures. All the sounds were modulated tones. Seals are found in this region and have a frequency range from 100 to 3 kHz. This event lasts approximately 200 ms and then fades slowly into the background noise.

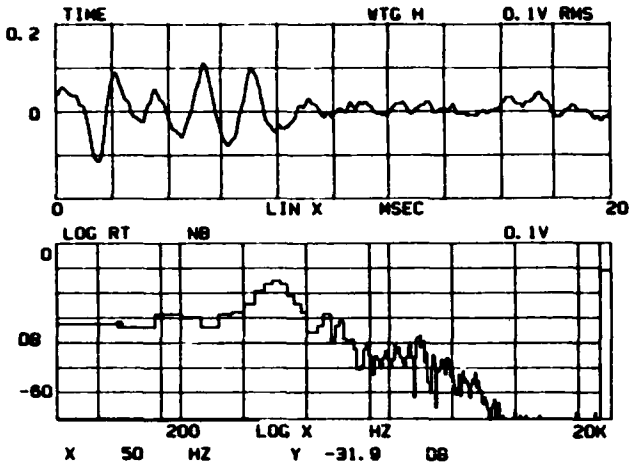

Figure 5.8a. FM Channel 1

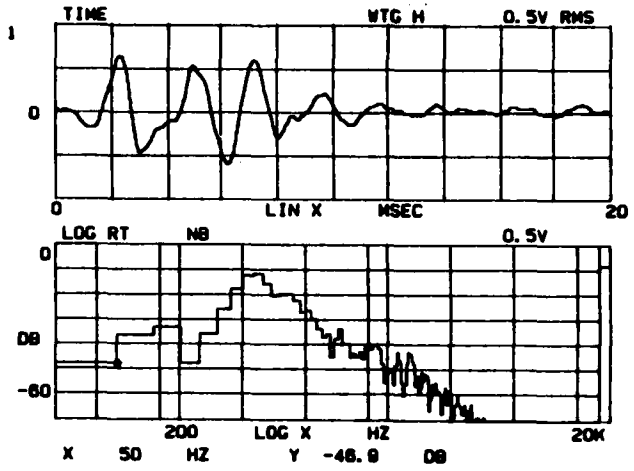

Figure 5.8b. FM Channel 2

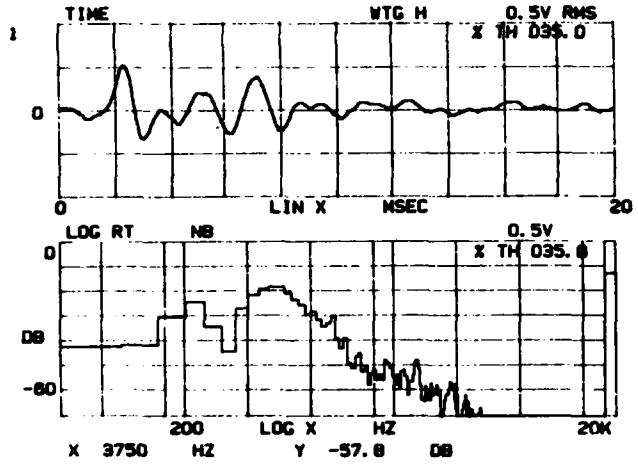

Figure 5.8c. FM Channel 4

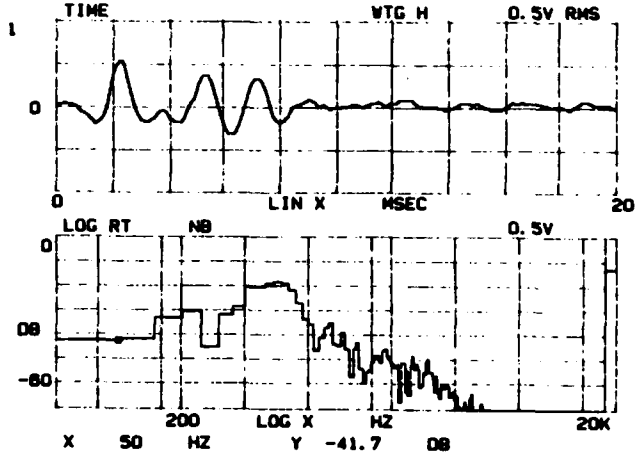

Figure 5.8d. FM Channel 6

Figures 5.8a-f. Sample (20 msec) of a Pop on Day 16 at 00:32:05 from Various FM Channels, Kronhite: 100-20K

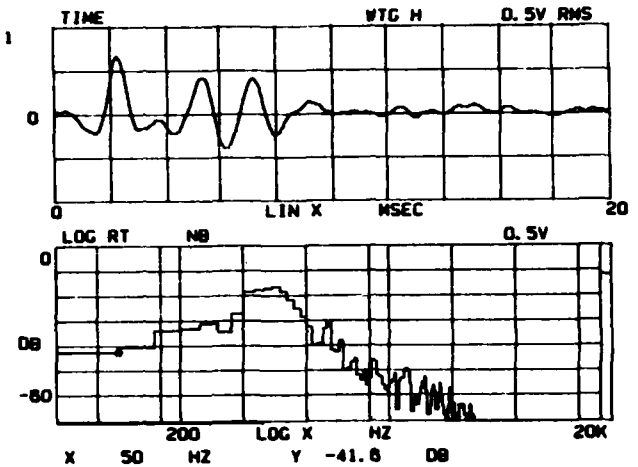

Figure 5.8e. FM Channel 8

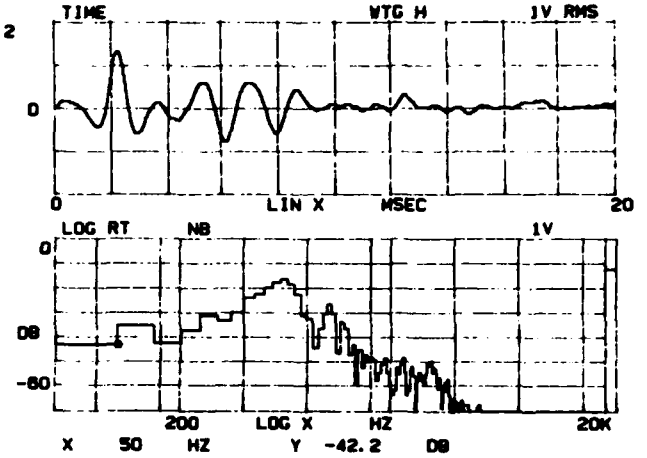

Figure 5.8f. FM Channel 10

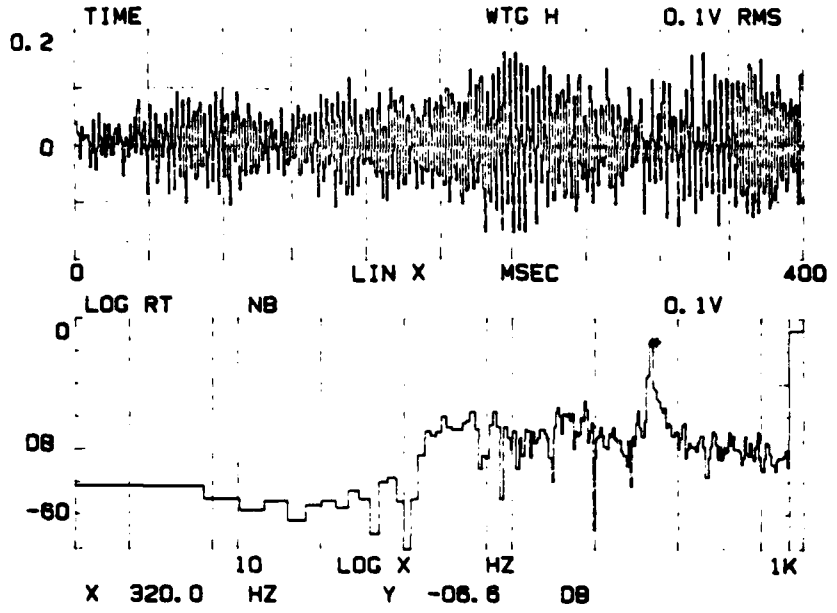

Figure 5.9a. Sample (400 msec) of Seal Sound on Day 15 at 09:53:56, FM Channel 2, Kronhite: 80-20K Hz

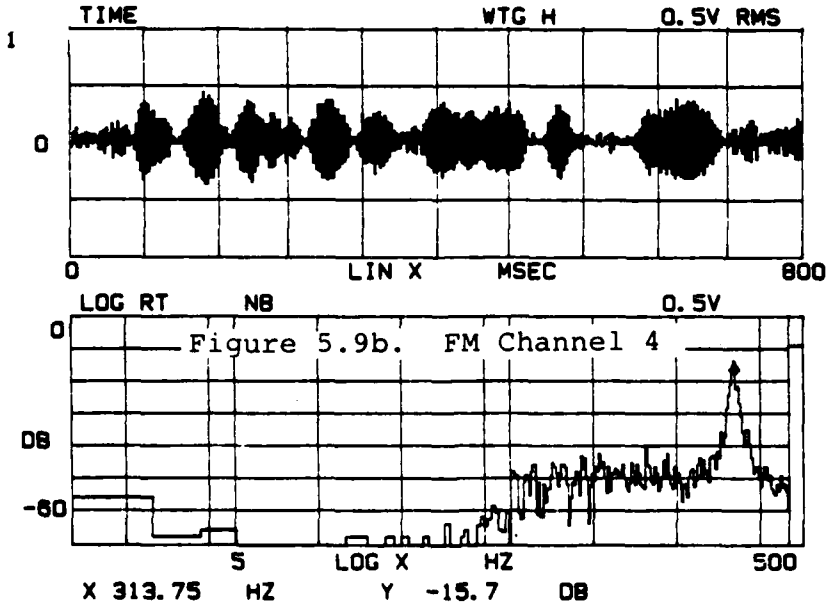

Figure 5.9b. FM Channel 4

Figures 5.9b-f. Sample (800 msec) of Seal Sound on Day 15 at 09:53:56 for Various FM Channels; Kronhite: 80-20K Hz

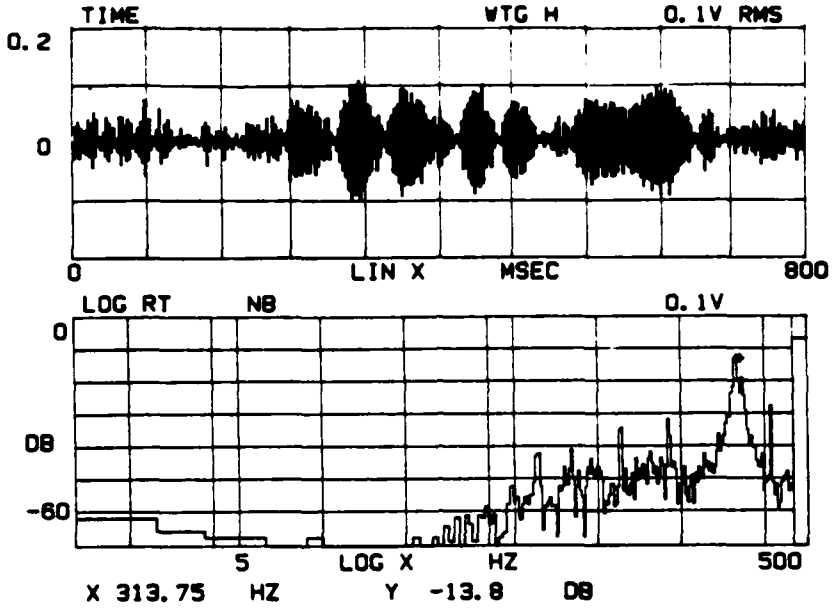

Figure 5.9c. FM Channel 5

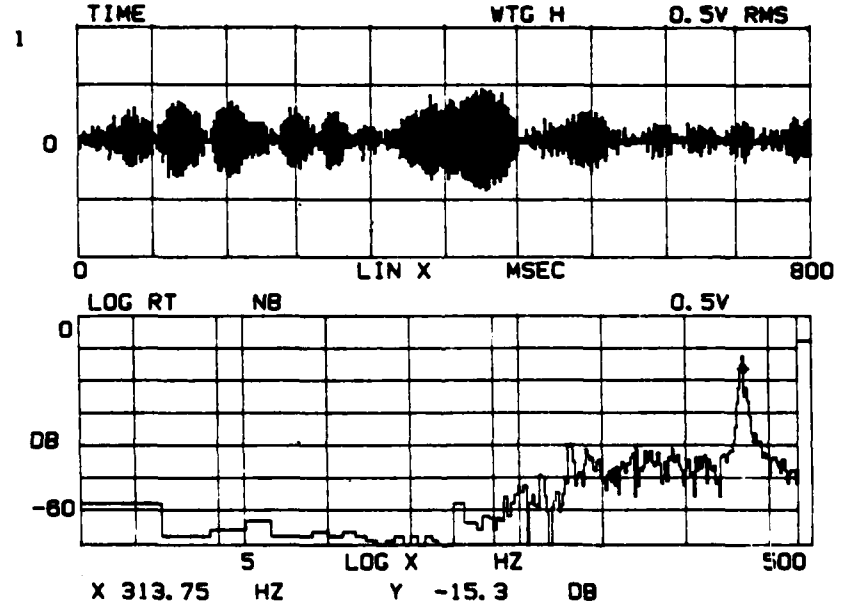

Figure 5.9d. FM Channel 6

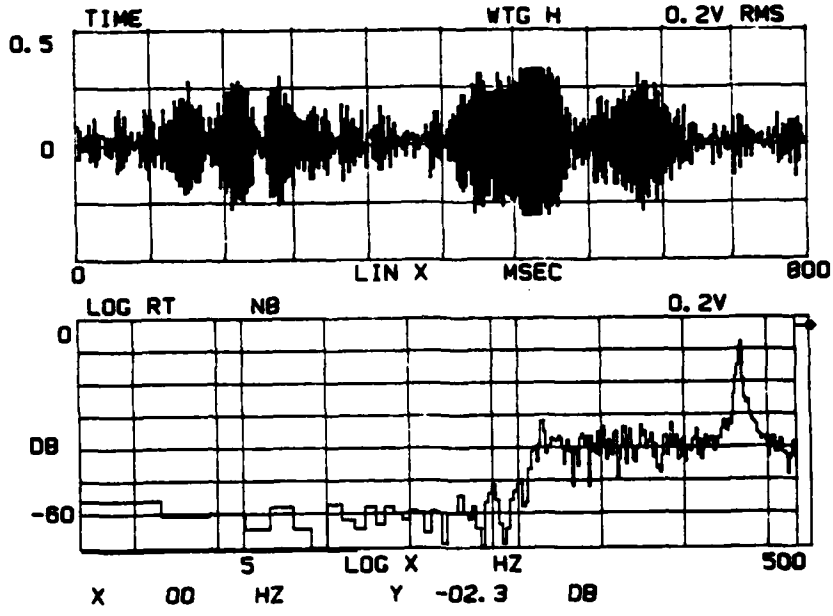

Figure 5.9e. FM Channel 8

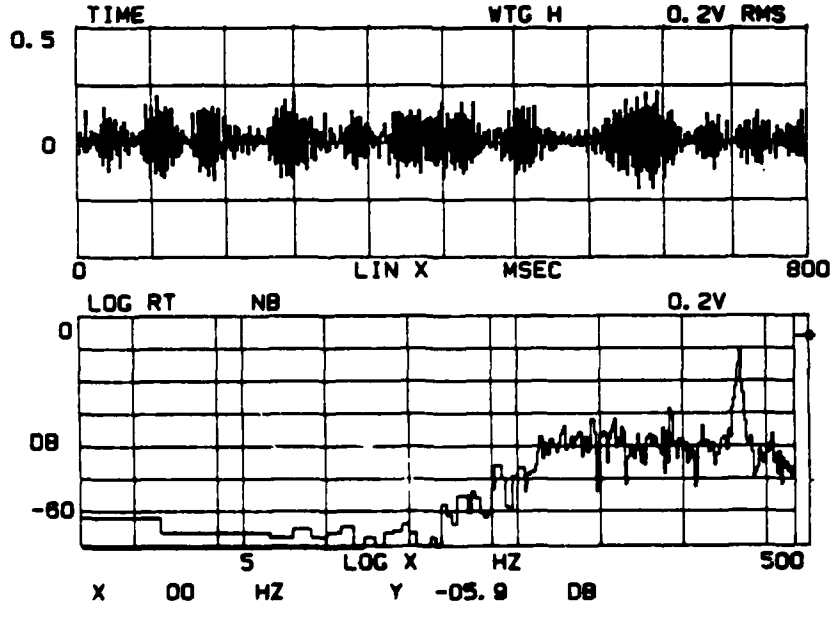

Figure 5.9f. FM Channel 10

5.10 Damped Sinusoids

Recall from Section 2 that Milne observed ice cracking events with damped sinusoid shapes (Figure 2.3). Although damped sinusoid patterns could be superimposed to model our straf events we also observed single damped sinusoid events that had a decidedly different character than the straf.

In Figures 5.10a,b,c the damped sinusoid sounded much like a tugboat whistle or someone blowing over the top of a Classic Coke bottle. These noises lasted several seconds and could be heard on all the vertical hydrophones and on horizontal hydrophones H1 (Figure 5.10a) and the hairy hydrophone (Figure 5.10c), which are the closest phones to the vertical array. The figures show a 400-ms time sample that captures one of the series of damped sinusoids and a 25.6-second average spectra. The spectra has a sharp peak about 117 Hz. These sounds could not be heard on H24, Figure 5.10d, but there was a straf event observed with a 100-Hz peak frequency at the same time.

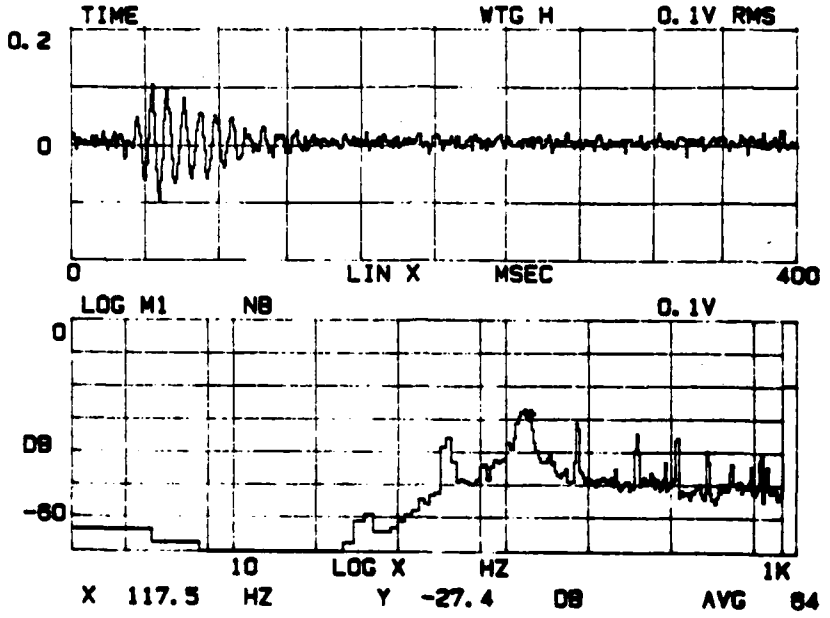

Figure 5.10a. Sample (400 msec) of Damped Sinusoid on Day 15 at 10:02:30 for FM Channel 1, Kronhite: 80-200 Hz

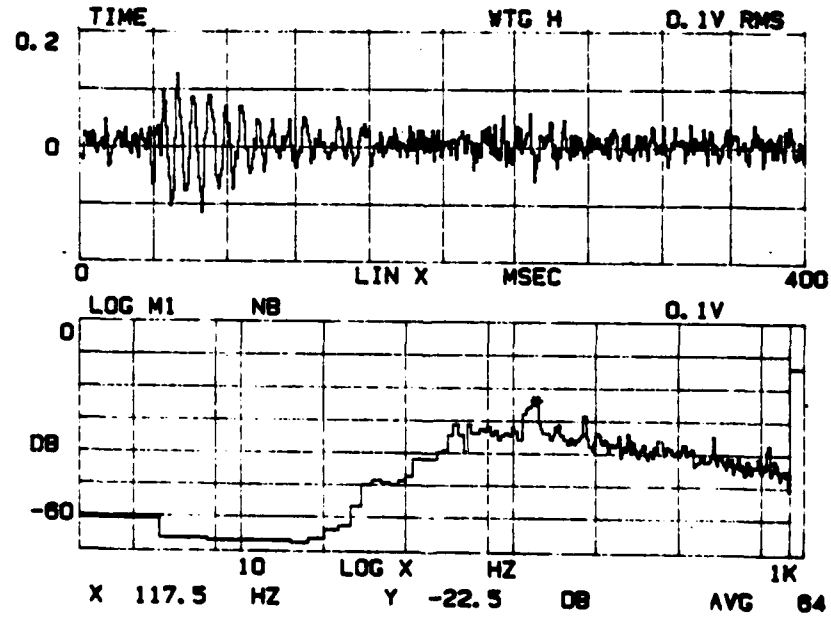

Figure 5.10b. Sample (400 msec) of Damped Sinusoid on Day 15 at 10:02:30 for FM Channel 2, Kronhite: 80-200 Hz

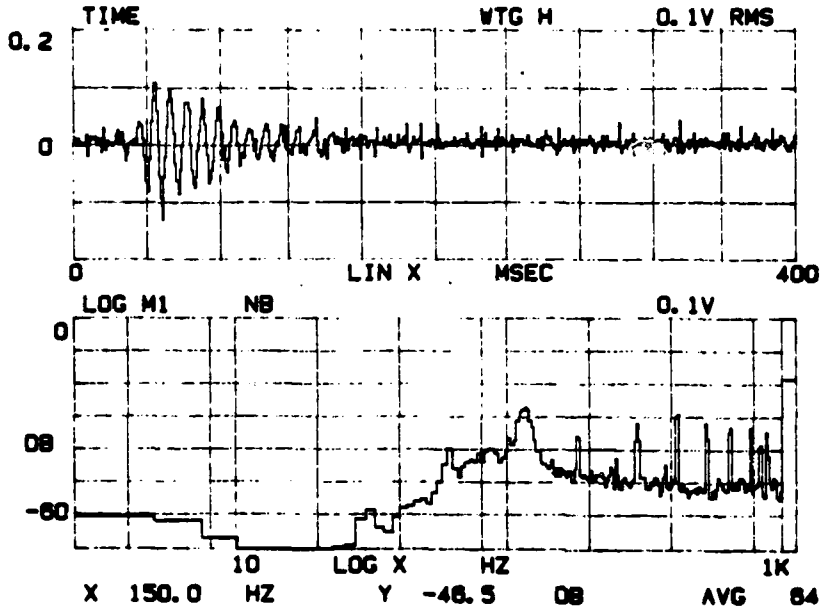

Figure 5.10c. Sample (400 msec) of Damped Sinusoid on Day 15 at 10:02:30 for FM Channel 5, Kronhite: 80-200 Hz

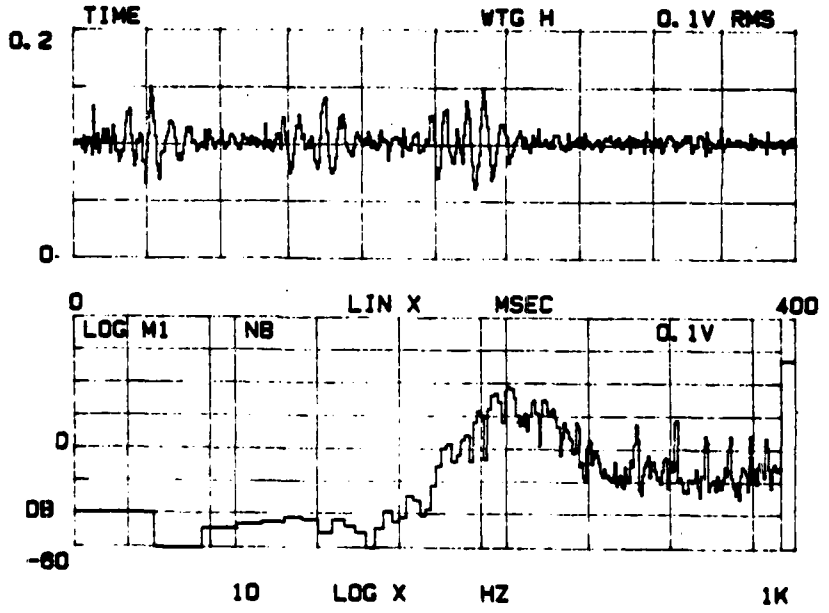

Figure 5.10d. Sample (400 msec) of Damped Sinusoid on Day 15 at 10:02:30 for FM Channel 9, Kronhite: 80-200 Hz

Section 6
SPECTRAL LEVELS

Thermal stress is the accepted mechanism for the generation of mid-frequency noise. Milne (Figure 2.3) has shown a striking temperature dependence, specifically with the temperature gradient. In this section the spectral levels at 100 Hz, 200 Hz and 300 Hz are compared with the temperature, temperature gradient, and large scale stress levels. The pressure levels in this data set do not show as marked a dependence on the temperature as observed by Milne.

The temperature was measured every 10 minutes during FRAM IV at 1m and 8m above the ice surface. This data is presented for the 24-day period in Figure 6.1. The 1m and 8m measurements are virtually identical. The diurnal variation of approximately 5°C is superposed on a larger scale temperature variation. The derivative of this curve was taken and plotted in Figure 6.2 (Makris, 1985). Figure 6.3 is the FRAM IV wind stress time series which is well correlated with the internal ice stress (Makris, 1985).

The 20-Hz and 100-Hz pressure spectral levels Mellen (1984) observed on the 30m vertical phone are presented in Figure 6.4 for comparison. Figures 6.5 and 6.6 are our measurements of the 100-Hz, 200-Hz and 300-Hz pressure levels. Figure 6.5 covers the period from 17:03 on Day 5 to 17:02 on Day 6. Figure 6.6 covers the period from 10:33 on Day 12 to 11:03 on Day 18. These measurements represent the average level of an approximate 30-second sample on different hydrophones (vertical and horizontal). If there was more than a 2-hour gap between data points they were left unconnected. Although each figure shows a different frequency,

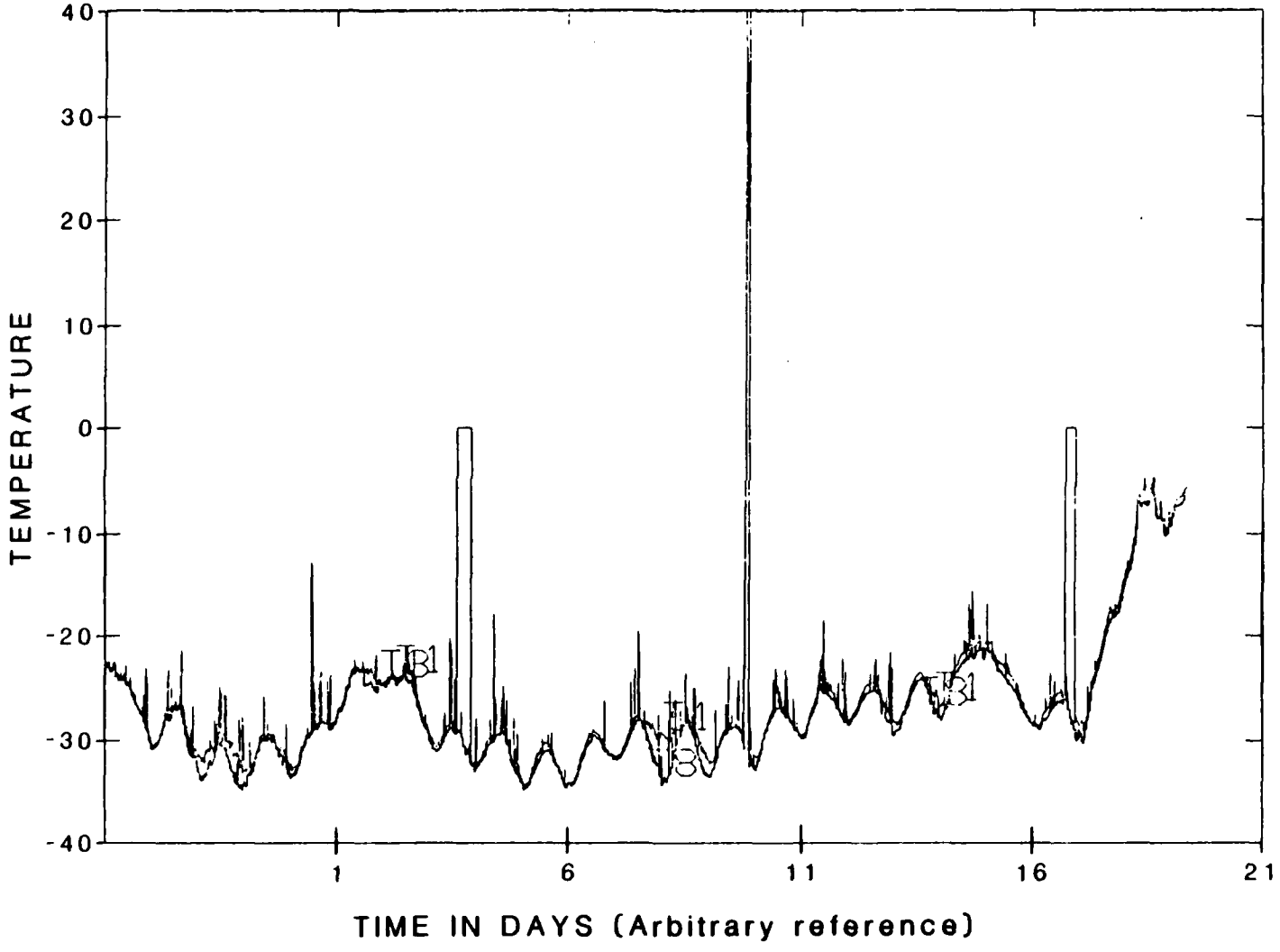

Figure 6.1. FRAM IV Temperature Time Series

AD-A174 880 FRAM IV AMBIENT NOISE: (100 HZ-500 HZ) DATA ANALYSIS (U) SCIENCE APPLICATIONS INTERNATIONAL CORP MCLEAN VA R E KEENAN ET AL. NOV 85 SAIC-85/1901 N00014-84-C-0180 2/2

UNCLASSIFIED F/G 20/1 NL

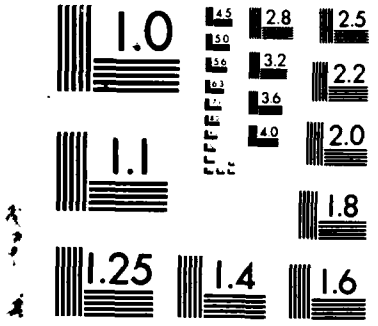

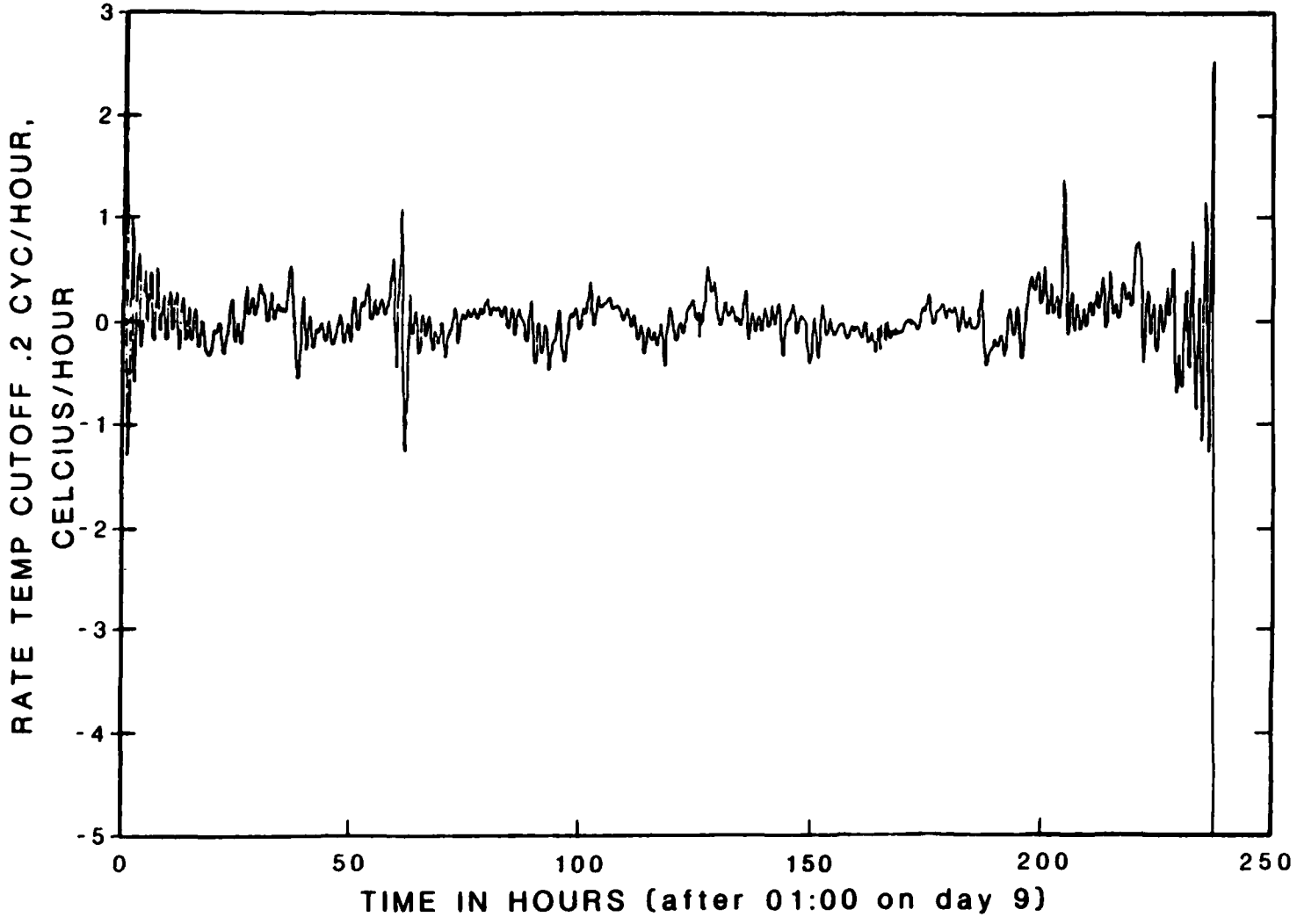

Figure 6.2. FRAM IV Temperature-Gradient Time Series

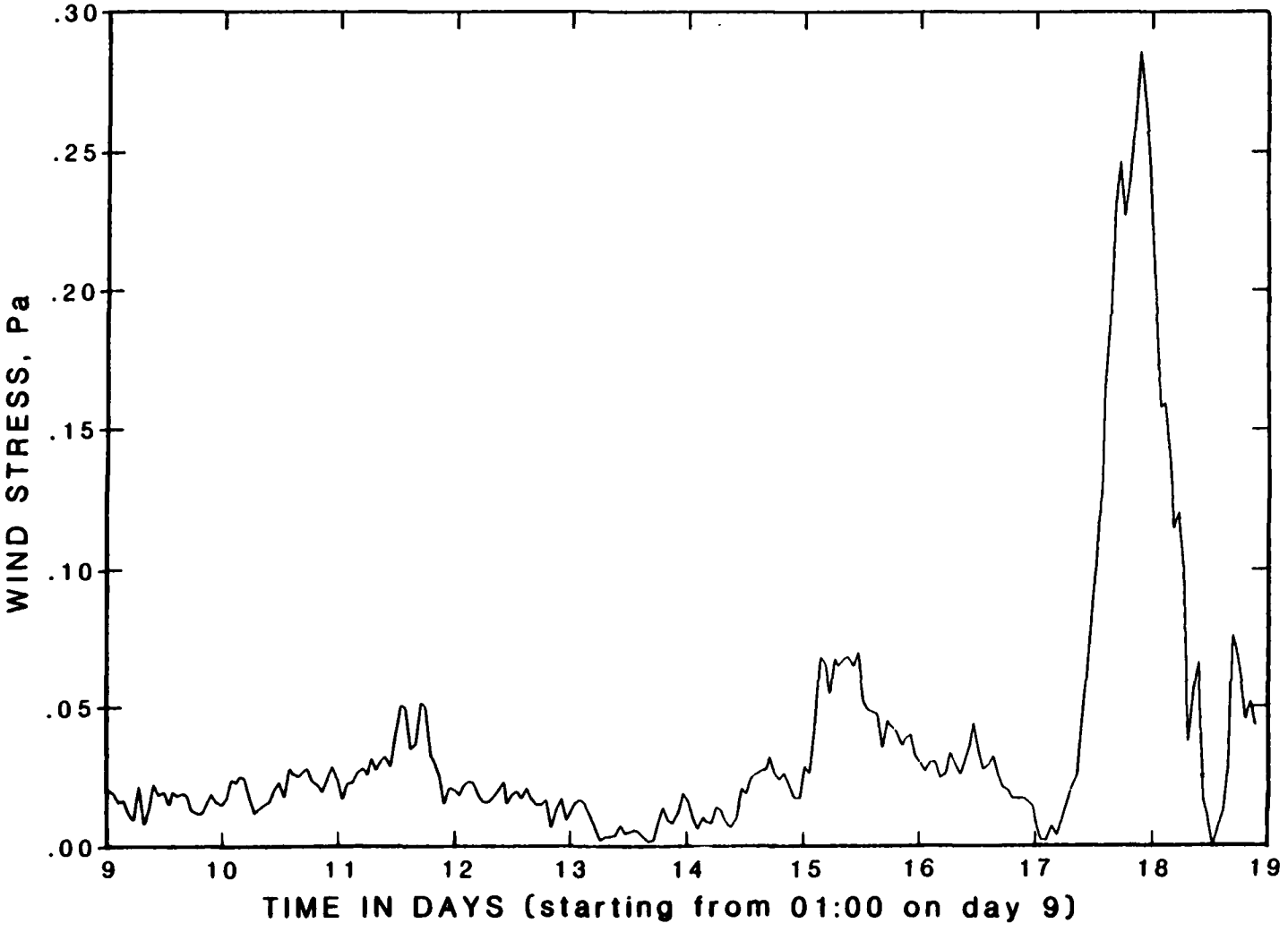

Figure 6.3. FRAM IV Wind Stress Time Series

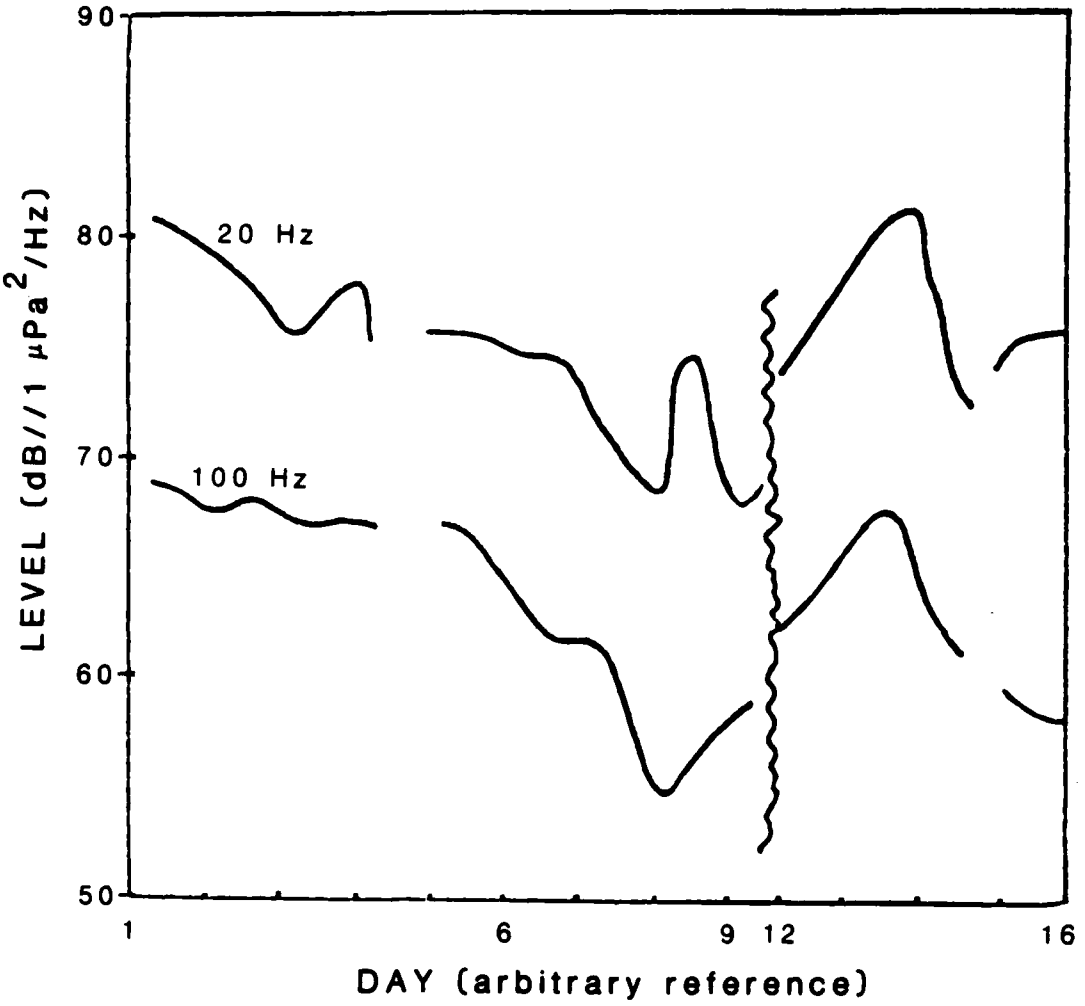

Figure 6.4. Mellon FRAM IV Ambient Noise Summary for 20 and 100 Hz

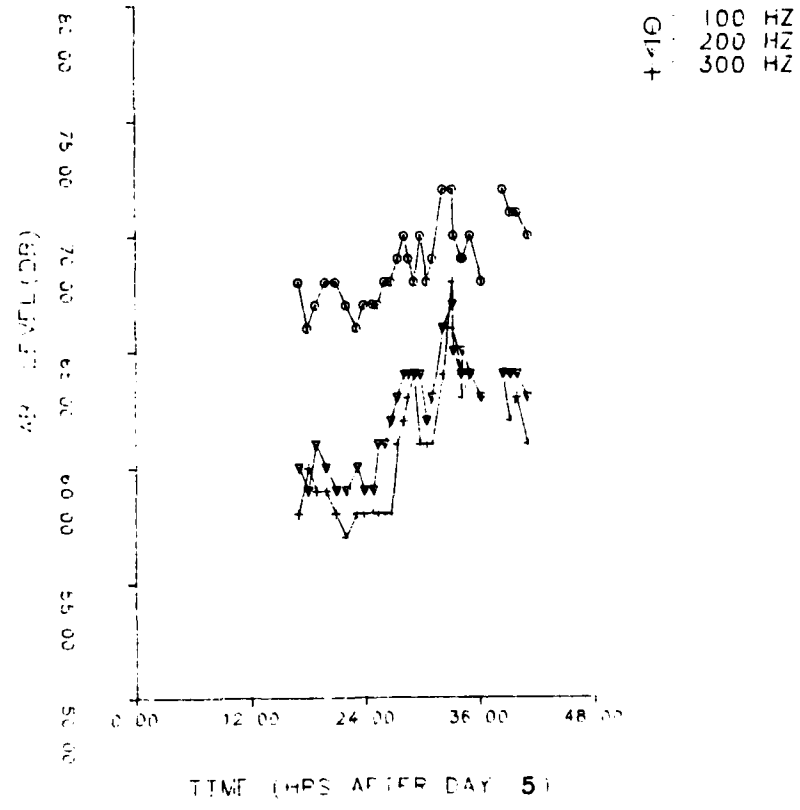

Figure 6.5. 100-Hz, 200-Hz and 300-Hz Spectral Levels on Days 5 and 6

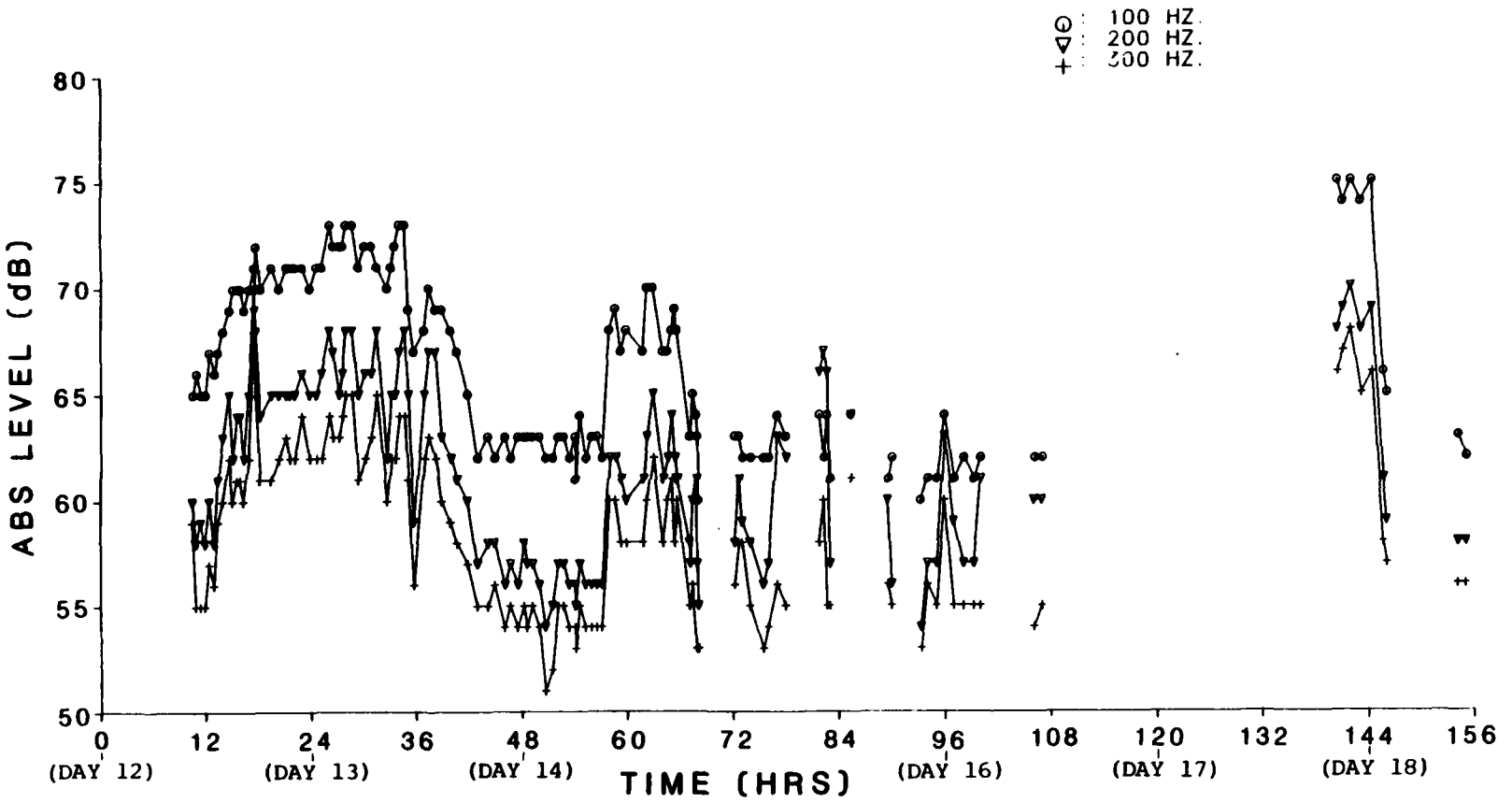

Figure 6.6. 100-Hz, 200-Hz and 300-Hz Spectral Levels on Days 12 Through 18

each exhibits the same temporal variations. The very high levels at 144 hours, or the beginning of Day 18, in Figure 6.6 were checked for consistency against the MIT/WHOI digital tapes and the levels were found to be in agreement. These high levels are probably related to the high internal ice stress levels calculated on Day 18 by Makris (see Figure 6.3) and not to any thermal ice stress levels, as the temperature was rising rapidly (Figure 6.1) at this time.

Qualitatively, the diurnal temperature component is not obvious although there does appear to be a correlation with the larger scale temperature variations. There could be a number of reasons why we do not see the pressure vary as illustrated in Figure 2.3. First, we have a more complicated temperature time series and the diurnal fluctuation is only half of what Milne observed. Second, we are in the Central Arctic, not the protected Canadian Archipelago, so this noise could be masked by other noises. The next step in analyzing this temperature dependence will be to take the spectra of this time series and examine it for a diurnal component.

Section 7
CONCLUSIONS

At the outset of this study we expected to correlate the pressure levels at different frequencies with the temperature and temperature gradient time series in order to determine the peak frequency of the thermal noise and the time delay between atmospheric changes and the acoustic response. However, this data has not provided what we expected. For one, given that both the vertical and horizontal hydrophone systems had flat responses, we are unable to account for the different spectral shapes between the two above 500 Hz - 700 Hz. For this reason we limited ourselves to the data below 500 Hz. The pressure levels do not rise and fall with the temperature as expected. Thermal noise is present and more events can be heard near midnight when the temperature drops, but these events are not the dominant ambient noise factor. A number of different kinds of noise events have been characterized, such as pops, straf and damped sinusoids. However, these events were rarely observed on all the hydrophones, although they were often heard in more than one location and when they were observed on the vertical array they were observed on all the vertical phones. These events, pops and straf, were usually less than 0.5 seconds in duration and rarely affected the 30-second average spectra used to plot the pressure time series.

These results, because they were unexpected, need to be further validated. In continuing this study we will look at the moveout between hydrophones and try to separate the thermal component from other noise sources. We will also examine the MIZEX 84 data set to corroborate these conclusions.

REFERENCES

Buck, B.M. and Rosser, K.A., "Arctic Underice Acoustic (Surveillance) Technology (URSA)," PRL TR38, 20 January 1982.

Dyer, Ira, "The Song of Sea Ice and Other Arctic Melodies," in Arctic Technology and Policy, I. Dyer and C. Chryssostomidis, ed., Hemisphere Publishing Co., Washington (1983).

Shepard, G.W., Arctic Ocean Ambient Noise, MIT Thesis (1979).

Chen, Y.M., Underwater Acoustic Ambient Noise in the Arctic, MIT Thesis (1982).

Milne, A.R. and Ganton, J.H., "Diurnal Variations in Underwater Noise Beneath Springtime Sea-Ice," Nature, Vol. 221, March 1, 1969.

Milne, A.R., "Sound Propagation and Ambient Noise Under Sea Ice," in Underwater Acoustics, Vol. 2, V.M. Albers, ed., Plenum Press (1967).

Mellen, Robert H., "Arctic Drift Station FRAM IV Ambient Noise Measurements," BKD-1341, prepared under NUSC Contract N00140-83-M-PJ12.

Ganton, J.H. and Milne, A.R., "Temperature- and Wind-Dependent Ambient Noise under Midwinter Pack Ice," The Journal of the Acoustical Society of America, Vol. 38, pp. 406-411, 1965.

Appendix A
FM CHANNEL CONFIGURATION

H denotes horizontal phones, V denotes vertical phones, G denotes geophones, SERVO is the channel devoted to tracking the tape speed and TCG is the time code generator

CHANNEL	HYDROPHONE	RANGE(M)	BEARING(DEG)	DEPTH(M)
Configuration on Day 15, 00:10:00				
1	H1	0	0	90
2	V29	40	270	30
3	H30	872	0	90
4	V27	40	270	90
5	HAIRY	50	225	90
6	V19	40	270	270
7	H29	160	90	90
8	V11	40	270	450
9	H24	971	270	90
10	V1	40	270	960
11	G2	23	0	90
12	HORGEO	19	180	90
13	SERVO	--	--	--
14	TCG	--	--	--
Configuration change (from Day 15: 00:10:00) at Day 15, 02:27:30				
5	H13	438	180	90
Configuration on Day 15, 16:08:12				
1	H5	161	0	90
2	V29	40	270	30
3	STRAPPED	155	354	90
4	V27	40	270	90
5	HAIRY	50	225	90
6	V19	40	270	270
7	90 lb	136	6	90
8	V11	40	270	450
9	H24	971	270	90
10	V1	40	270	960
11	G2	23	0	90
12	HORGEO	19	180	90
13	SERVO	--	--	--
14	TCG	--	--	--
Configuration change (from Day 15: 16:08:12) Day 16 02:07:50				
1	H1	0	0	90
11	H5	161	0	90
Configuration change at Day 16, 09:42:00 (revert to configuration at Day 15: 16:08:12)				
Configuration change (from Day 16: 16:08:12) at Day 16, 20:20:00 (replaces all vertical phones with horizontal phones)				
2	H1	0	0	90
4	H21	160	270	90
6	H19	20	270	90
8	H10	80	180	90
10	H16	80	90	90

END

1-87

DTIC